Surface–Based Electrical Surveys

For

Injection Well Fluids

By
Roy B. Evans, Ph.D.
Pieter Hoekstra, Ph.D.
Aldo T. Mazzella, Ph.D.

SURFACE-BASED ELECTRICAL SURVEYS

FOR

INJECTION WELL FLUIDS

by

Roy B. Evans, Ph.D.
Environmental Research Center
University of Nevada-Las Vegas

and

Pieter Hoekstra, Ph.D.
The Earth Technology Corporation

and

Aldo T. Mazzella, Ph.D.
Environmental Monitoring Systems Laboratory

for

Aldo T. Mazzella, Project Officer
Advanced Monitoring Systems Division
Environmental Monitoring Sytems Laboratory
U.S. Environmental Protection Agency
Las Vegas, Nevada

August 1988

NOTICE

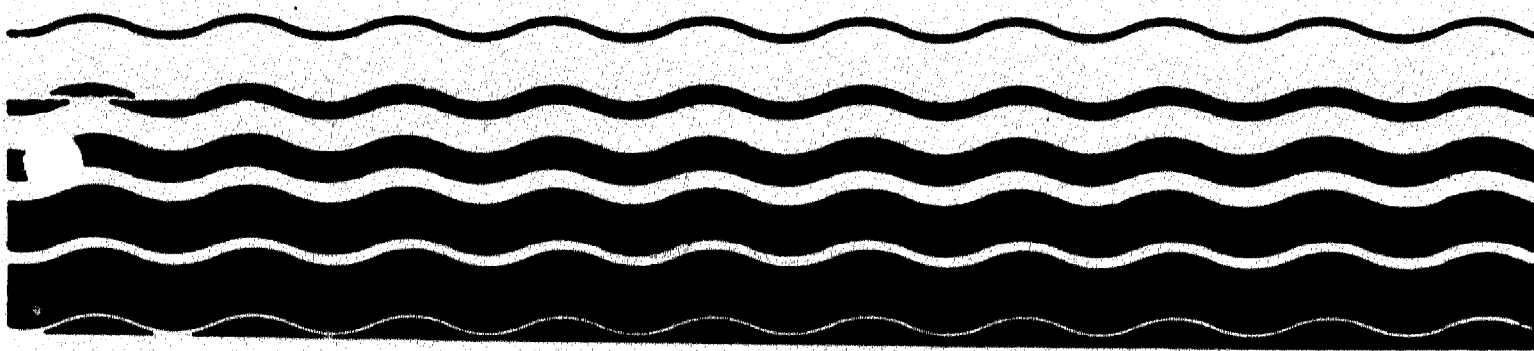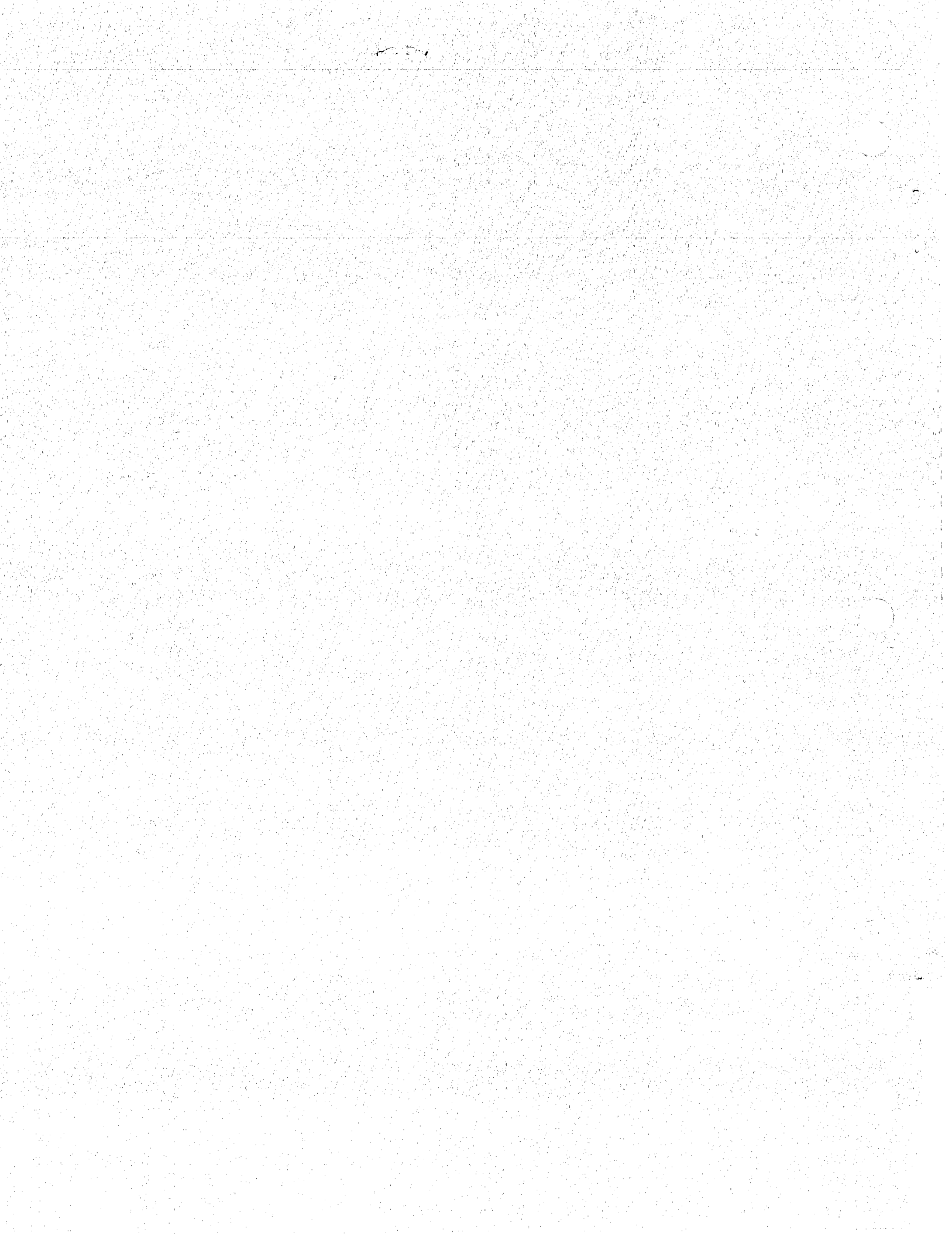The information in this document has been funded wholly or in part by the United States Environmental Protection Agency under cooperative agreement number CR 812189-01 to the Environmental Research Center of the University of Nevada-Las Vegas. It has been subject to the Agency's peer and administrative review, and it has been approved for publication as an EPA document.

Mention of trade names or commercial products does not constitute endorsement or recommendation for use.

ABSTRACT

Injected fluids present difficult electrical targets. Detection of target objects, formations, or strata by electrical geophysical techniques depends on the contrast in some electrical property between the target of interest and the material within which it is imbedded. Electrical conductivity is the principal property of interest for most electrical methods. The conductivity of injected fluids is usually roughly proportional to their total dissolved solids content. Injection usually takes place at depths of a few thousand feet, beneath confining strata which are often highly conductive, such as shale. Often the injection zone already contains connate water high in total dissolved solids and hence of high conductivity. In such situations, with properly constructed and operated injection wells, surface electrical methods probably will not be very useful for directly monitoring injected fluids because the contrast between the injected fluids and the connate water of the injected stratum, as well as the conductive overburden, would not be great. However, in cases where wells are improperly constructed and operated or cases in which fractures connect the injection zones with overlying fresh water aquifers, movement of the highly conductive injected fluids into the overlying fresh water aquifers could create a conductive electrical target which contrasts sharply with the surrounding material. In such cases, electrical methods may indeed be useful in detecting and mapping the contaminated zones.

The important criteria for evaluating the applicability of various electrical methods to exploration objectives are the practical depth of exploration, lateral resolution, vertical resolution, sensitivity to geologic noise, and survey productivity.

For cases where conductive contamination lies very near the surface (<30 meters depth), continuous, frequency-domain electromagnetic induction is likely to be useful in mapping the areal extent of the brines. D.C. resistivity may be successful at slightly greater depths, although cultural interferences (power lines, pipelines, fences) are likely to cause problems. Neither of these methods are likely to produce useful information at depths approaching a typical injection horizon (thousands of meters).

Because of its relative insensitivity to near-surface geological noise and its ability to achieve substantial depths of exploration with relatively small loop arrays, time-domain electromagnetic induction (TDEM) appears to offer the greatest chance of success of the methods discussed here at depths approaching injection horizons. However, even TDEM will need a relatively large conductivity contrast (factor of 2 or greater) between the target and surrounding background to do successful mapping. To be detectable, the target must have lateral dimensions which are a substantial fraction of the depth of exploration; mapping requires targets which have dimensions greater than the depth of exploration.

iii

CONTENTS

CONTENTS (Continued)

FIGURES

SURFACE-BASED ELECTRICAL SURVEYS FOR INJECTION-WELL FLUIDS

I. INTRODUCTION

1.0 Purpose and Scope of the Document

This document surveys available and potentially useful surface-based electrical geophysical methods for mapping contaminant fluids from injection wells. The goal has been to present a "snapshot in time" of the presently available technology in this field. The approach has been to survey current literature to determine the extent to which surface-based electrical geophysical methods have been used to map plumes of contaminant fluids from injection wells, and the success of these efforts to date. Emphasis has been placed on the definition of the problem: injection wells and injected fluids as electrical targets.

In 1974, Congress mandated the EPA (Safe Drinking Water Act, Part C) to promulgate regulations to protect underground sources of drinking water (USDW's) from improper injection practices. As a response, injection wells were regulated by EPA in 1980 in the Underground Injection Control Regulations which today are codified in 40 CFR, Parts 124, 144, 145, 146, and 147. Because injection takes place at depths of hundreds or thousands of feet below the surface, direct monitoring of injected fluid movement has usually been difficult or impossible. The construction of monitoring wells for the purpose would be very expensive, and such monitoring wells would themselves present potential conduits for undesirable fluid movement. Monitoring of the injection process is usually limited to such data as injection pressures and volumes and the chemical characteristics of the injected fluids. Some investigators have also used nearby wells to measure changes in pore pressure as injection occurs. Monitoring wells in surficial aquifers have also been used. Electrical geophysical measurements at the surface have also been suggested as a possible means of monitoring injected fluid movement; surface-based electrical measurements, if feasible, would be much less expensive than the construction of monitoring wells. The feasibility of electrical measurements is still unresolved as of the preparation of this document.

To help understand the kinds of ground-water contamination problems which can be created by injection wells and the potential uses of surface-based electrical geophysical methods in mapping these problems, background material is presented on the Underground Injection Control Regulations; on the types, numbers, and geographical distribution of injection wells; on the volumes and chemical/electrical characteritics of injected fluids; on pathways of migration for injected fluids; and on injected fluids as electrical targets. With this background, the

1

surface-based electrical geophysical technology currently available for monitoring injected fluids is reviewed.

2.0 UIC Regulations

Underground injection began to be widely used about 50 years ago in secondary petroleum recovery. In the 1930's underground injection became a common alternative to surface disposal of produced brines from petroleum wells. Disposal of industrial wastes began in the 1950's as a method to isolate difficult-to-treat wastes by placing them into deep formations where they would presumably remain through geologic time. Construction of injection wells grew rapidly. EPA estimated the total number of injection wells for all purposes at 500,000 in 1979; an inventory in 1984 placed the total number at approximately 246,000, with oil and gas secondary recovery operations accounting for about 167,000, roughly 68 percent of the total.

Hydrogeologic concepts behind the process are simple. In several areas of the United States, the basement rock is covered by up to 20,000 feet of sedimentary rocks, which have been deposited over millions of years and have remained relatively undisturbed. These rocks were stratified as they were deposited, and the strata vary widely in composition, structure, permeability, and porosity. They also contain water whose quality varies considerably with depth. Generally, the total dissolved solids (TDS) concentrations increase with depth. To place TDS concentrations in perspective, the health-based national (secondary) drinking water standard for TDS is 500 mg/l; California classes waters with TDS > 2100 mg/l as "unsuitable under most conditions" for irrigation (McKee, 1963). The Underground Injection Control Regulations protect ground water with TDS < 10,000 mg/l since such water could conceivably be rendered potable through treatment. Seawater usually has TDS of about 35,000 mg/l. In comparison, brines associated with oil and gas production generally contain 30,000 to 100,000 mg/l TDS. The fact that there are large differences between the composition of surficial and deep water indicates that the various impermeable strata act as barriers to the upward movement of the deep saline water. Sedimentary rocks with adequate permeability, thickness, depth, and areal extent provide the most satisfactory injection zones. The location of such thick sedimentary sequences is one important factor in determining where deep well injection can occur.

The engineering of injection wells was based on oil-field technology and was further developed by industrial firms to dispose of specific waste streams. A typical injection well is several thousand feet deep and injects wastes directly into highly saline permeable injection zones. As shown schematically in Figure 1.1, the well consists of concentric pipes. The outer pipe or surface casing ideally extends below the base of any USDW and is cemented back to the surface. Two pipes extend to the injection zone, the long string casing which is also usually cemented back to the surface, and the injection tubing, placed within the long string. Waste is injected through the tubing and perforations in the bottom of the long-string casing. The space between the tubing and the casing (called the annulus) is closed off at the bottom by a device called a packer, which keeps injected fluids from backing up into the annulus. This annular space

Gauge on injection tubing

Gauge on tubing-casing annulus

Water table

Land surface

Surface casing ▶ Surficial aquifer (USDW)

400 Feet

800

Annulus ▶
(positive pressure) Confined aquifer (USDW)

1200

Cement ▶
Long-string
casing ▶ Saline aquifer >10,000 TDS

1600

2000

Saline aquifer <30,000 TDS

2400

Injection tubing ▶

2800

Confining zone

3200

Packer ▶

3600

Perforations ▶

4000

Injection zone >30,000 TDS

4400

Figure 1.1. Ideal injection well and site.

3

is typically filled with an inert, pressurized fluid. The inert fluid is kept at a higher pressure than the injection pressure in the tubing to prevent escape of the waste into the annulus if a leak should occur. Capping the well is the well head, which contains valves and gauges to control and to monitor injection.

Underground injection came under Federal control in 1974 with the enactment of the Safe Drinking Water Act; Part C of the Act established the Underground Injection Control (UIC) Program to protect underground sources of drinking water (USDW's). The law required the Environmental Protection Agency to establish minimum standards and technical requirements which the States were to adopt before assuming primary enforcement responsibility. (primacy). The UIC regulations which were adopted in 1980 have the following chief provisions:

- They defined underground sources of drinking water (USDW's) as the resource to be protected; the definition includes all aquifers containing water with less than 10,000 mg/l TDS.

- They categorize injection wells into five classes:

Class I wells inject hazardous and non-hazardous waste below the deepest USDW.

Class II wells are associated with oil and gas production and with hydrocarbon storage and comprise the majority of all U.S. injection wells.

Class III includes special process wells used in conjunction with solution mining of minerals, in situ gasification of oil shale, coal, etc.

Class IV wells inject hazardous wastes into or above USDW's. These wells were banned by the 1984 amendments to the Resource Conservation and Recovery Act of 1976 (RCRA), Section 7010, and by the UIC regulations (40 CFR, Part 144.13).

Class V wells are non-hazardous waste injection wells that do not fit into the other four classifications: recharge wells, air conditioner return flow wells, drainage wells, etc.

- Minimum technical requirements were established to ensure that injected fluids will go into the proper horizon and remain there.

The technical requirements include the following:

- siting in areas which are free of faults and abandoned wells and which possess adequate confining zones;

- construction requirements for casings, tubing and packer, cementing, logging, and testing;

4

-       <u>operation</u> to prevent fracturing of the injection zone;

-       <u>monitoring</u> which includes periodic testing of the integrity of the well and reporting; and

-       <u>plugging and abandonment</u> procedures which include demonstration of financial responsibility.

For a State to have a federally-approved UIC program and to assume primacy, it must meet minimum regulatory standards. The 1980 amendments to the SDWA created Section 1425. States can be delegated primary responsibility for oil and gas injection wells if they can show that their program is effective in protecting USDW's and includes permitting, surveillance, reporting, and enforcement. The EPA oversees State programs to ensure that the standards are implemented. EPA has to follow the same standards in States where the Agency implements the UIC program. As of January 9, 1987, 33 States had been approved for full primacy and 6 for partial primacy. EPA is implementing a full program for 18 States and a partial program in 6.

3.0 Injection Wells

3.1 Numbers and Types of Injection Wells

In 1983 the EPA conducted a nationwide inventory of injection wells, utilizing a computerized system called FURS (Federal UIC Reporting System). FURS contains data on owner, operator, location, well status, general comments, date of construction or conversion, volume injected, injection pressure, and construction features. As of November 1983, the total number of injection wells in the inventory was approximately 240,000; this figure included wells in the U.S. territories of Puerto Rico, the Virgin Islands, Guam, the Pacific Islands Trust Territory, and American Samoa. For the purposes of this report, only wells in the 50 states will be discussed. Table 1.1 summarizes the results of this inventory, showing the number of injection wells known to FURS as of November 1983 by class and EPA region for the 50 United States (Fairchild, 1984). Regions VI, VII, and V had the largest numbers of wells in this inventory and have had the largest numbers historically (Fairchild, 1984). Appendix 1 presents a table of the distribution of injection wells by class, State, and EPA region. Figures 1.2, 1.3, and 1.4 graphically summarize the data in Appendix 1. Figure 1.2 shows that EPA Regions V, VI, and VII together contained 70 percent of the approximately 246,000 injection wells in the 1983 EPA inventory. Figure 1.3 shows that 6 states--Texas, Kansas, Pennsylvania, Illinois, Oklahoma, and California--together contained about 73 percent of the national total. Figure 1.4 shows that the most numerous well types nationwide were Class 2 (68 percent of the total), Class 5 (19 percent), and Class 3 (14 percent). However, the contributions of the different well types to the totals vary considerably in individual states, as shown by Figures 1.5 and 1.6. Figure 1.5 shows oil and gas injection wells (Class 2-60 percent) and solution mining wells (Class 3-39 percent) predominating in Texas. Figure 1.6 shows

Table 1.1. 1984 EPA INJECTION WELL INVENTORY

EPA REGION	Class I	Class II	Class III	Class IV	Class V	Regional Totals
I	0	0	0	0	0	302
II	23	3859	249	0	3651	7782
III	12	4444	41	17	18827	23341
IV	127	5936	10	20	5149	11242
V	129	27395	112	0	6001	33637
VI	264	71195	31080	1	595	103135
VII	59	31323	394	0	1978	33754
VIII	5	7943	991	2	24	8965
XI	39	14374	490	27	43	14973
X	1	161	0	11	9114	9287
Totals	659	166630	33367	78	45684	246418
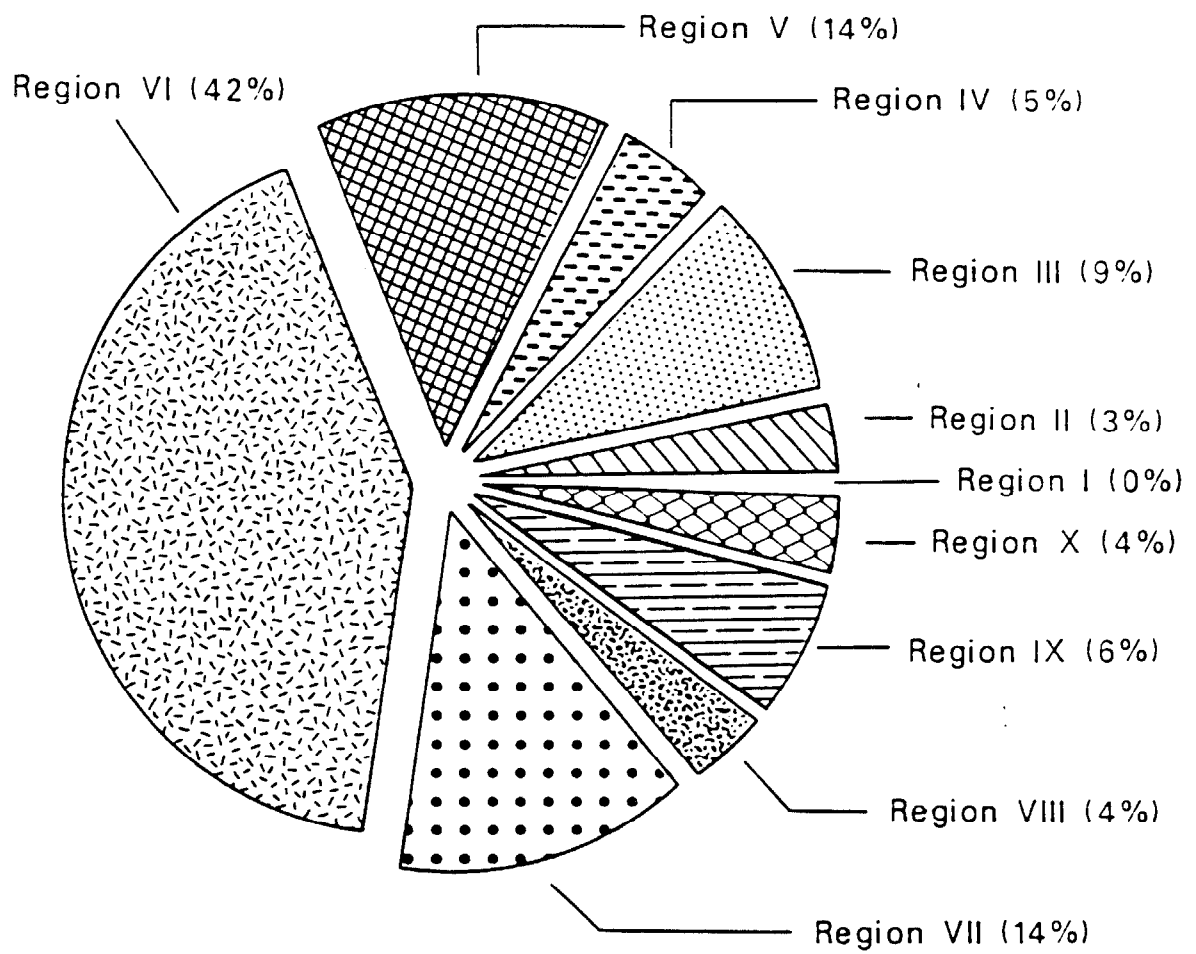
Figure 1.2. Injection well totals by EPA region.

7
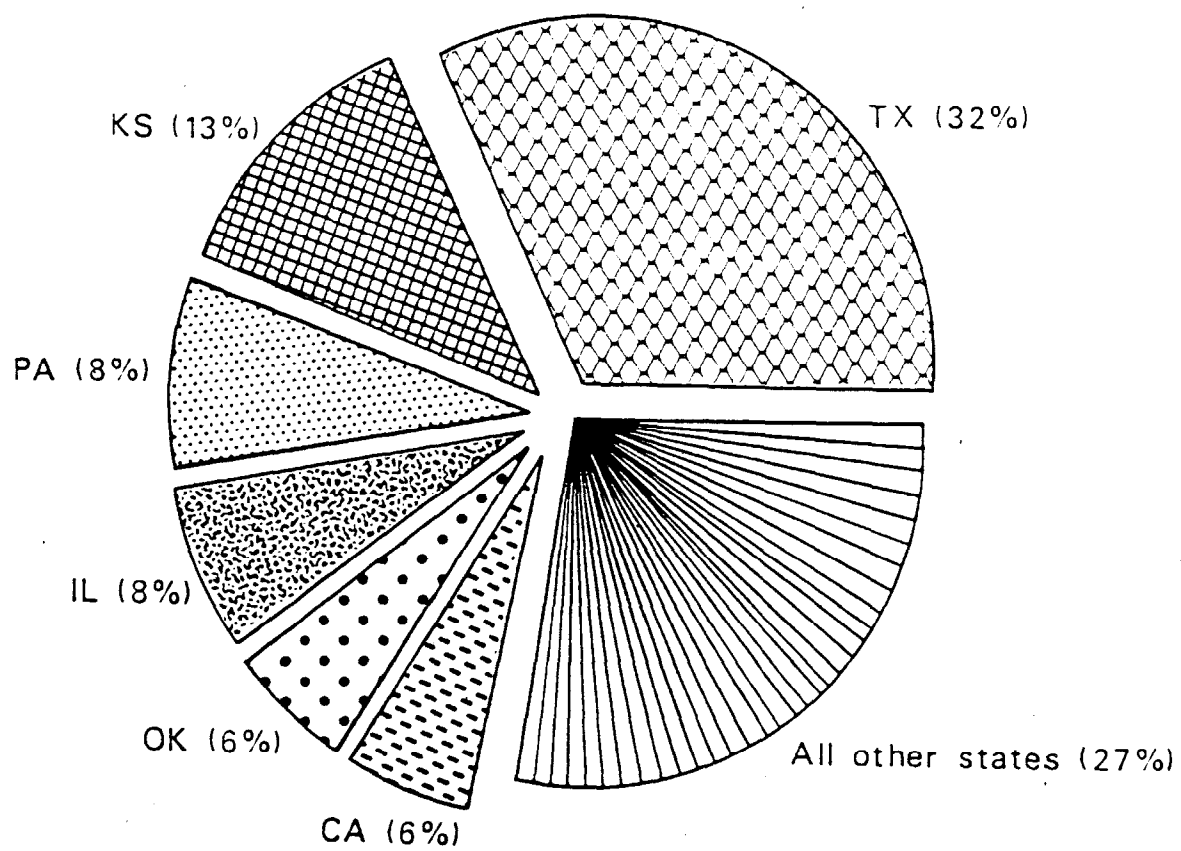
Figure 1.3. Injection well totals by state.

Class 2 (65%)

Class 1 (< 1%)

Class 5 (19%)

Class 4 (< 1%)

Class 3 (14%)
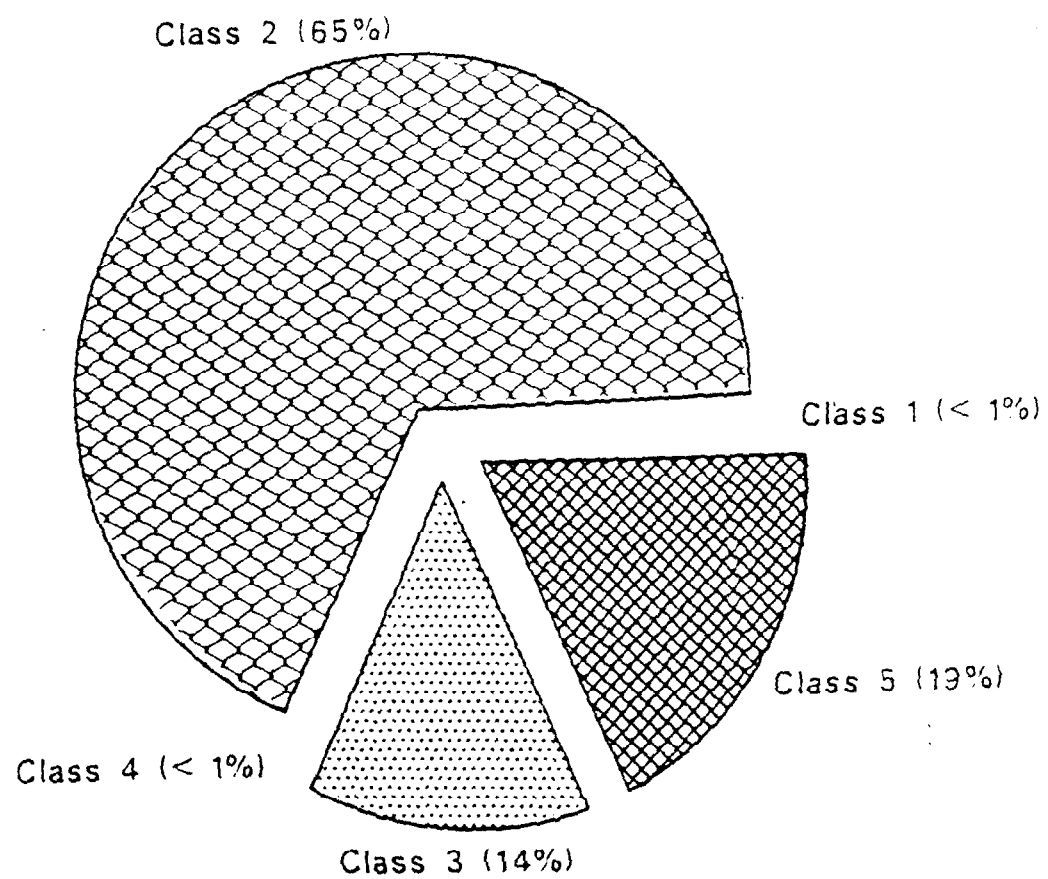
Figure 1.4. Injection well totals by well type.

9

Class II (60%)

Class I,IV,V
(< 1%)

Class III (39%)
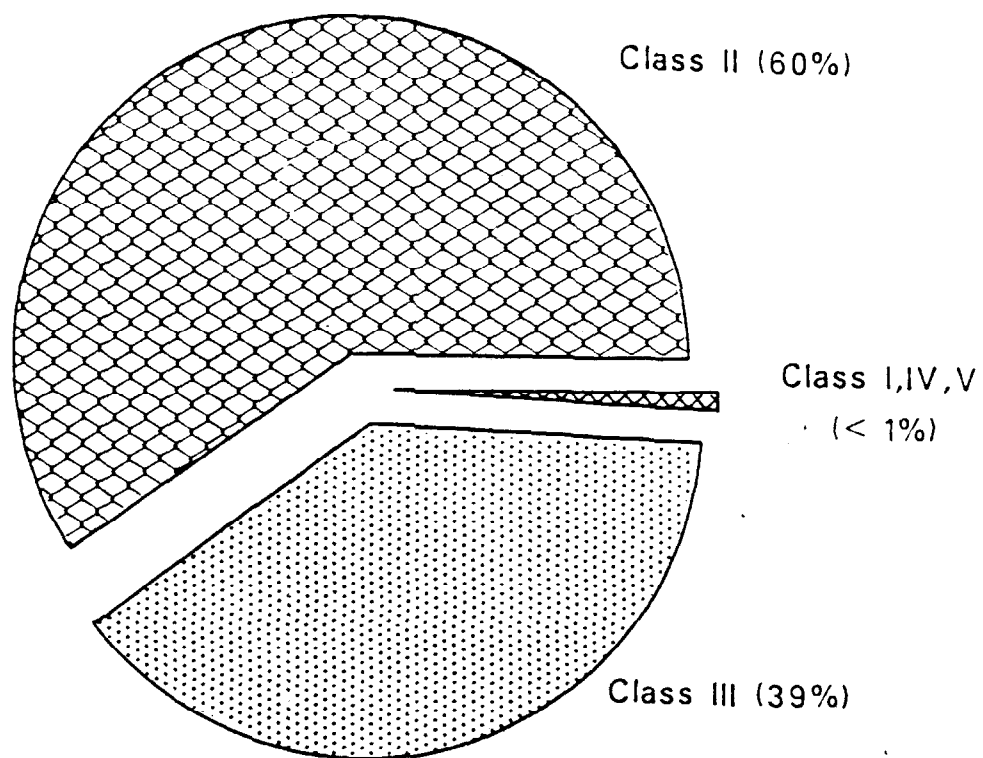
Figure 1.5. Texas injection wells by well type.

10
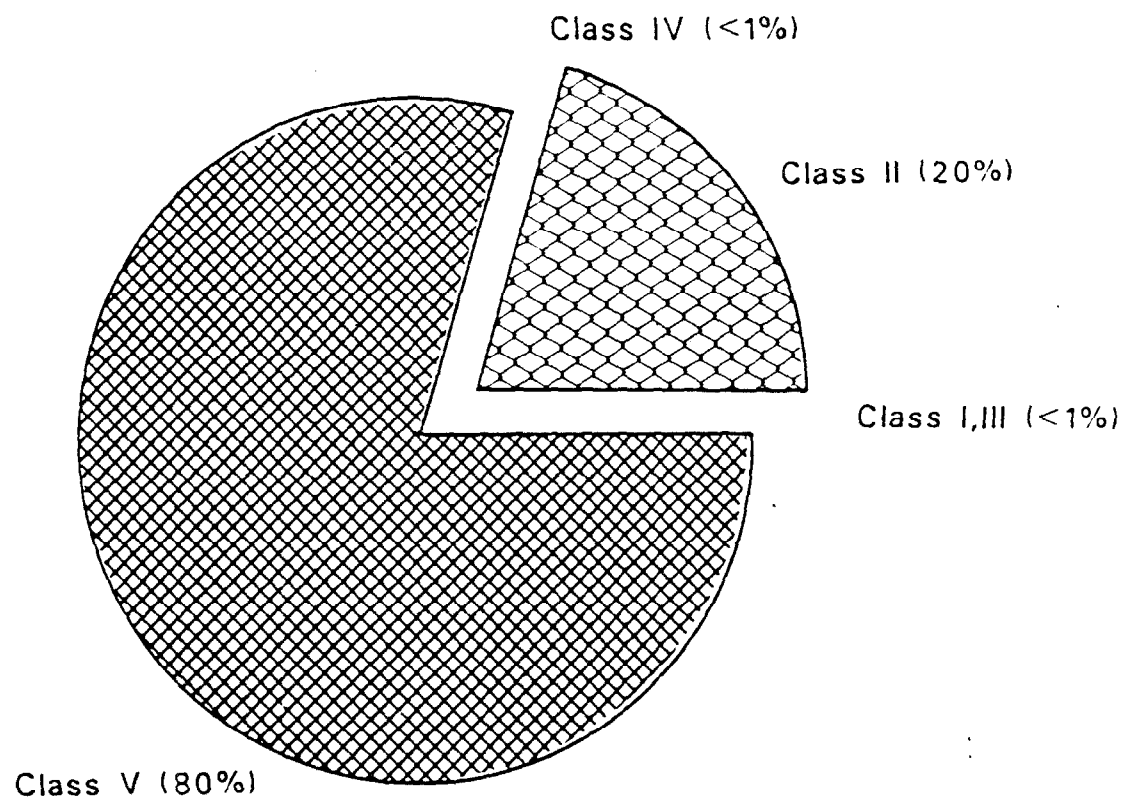
Figure 1.6. Pennsylvania injection wells by well type.

20 percent of the Pennsylvania state total in oil and gas injection wells and 80 percent in Class 5 ("other").

The numbers in the 1983 EPA inventory should be regarded as preliminary and indicative only of the relative geographic distribution and the relative numbers of wells in the various classes. For example, Table 1.1 (from the 1983 inventory) shows a nationwide total of 670 Class 1 (waste disposal) wells; in a May 1985 report to Congress on injection of hazardous waste, EPA identified 252 existing Class 1 wells (EPA, 1985). In particular, the numbers of Class 5 wells in the 1983 survey are suspect since the various states had not yet completed their own inventories of Class 5.

3.2 Geologic and Chemical Characteristics

3.2.1 Available Information

Fairchild (1984) reviewed available information on injection wells in 1984 and concluded that nationwide characteristics for the five classes of injection wells could not be identified. One reason is the lack of information; comprehensive data collection on injection well numbers, uses, and characteristics did not begin until the late 1960's. Organized data for Class II wells is probably most complete; state files contain considerable information on Class I wells particularly on their operation and maintenance, but such data are not readily accessible. Data on Class III wells are scarce because such wells are few in number, many are experimental, and their data are regarded as proprietary. Since states were not required to inventory and assess Class V wells until 3 years after achieving primacy, data on their numbers and characteristics are nearly nonexistent.

Completeness of available information depends on the particular characteristic of interest. Much has been published about recommended or proper injection well construction, but there are relatively few published case studies of actual installations for each of the five classes. Data on general waste characteristics are available for particular industries, and chemical analyses of injected wastes can be found in state files. The literature contains little geological information except on large scales. Applications approved under the UIC program contain limited hydrological information such as location and depth of water wells, monitoring wells, piezometric gradients, and depth to the base of fresh water.

3.2.2 Hydrogeology

As mentioned above, the literature contains several discussions of recommended injection well construction practices but relatively little about actual case studies. The recent report made by the EPA to Congress on Class I wells summarizes characteristics of 252 waste disposal wells (EPA, 1985). Fairchild (1984) summarized available information on wells of all types. Rocks are generally classified by their origin as igneous, metamorphic, or sedimentary. While nearly all rock types may occasionally have the proper engineering characteristics to serve as injection zones,

12

sedimentary rocks are most likely to have sufficient porosity, permeability, thickness, and areal extent to permit the rock to act as a liquid storage reservoir at safe injection pressures. Sedimentary rocks with sufficient porosity and permeability to accept relatively large volumes of fluids in the unfractured state include sandstones, limestones, and dolomites. Naturally fractured limestones and shales may provide satisfactory injection horizons, since oil and gas are commonly produced from such strata. Impermeable confining strata must overlie and underlie the injection zone to prevent the vertical migration of injected fluids. Unfractured shale, clay, salt, anhydrite, gypsum, marl, and bentonite often provide good seals against the upward flow of oil and gas. Most sedimentary rocks with appropriate characteristics for injection wells were deposited in marine environments and contain saline water at depths below the present level of fresh water circulation.

Folding and fracturing of sedimentary strata must also be considered in the evaluation of an injection well site. Structural geology on both the regional and local scale influences subsurface liquid flow, the engineering properties of rocks, the location and distribution of minerals, and earthquakes. Simple folds are either synclines (downward folds) or anticlines (upward folds). Synclinal basins are particularly attractive as injection well sites because they contain relatively thick sequences of saltwater bearing sedimentary rocks, and because the subsurface geology of these basins is usually well-known from oil and gas exploration.

3.2.3   Hydrogeology of Class I Wells

The EPA 1985 report to Congress on hazardous waste disposal with injection wells summarized the pertinent geologic characteristics of 252 Class I wells (EPA, 1985); summaries of this information are given in Appendices 2 and 3. The EPA found that, nationwide, most of the injection wells are constructed to inject wastes into sand and sandstone formations (76 percent); fewer are constructed to inject into limestone or dolomite formations (14.3 percent) and sandstone shale formations (9.7 percent). The EPA found that the most common confining zones were composed of shale (42.7 percent), sandstone shale (20.8 percent) and limestone shale (10.0 percent). The rest of the confining zones (for the 252 Class I wells) are composed of silt, clay, dolomite, and other impermeable materials.

The greatest concentrations of Class I wells are found in the Great Lakes and Gulf Coast areas. The EPA found that Class I injection wells in the Great Lakes vicinity typically inject into the Mt. Simon sandstones with an average thickness of about 600 feet or into dolomite at an average depth of about 2,500 feet. In the Great Lakes area, confining zones of shale with some limestones, dolomite, or siltstone average about 630 feet thick. The average separation between the lowermost USDW and the injection zone in the Great Lakes was found to be about 2,300 feet (EPA, 1985). Figure 1.7 shows these average Great Lakes Class I injection well regional characteristics in an idealized cross-section.

13
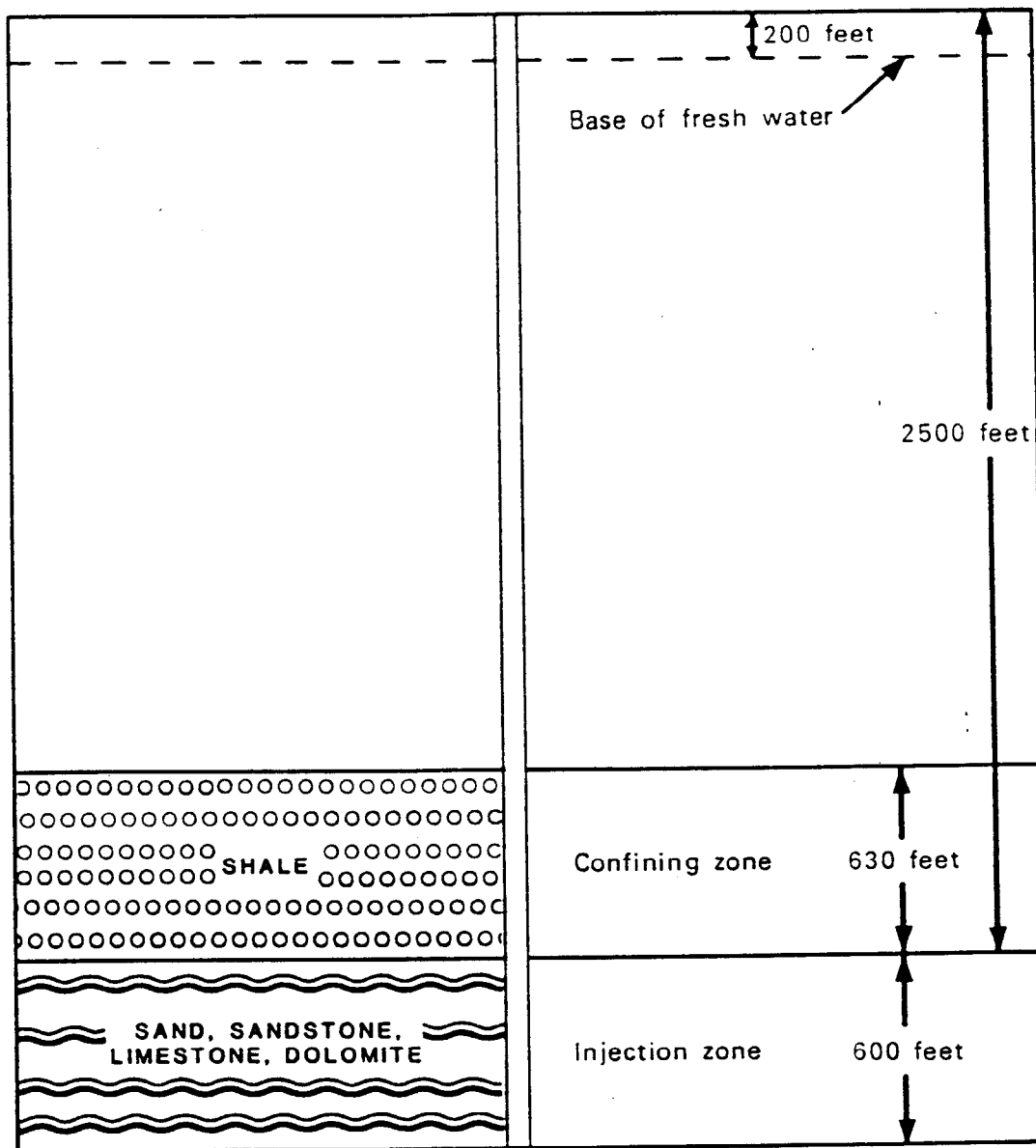
Figure 1.7. Average hydrogeological characteristics of Class I injection wells in the Great Lakes region.

In the Gulf Coast area, the injection zones were typically sand or sandstone averaging about 500 feet thick and lying at an average depth of about 4,600 feet. The Gulf Coast confining zones were mainly shale with some marl or clay and averaged about 1,000 feet thick. The average separation between the lowermost USDW and the injection zone is about 3,300 feet in the Gulf Coast (EPA, 1985). Figure 1.8 shows the average Gulf Coast Class I injection well characteristics as an idealized cross-section.

The EPA found a nationwide average for Class I injection well thicknesses of about 560 feet, under a confining zone with an average thickness of about 930 feet. The nationwide average depth to the top of the injection zone was about 4,100 feet, and the nationwide average separation of the lowermost USDW from the top of the injection zone was about 2,900 feet (EPA, 1985). Table 1.2 summarizes the Class I hydrogeological characteristics for the Great Lakes and Gulf Coast regions and the nationwide (by well) averages.

3.2.4   Hydrogeology of Class II Wells

About 68 percent of all injection wells fall into Class II, as indicated by Figure 1.4. Class II includes wells injecting fluids (1) brought to the surface in the process of conventional oil or natural gas production; (2) to enhance recovery of oil or natural gas; or (3) for storage of hydrocarbons which are liquids at STP. Because of the large numbers of Class II wells (over 166,000), they probably constitute the most important injection category in terms of their impact on groundwater and USDW's. In a 1974 EPA national survey, Keely (Scalf, 1983) ranked Class II brine injection wells as the sixth and seventh worst causes of ground-water pollution in the northwest and southeast, respectively (Scalf et al, 1973). In a 1980 prioritized listing, EPA ranked petroleum exploration and development as the second worst specific source of ground-water contamination in the U.S. (Miller, 1980).

Perhaps because of the large numbers of Class II wells, national summary statistics of their hydrogeological characteristics are not available in the literature. While these data are probably available in State and petroleum company files, compilation of summary statistics would be a very large task. Fairchild was unable to present nationwide statistics in her survey (Fairchild, 1984). She did describe practices in several wellfields across the country. In most Class II wells, fluids are injected into the "pay zones" of producing fields. In general, such practices occur or will occur in most (if not all) petroleum and natural gas producing fields in the country. In many cases, fields which are exhausted or nearly exhausted are used for storage of gas or petroleum products produced elsewhere. In her 1984 summary, Fairchild describes a gas storage operation in the Richfield formation in Upper Peninsula Michigan; the Richfield had been a producing formation in previous years.

15
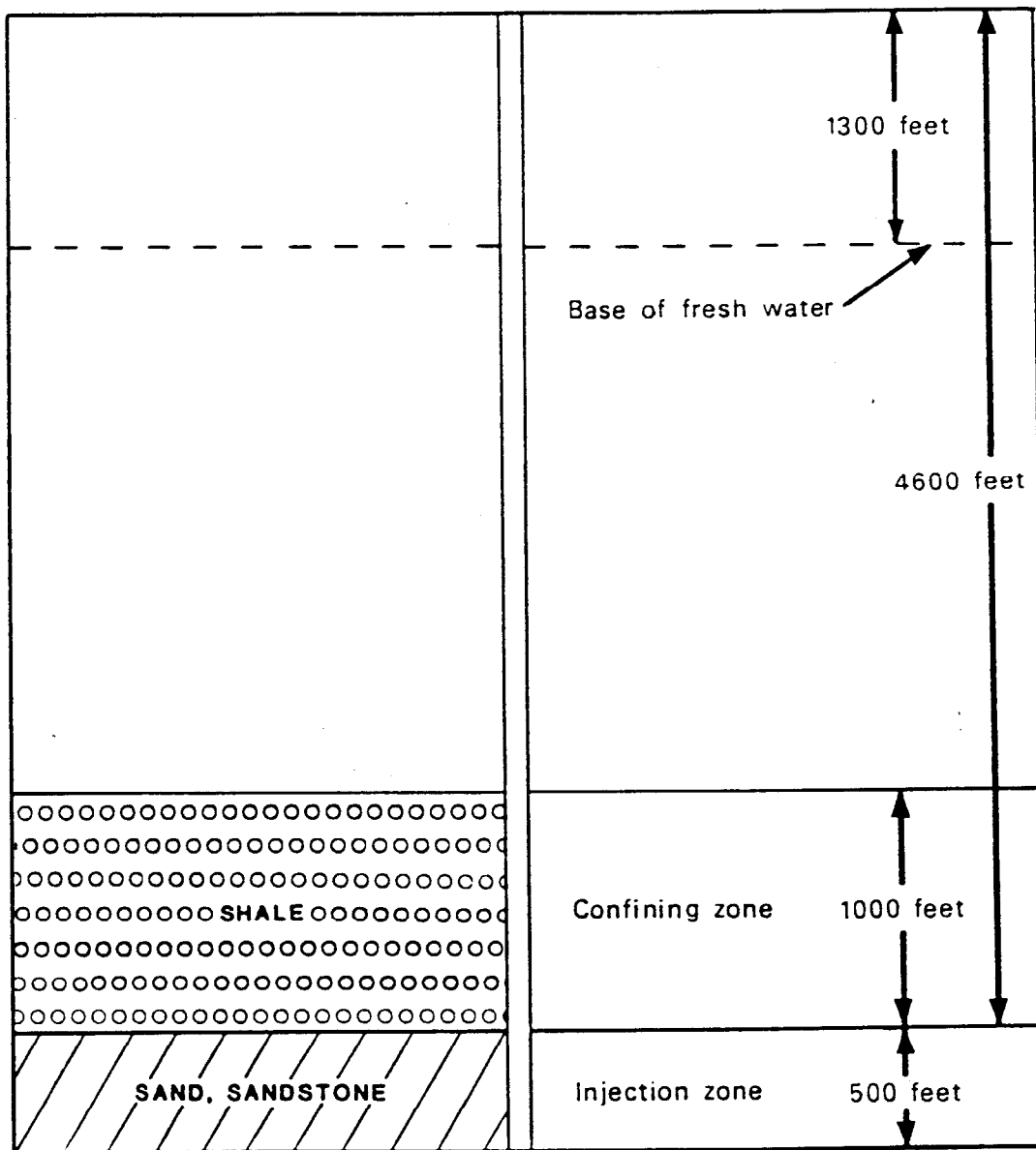
Figure 1.8. Average hydrogeological characteristics of Class I injection wells in the Gulf Coast region.

16

TABLE 1.2. HYDROGEOLOGICAL CHARACTERISTICS OF CLASS I INJECTION WELLS

Characteristic	Great Lakes Region	Gulf Coast Region	Nationwide Average by well
Principal Injection zone	Sand, sandstone; limestone, dolomite	Sand, sandstone	
Injection zone thickness (ft)	600	500	560
Injection zone depths (ft)	2500	4600	4100
Principal confining zone rock types	Shale	Shale	
Confining zone thickness (ft)	630	1000	930
Separation from lowermost USDW	2300	3300	2900

Table 1.3 presents hydrogeologic characteristics from some of the cases described in Fairchild's summary. In the absence of summary statistics for Class II injection well hydrogeology, Table 1.3 will be assumed to be generally representative of characteristics found nationally.

3.3 Volumes and Characteristics of Injected Fluids

3.3.1 Class I Wells: Injected Fluids

The EPA compiled data on waste characteristics of 108 hazardous waste injection wells for the year 1983 (EPA, 1985). Utilizing their annual flow volumes and waste concentrations, the EPA found that during 1983 the 108 wells disposed of 228,021,900 gallons of non-aqueous waste with 6.2 billion gallons of water. These figures would yield an average dissolved solids concentration of about 35,500 mg/l, with an average injected volume of about 59 million gallons per well. The composition of this waste is given in Table 1.4. Table 1.5 lists the individual waste components classified as either acids, heavy metals, organics, or hazardous inorganics.

3.3.2 Class II Wells: Injected Fluids

Class II wells used for brine disposal constitute a large percentage of all disposal wells. In 1970, 3.5 billion barrels of oil were produced in the United States, and most of the associated brine was reinjected through approximately 7,400 saltwater disposal wells. Half of these wells were in Texas, and another 1,500 existed in Oklahoma (Scalf et al., 1973). For 1980, it was estimated that 11 billion barrels of brine (equivalent to 140,000,000 tons of salt) would be injected back into the ground (Miller, 1980). (This corresponds to an approximate average brine concentration of 55,000 to 60,000 mg/l.)

From a water pollution standpoint, brine waters are of concern because of the presence of dissolved ions. Those dissolved ions which are most commonly present in greater than trace amounts are sodium, calcium, magnesium, potassium, barium, strontium, ferrous iron, ferric iron, chloride, sulfate, sulfide, bromide, and bicarbonate. Dissolved gases in these waters often include carbon dioxide, hydrogen sulfide, and methane (Collins, 1974). The chlorides of sodium, calcium, and magnesium comprise 95 percent or more of the dissolved salts in most brines. Table 1.6 contains a summary of some brine analyses from various locations in the United States. An analysis of ocean waters is included for purposes of comparison (EPA, 1977). Brine waters from different strata vary considerably in their dissolved chemical constituents, and this makes difficult the identification of a water from a particular strata. As some petroleum wells become older, the produced fluids may be more than 99 percent brine. Produced brines differ in concentration but usually consist primarily of sodium chloride in concentrations ranging from 5,000 to 400,000 mg/l and averaging 50,000 mg/l, 2.5 times the NaCl concentration in seawater.

TABLE 1.3. HYDROGEOLOGICAL CHARACTERISTICS OF CLASS II INJECTION WELLS

Characteristic	Pennsylvania	Michigan gas storage	Michigan Oil Production	Oklahoma saltwater disposal % waterflood well (Anadarko "A" No. 1)
Principal injection zone rock types	Devonian sands	Stray sandstone (Mississippian)	Richfield formation (dolomite pay zones)	Runnymede silt
Injection zone thickness (ft)		12	12	67
Injection zone depths (ft)	600 to 2000	1300	4613	1407
Principal confining zone rock types	Shale	Gypsum, limestone		Shale
Confining zone thickness (ft)				1000
Separation from lowermost USDW				

19

TABLE 1.4. WASTE CHARACTERISTICS OF 108 CLASS I INJECTION
ACTIVE IN 1983 IN THE UNITED STATES
(EPA 1985)

Waste type	Gallons	Percent of total gallons	Pounds	Well count
Acids	44140900	20.26	367250000	35
Heavy metals	1517600	.7	12626100	19
Organics	39674500	17.4	330090000	17
Hazardous organics	89600	.04	745800	4
Non-hazardous organics	118679700	52.04	987410000	50
Other	22964600	9.91	191070000	33
Total (non-aqueous)	227066900	100.35	1889191900	

Actual total   228021900
(minus overlaps, e.g. "organic acids")

TABLE 1.5.   HAZARDOUS WASTE STREAM COMPONENTS AND CONCENTRATIONS
IN CLASS I INJECTION WELLS IN THE UNITED STATES IN 1983

Waste stream type	Waste components	Incidence of injection by wells	Average concentration (ag/l)
Acids	Hydrochloric acid	15	78573
	Sulfuric acid	6	43000
	Nitric acid	2	75000
	Formic acid	2	75000
	Acid, unspecified	12	44900
Heavy metals	Chromium	11	1.4
	Nickel	5	600
	Metals, unspecified	2	5500
	Metal hydroxides, unspecified	1	1000
Organics	Total organic carbon (TOC)	24	11413
	Phenol	22	805
	Oil	6	3062
	Organic acids	3	10000
	Isopropyl alcohol	3	1775
	Organic cyanide	3	400
	Formaldehyde	2	15000
	Acteophenone	2	650
	Urea "N"	2	1250
	Chlorinated organis	2	35000
	Formic acid	2	75000
	Organic peroxides	2	4950
	Pentachlorophenol	2	7.6
	Acetone	2	650
	Nitrile	1	700
	Methacrylonitrile	1	22
	Ethylene chloride	1	970
Hazardous	Selenium	2	.3
Organics	Cyanide	2	391

TABLE 1.6. ANALYSES OF OIL FIELD BRINES (in ppm)

Field	Formation	Chloride	Sulfate	Car-bonate	Bicar-bonate	Sodium	Potassium*	Calcium	Mag-nesium	Misc.	Total
Kawkawlin MI	Dundee limestone	161,200	155	-	60	66,280	-	25,740	4,670		258,105
Seminole OK	Wilcox sand	89,990	515	-	65	44,020	-	9,460	1,990		146,060
Glenn OK	Arbuckle limestone	101,715	120	-	60	50,345	-	10,160	2,120		164,520
Nikkel KA	Hunton limestone	76,797	207	-	61	40,284	-	5,440	1,790		124,579
Yates TX	Sanandres dolomite	2,518	2,135	-	-	1,624	-	587	288		7,445
Monument NM	Grayburg limestone	6,630	160	-	1,740	3,735	-	515	365		13,145
Shelby MT	Madison limestone	1,179	659	71	1,270	1,322	-	143	66		3,388
Frannie Dome WY	Tensleep sand	27	2,303	0	691	51	-	760	240		4,022
Grass Creek WY	Frontier sand	256	6	1,211	-	1,087	-	5	2		2,565
Edison CA	Upper Duff sand	79	4	29	648	299	-	17	1		962
Ventura Ave. CA	Pico Repetto sand	14,212	59	-	1,846	8,607	-	729	242		26,091

22

(Continued)

TABLE 1.6. ANALYSES OF OIL FIELD BRINES (in ppm)

Field	Formation	Chloride	Sulfate	Car-bonate	Bicar-bonate	Sodium	Potassium*	Calcium	Mag-nesium	Misc.	Total
Bay City MI	Salina dolomite	403,207	0	-	1,208	21	-	206,300	7,300		642,798
Sharon PA	Berea sand	6,740	0	0	250	-	3,440*	700	160		11,290
Evans City PA	3d Venango sand	88,820	180	0	40	-	38,660*	13,790	2,220		143,710
Bell Run WV	Salt sand	64,930	0	0	90	-	30,450*	7,580	1,620		104,670
Reed City MI	Marston dolomite	156,225	265	-	20	59,080	-	28,440	5,155		249,185
Burbank OK	Bartlesville sand	107,895	-	-	35	50,000	-	14,340	1,875		174,145
East Texas TX	Woodbine sand	40,958	278	-	569	-	24,540*	1,388	282		67,649
Ventura CA	Pico-Re-petto sand	14,212	59	-	1,846	8,607	-	729	242	NH3:66; SI:170; Fe,Al:160	26,091
Fruitvale CA	Fairhaven sand	245	11	60	2,235	-	1,024*	8	10		3,593
Ocean Waters (mean)	-	19,410	2,700	70	-	10,710	-	420	1,300		35,000

*In most brine analyses Na and K are determined together and reported as Na. For those cases, however, where the alkali content was listed as Na + K, the values are tabulated between the Na and K columns. A similar uncertainty exists in the case of some of the reported values of CO_3 and HCO_3 concentrations.

Brine disposal wells in oil fields range considerably in injection rate and depth. Injection pressures vary from a vacuum to 2,000 psi, and flow rates range from 35 to 150 gpm per well. One well in the Arbuckle formation is reported to have taken water at an average rate of 17,730 barrels per day (750,000 gpd) for periods of 600 days. If the operation is one of combined discharge-recharge, the well depth is the same as the producing oil formation. However, if it is desired to merely dispose of the brine, the well depth is dictated by the depth of the formation suitable for injection.

As an example of a salt water disposal operation, Fairchild (1984) cited the East Texas Salt Water Disposal Company of Kilgore, Texas. This company was organized in January 1942 and was subscribed to by about 250 large and small operators in the East Texas oil field. In 1958 there were 82 injection wells operating in the East Texas oil field which returned 165 million barrels to the reservoir. 60 of these wells, operated by the East Texas Salt Water Disposal Company, returned 138 million barrels of brine to the reservoir, an average of roughly 2 million barrels/year per well.

Figures 1.9 and 1.10 show schematically the significant geometrical factors for two Class II wells in Oklahoma, as given by their permit applications to the Oklahoma Corporation Commission (Fairchild, 1984). Figure 1.9 shows a Class II well injecting brine into a 67-foot thick silt formation at a depth of about 1,400 feet. In this well, the Corporation Commission limited injection pressures to 300 psi and the brine injection rates to 300 barrels/day. Brine TDS concentrations are reported as about 60,000 mg/l (95 percent NaCl). Figure 1.10 shows brine injection into a 114-foot thick lime formation at a depth of about 3,900 feet. Here injection pressures are limited in the permit to 2,000 psi, and the injection rates are limited to 2,000 barrels/day. Brine TDS concentrations are reported as about 166,000 mg/l (92 percent NaCl). In both cases, the principal confining zones are shale.

4.0 Pollutant Pathways

Some possible causes of leakage and subsequent contamination from injection well operations include: (a) corrosion of injection well casing; (b) fracturing of reservoir and confining units; (c) poor cementation between the well casing and borehole; and (d) conduits to overlying USDW's (abandoned wells and existing fractures in the confining zones). Figure 1.11 schematically depicts these various pollutant pathways and suggests the geometry of their attendant injected fluid migration.

However, in cases where wells are improperly constructed and operated or in cases in which fractures connect the injection zones with overlying fresh water aquifers, movement of the highly conductive injected fluids into the overlying fresh water aquifers could create a conductive electrical target which contrasts sharply with the surrounding material. In such cases, electrical methods may indeed be useful in detecting and mapping the contaminated zones. Unfortunately, the literature does not contain case studies delineating the actual geometries and conductivities of such contamination incidents.

SAND

SHALE AND RED BEDS

RED BED

SHALE AND SAND

SHALE

Fresh water
TDS 400 mg/l

500 feet

Base of fresh water
(10,000 mg/l TDS)

1407 feet

Injection zone
(Runneymede silt)

Injection fluid TDS
≅ 60,000 mg/l
(~ 95% NaCl)

67 feet
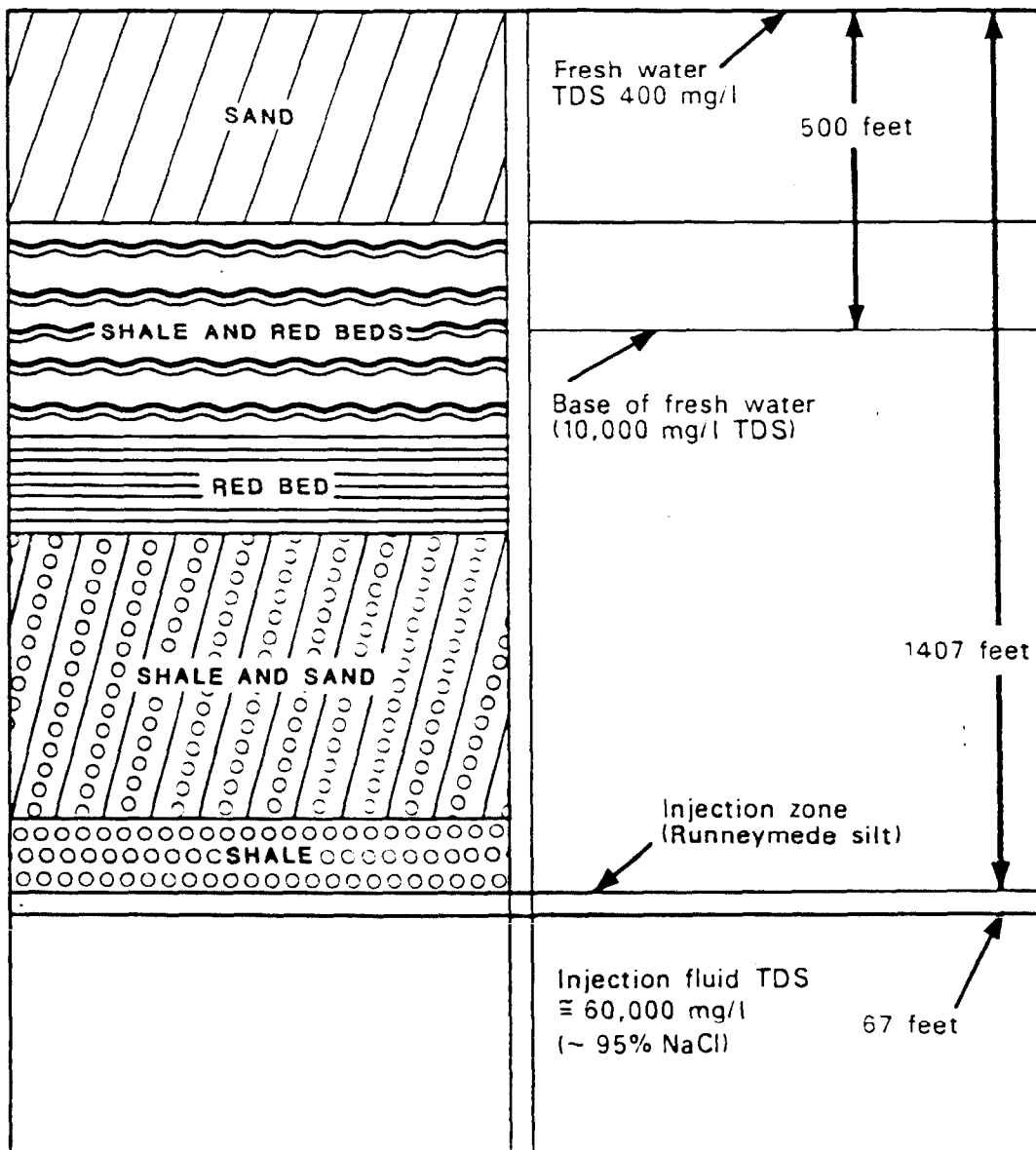
Texas county, Oklahoma

Injection pressure = 300 psig
Injection rate = 300 BWPD
Injection zone porosity = 10%

Figure 1.9.   Idealized cross-section of Anadarko Well No. "A" No. 1 (Class II injection well).

25

```
                              200 feet
       SHALE
                         Base of fresh water
                         (10,000 mg/l TDS)

                    1060

       SHALE AND SAND

                    1670                    3880 feet

       SAND AND SHALE

           SAND


       SHALE

                              Injection zone
    LIME (Hunton-Viola)

                                            114 feet
                         Injection fluid TDS
                         ≅165,984 mg/l
                         (~92% NaCl)
```
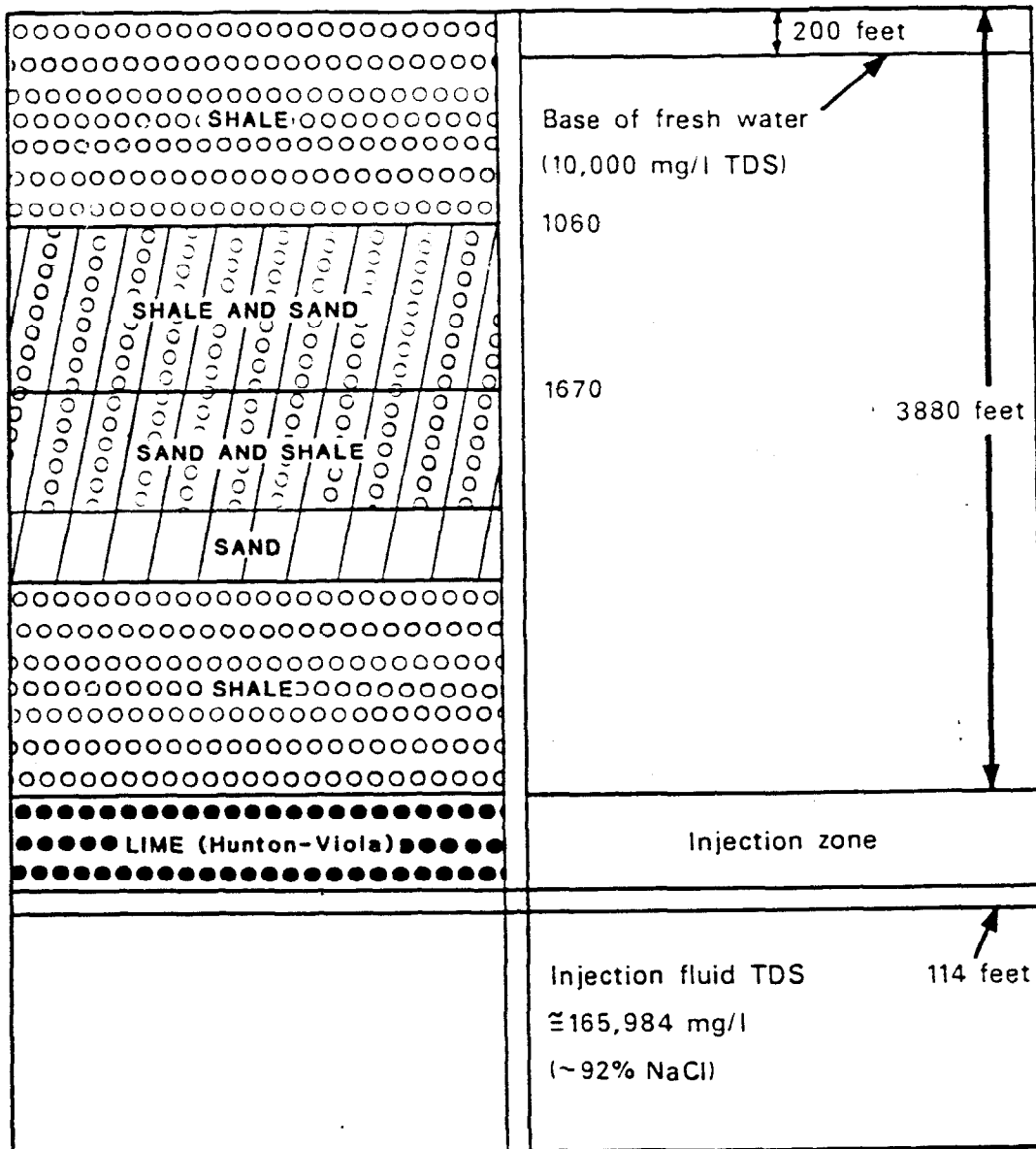
Sun well no. 6-46
Pontotoc county, Oklahoma

Max. injection pressure = 2000 psi
Max. injection rate = 2000 B/D
Injection zone porosity = 11%

Figure 1.10. Idealized cross-section of Sun Well No. 6-4L (Class II injection
              well).

26
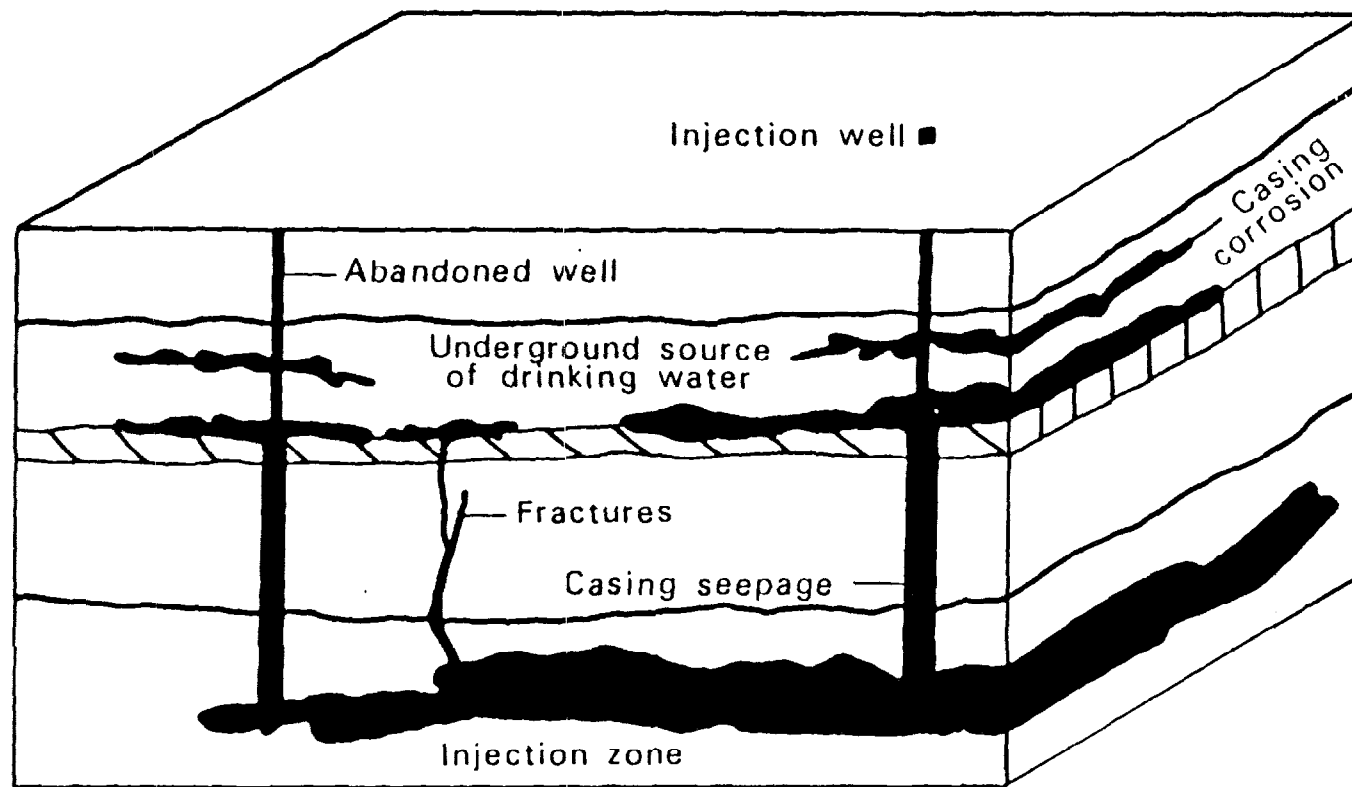
Figure 1.11.   Migration pathways for injected fluids.

II. ELECTRICAL PROPERTIES OF FLUIDS, ROCKS, AND GEOLOGIC FORMATIONS

The preceding section discussed injection wells as a water quality problem and attempted to present some general information on their hydrogeology, on the volumes and chemical properties of the injected fluids, and on the potential pathways for migration of injected fluids. To understand injected fluids as electrical targets, we now need to discuss the effects of soils, rocks, and their pore fluids on the electrical conductivity of subsurface strata.

The bulk resistivity of a rock formation depends on the resistivity of the contained fluids, the resistivity of the rock itself, and on the geometry in which the two phases coexist. In clays and shales (and in metallic mineral deposits) the rock itself is conducting. In clean aquifers (i.e., aquifers with no clay or shale component), however, the resistivity of the rock matrix (e.g., sand) is usually so large as to have no influence on the conduction of current.

Electrical resistivity is defined by Ohm's law:

$$\vec{J} = \vec{E}/\rho$$

where $\vec{J}$ is the current density in amperes/meter^2, $\vec{E}$ is the electric field in volts/meter, and ρ is the resistivity in Ohm-meters. A homogeneous material of resistivity ρ, cross-section A, and length ℓ(see diagram below) has a total resistance along its length of
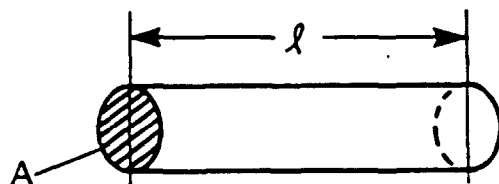
$$R = \rho\ell/A \qquad (i)$$

Now consider a non-conducting rock which has a porosity φ and whose pores are filled with a fluid of resistivity ρ_w. The current is confined to a cross-section which on average is φ A and must travel a tortuous path from one end of the cylinder through connecting pores. The more porous the material, the less tortuous the path is likely to be (see diagram below).
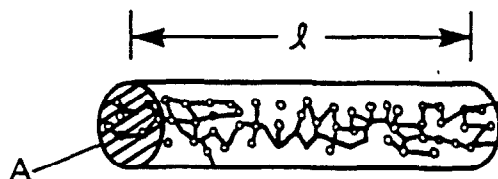
Tortuous path or current flow through connected pores, effective length ℓ_e

In this case, we can describe the relationships between the fluid resistivity, bulk aquifer resistivity, and porosity by an empirical relationship known as Archie's Law:

28

$$F = (\rho_t/\rho_w) = a/(\varphi^m) \qquad\qquad \text{(ii)}$$

where a and m are constants and F is known as the "formation factor." This equation implies that, in a clean formation with constant porosity, the bulk resistivity ρ_t (which can be measured with surface and borehole geophysical methods) is linearly related to the resistivity of the pore water. Alternatively, if the pore water is unchanged, it relates changes in bulk resistivity to changes in porosity. The exponent m is sometimes called the cementation index and has a value in the range from 1 to 3 depending on the rock type. Usually, larger values of m are associated with "tighter" rocks and low porosities (Greenhouse, 1982; McNeill, 1980).

For poorly consolidated aquifers, Archie's Law is often taken as

$$F = 0.62 \; \varphi^{-2.15} \qquad\qquad \text{(iii)}$$

The relationship between fluid resistivity and sodium chloride concentration for a range of temperatures is shown in Figure 2.1. Note that resistivity in ohm-meters is related to conductivity σ in mhos/meter by

$$\rho \; (\text{Ohm-meters}) = \frac{1}{\sigma(\text{mho/meter})} \qquad\qquad \text{(iv)}$$

If ions other than sodium chloride are present, the factors given in Table 2.1 can be used to convert to electrically-equivalent sodium chloride concentrations. A general rule of thumb is often used, sometimes erroneously, that relates total dissolved solids to resistivity as (Greenhouse, 1982; Sawyer et al., 1967)

$$\text{Total Dissolved Solids (ppm)} = 7000/\rho_w(\text{ohm-m}) \qquad\qquad \text{(v)}$$

Finally, the bulk resistivities ρ_t of granular aquifers can be plotted as a function of φ and salinity on the basis of Equation (iii) and Figure 2.1 (18°C). This is done in Figure 2.2.

The presence of clays or shales in an aquifer complicates matters because (wet) clays are conductive. The clay particles have a conductive surface layer resulting from a net negative charge in the clay lattice and a compensating positive charge of exchange cations (typically Ca, Mg, H, K, Na, NH_3) on the outer surface of the clay particles. Table 2.2 lists typical values for sedimentary rocks and unconsolidated formations and illustrates the point that typical clays, marls, and shales are appreciably less resistive (i.e., more conductive) than typical sands, sandstones, and limestones. Table 2.2 also shows that the ranges of resistivity which can be expected for particular rock types are very broad; the determination of the electrical properties of rocks at a particular site must, in general, be based on actual measurements at that site.
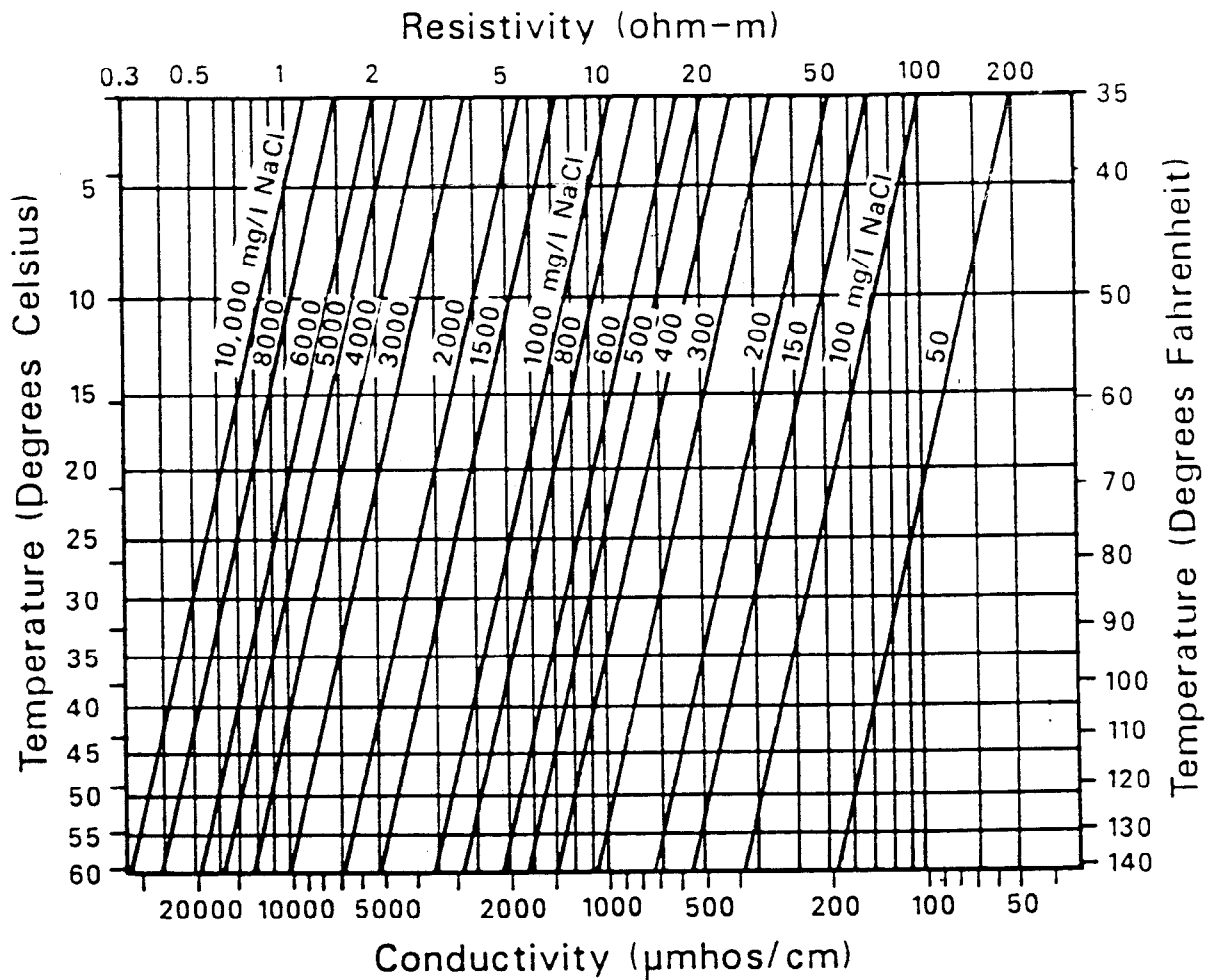
Figure 2.1.   Electrically equivalent concentrations of a sodium chloride
solution as a function of resistivity (or conductivity) and
temperature (from Keys and MacCary, 1972).

30

$$R_1 = \frac{4000}{\text{ppm} \times \emptyset^{2.15}}$$
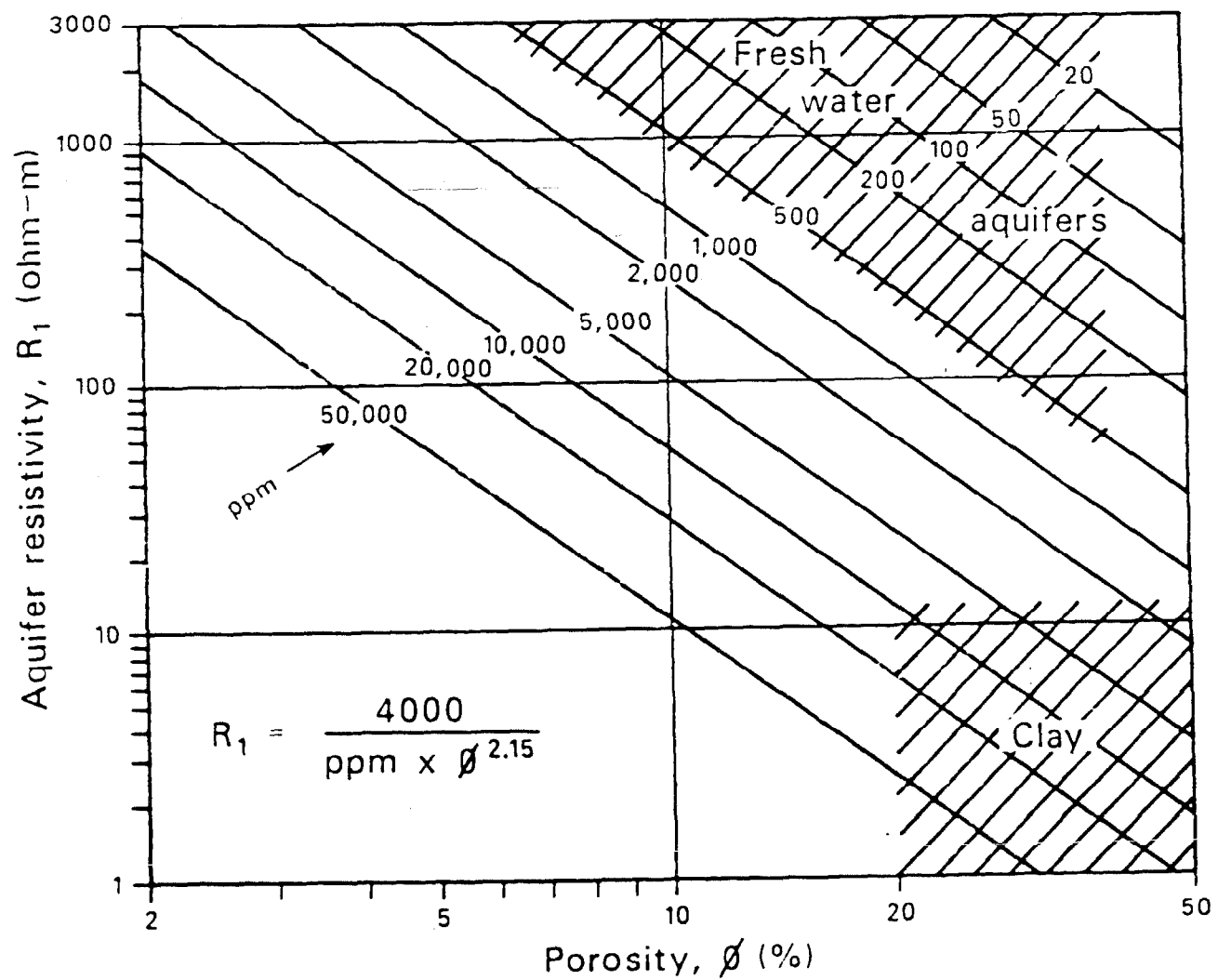
Figure 2.2. Approximate resistivity of granular aquifers versus prosity for several water salinities (from Guyod, 1966).

31

TABLE 2.1: Contributions of Various Ions to
Fluid Conductivity
(after Greenhouse, 1982; McNeill, 1980)

ION	RATIO OF ION CONDUCTIVITY TO CONDUCTIVITY OF EQUAL CONCENTRATION OF NaCl
Ca^{+2}	0.95
Mg^{+2}	2.00
K^+	1.00
SO_4^{-2}	0.50
HCO_3^{-1}	0.27
CO_3^{-2}	1.26
NO_3^{-1}	0.53

TABLE 2.2: Resistivities of Sediments
(after Telford, 1976)

Rock Type	Resistivity Range (ohm-m)
Consolidated Shales	$20 - 2 \times 10^3$
Argillites	$10 - 8 \times 10^2$
Conglomerates	$2 \times 10^3 - 10^4$
Sandstones	$1 - 6.4 \times 10^8$
Limestones	$50 - 10^7$
Dolomite	$3.5 \times 10^2 - 5 \times 10^3$
Unconsolidated wet clay	20
Marls	3 - 70
Clays	1 - 100
Alluvium and sands	10 - 800
Oil sands	4 - 800

In general, aquifer conductivity is directly proportional to the electrolyte concentrations in the pore water and takes place through the moisture-filled pores and passages which are contained within the (usually insulating) aquifer matrix. The conductivity is determined for both rocks and soils by

(1)   porosity (shape and size of pores, number, size, and shape of interconnecting passages);

(2)   moisture content (the extent to which the pore passages are filled with water);

(3)   concentration of dissolved electrolytes in the pore water (for us, a function of the salts present and of the pollutant concentration);

(4)   amount and composition of clays and shales in the aquifer matrix.

With the foregoing theoretical considerations, the kind of highly simplified cross-sectional schematics of injection wells presented earlier in Figures 1.7 - 1.10 can be interpreted in terms of geoelectric sections: vertical sections of the earth composed of horizontal layers of different resistivities. Assume a "typical" Class I injection well has been operating for 10 years and has been injecting about 60 million gallons per year of wastes with a TDS concentration of about 40,000 mg/l. Furthermore, assume that the porosity of the injection zone and the overburden above the confining zone is approximately 10 percent and that the TDS concentrations of fluids in the entire vertical column under the base of fresh water are about 10,000 mg/l. Also assume that the overlying (confining zone) shale has a resistivity which is about the midpoint of the range given by Table 2.2, about 200 ohm-meters (or a conductivity of about 5 millimhos/meter). Then, by using Equation (iii) for Archie's Law and a rough relationship between TDS concentrations and injected fluid conductivity (Equation v), the conductivity of the cylinder of injected fluids can be estimated to be about 65 millimhos/meter. The overburden (assumed to be free of clays) would have a conductivity of about 16 millimhos/meter. The TDS concentration of the freshwater aquifer is assumed to be about 350 mg/l which corresponds to a conductivity of about 0.6 millimhos/meter when a porosity of about 10 percent is assumed. The diameter of the cylinder of injected fluids will be about 450 feet after 1 year of operation, and about 1,400 feet after 10 years of operation. This geometry is indicated in Figure 2.3 with these resistivity values converted to conductivities in millimhos/meter.

Figure 2.3 shows an injected cylinder about 450 feet in diameter and about 500 feet thick, covered by a confining zone 1000 feet thick and an overburden of another 3600 feet. The injected cylinder has a conductivity about 4 times that of the rest of the injected zone and 13 times larger than the confining layer. The overburden, up to the base of fresh water, will have a conductivity about one-fourth of the injected cylinder This geometry is not promising for the application of surface-based electrical methods. A target which is about 4 times more conductive than its

34

surroundings is buried at a depth approximately 10 times its diameter. In a situation where the surface was free of interferences such as buried pipes, fences, powerlines, buildings, and scrap metal, the injected cylinder may be detectable. However, the use of surface methods to map the outlines of this target would probably not be successful. However, a series of annual measurements commencing prior to injection probably would be able to detect a change in apparent resistivities over time. For example, the results of computer model calculations indicate only a 14% increase in apparent resistivity would be observed for the model in Figure 2.3 if the entire injection layer conductivity increased from 16 to 65 mhos/meter. These results are for a Wenner array with an electrode spacing of 6000 feet. The apparent resistivity changes for the finite three dimensional injection zone of Figure 2.3 would be less than this 14%. The overall Wenner array electrode spread in the above example would be 18,000 feet. Such large spreads have poor lateral resolution for detecting deep structure boundaries. In addition, changes in the near surface geology would likely be encountered over distances of 18,000 feet and the associated near surface variations in conductivity would easily mask the detection of the deeper structures. However, a series of repeated measurements commencing prior to injection probably would be able to detect a change in apparent resistivity over time. These changes could then be interpreted to give information on the injection zone.

(TDS ≈ 350 mg/l)

Fresh water aquifer

1300 feet

(σ ≅ 0.6 millimhos/meter)

Base of fresh water

4600 feet

(TDS ≈ 10,000 mg/l)
over burden

(σ ≅ 16 millimhos/meter)
(∅ ≈ 10%)

SHALE

1000 feet

Confining zone
(σ ≅ 5 millimhos/meter)

SANDSTONE

Injection zone
(TDS ≈ 10,000 mg/l)   500 feet
(σ ≅ 16 millimhos/meter)

Cylinder of injected fluids
(TDS ≈ 40,000 mg/l)

Cylinder of injected fluids
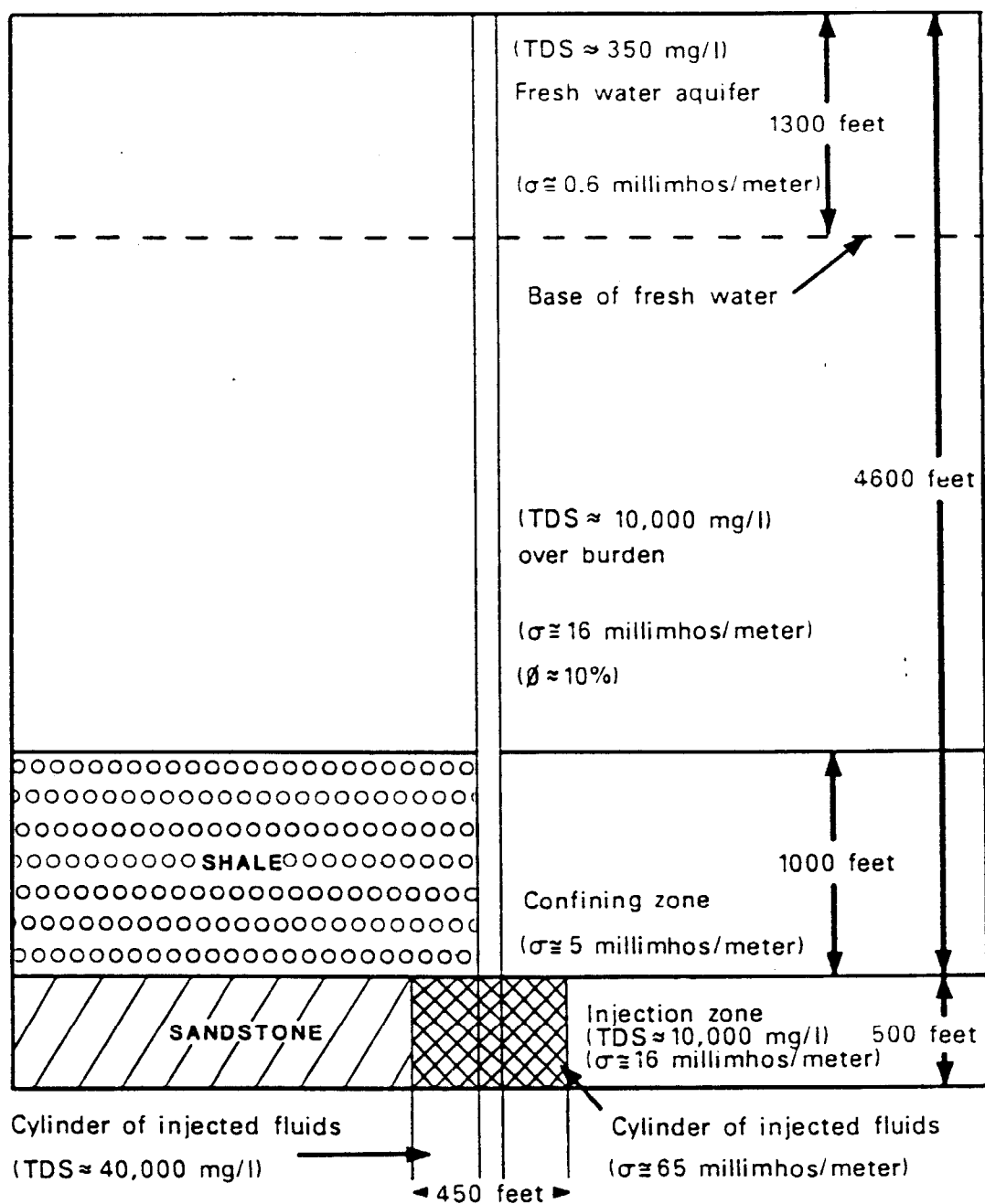(σ ≅ 65 millimhos/meter)

◄ 450 feet ►

Figure 2.3.   Electrical conductivities corresponding to Figure 1.8.

III. PHYSICS OF RESISTIVITY MAPPING

1.0 GENERAL

Measurement of the electrical properties of the subsurface with geophysical tools employed from the surface is one of the oldest geophysical techniques. Electrical techniques figure prominently in ground-water contamination and salinity mapping because the resistivity of formations is highly dependent on the concentration of dissolved solids in ground water. Other physical techniques that measure such properties as seismic velocity, density, and magnetic susceptibility are barely influenced by dissolved solids in ground water and are, therefore, ineffective in mapping changes in ground-water quality or contamination. They are effective for other exploration objectives. In the past 60 years, electromagnetic methods have been used principally for exploration for mineral ores where exploration targets generally have had very high conductivity values compared to the rocks hosting the ore. The objectives in development of techniques consisted of detecting anomalous responses from smaller and smaller ore targets at greater and greater depths.

The objectives in ground-water investigations are somewhat different. First, the resistivity contrast between formations with different concentrations of dissolved solids in ground water is often considerably less than is encountered in minerals exploration. In the last 5 years, equipment manufacturers have begun to address seriously the requirements of geophysics for ground-water objectives. This trend has been helped along by the increased use of electrical methods for hydrocarbon exploration in frontier areas such as volcanic-covered terrain, the Rocky Mountain overthrust, and for permafrost mapping in Alaska.

Although the use of electrical techniques for ore detection has different objectives than their use in ground-water exploration, much has been learned in the last 60 years about electrical techniques. This knowledge forms a firm foundation for applying electrical methods to ground-water investigations.

The electrical resistivity of the earth is measured by determining the response of the earth to current flow. The various methods in use differ mainly in the manner currents are generated. Figure 3.1 schematically illustrates the geometry of current flow in the subsurface for several methods discussed in this report.

In both electromagnetic induction and magneto-telluric (MT) type methods, the current flow in a horizontally-layered earth is horizontal and has no vertical component. In the electromagnetic induction methods the currents are horizontally-closed rings concentric about the transmitter, for both horizontal and vertical co-planar coils (Kaufman et al., 1983). The current flows in horizontal sheets for the MT-type methods. In the direct current (D.C.) method there is a vertical component of current flow, so that currents will cross the boundaries of layers with different resistivities.

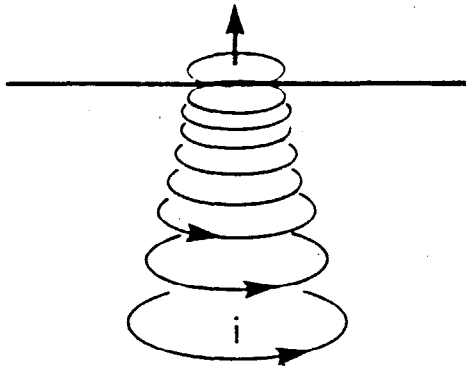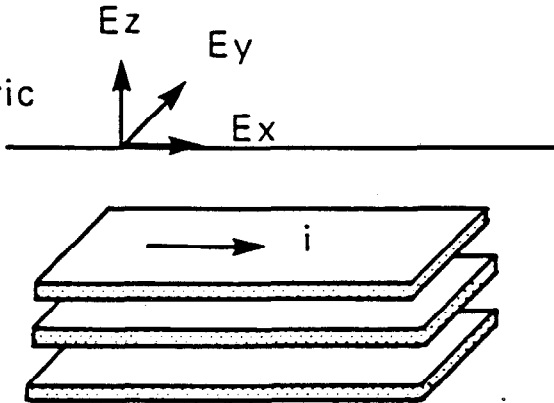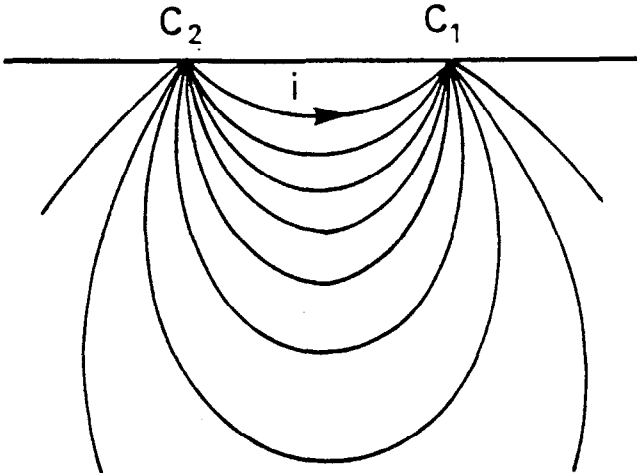| Method	Schematic	Comments
Magnetic induction		Transmitter is a local source which generates a time-varying primary magnetic field which induces eddy currents in the ground.
Magnetotelluric – type MT AMT CSAMT		Transmitter is a distant source (radio stations, geomagnetic storms).
Direct current		Current flows from one electrode to the other.

Figure 3.1. Geometry of current flow in electrical methods.

Whenever a current crosses a boundary of change in electrical resistivity, electrical charges will arise (Kaufman, 1985). Figure 3.2, for example, shows the formation of charges in a horizontally-layered medium for the DC method (Alpin, 1947). This phenomenon is called electrostatic induction and is observed in any conductive medium regardless of its resistivity. The phenomenon is further illustrated in Figure 3.3 with a conductive body embedded in a uniform earth. Under the influence of an electric field, the positive and negative charges residing inside the conductor move in opposite directions. As a consequence of this movement, electric charges develop on both sides of the conductor. These charges in turn create a secondary electric field (Coloumb's Law) inside the conductive medium. For a perfect conductor, the electric charges distribute themselves in such a way that the total electric field inside the conductor will disappear. These charges form on boundaries of lateral resistivity variations in all electrical methods and on horizontal layers in the D.C. method. This principle of electrostatic induction holds for steady-state as well as time-varying electric fields and for perfect and finite conductors (Kaufman, 1985; Alpin, 1947).

It is common to all electrical methods to define apparent resistivity and to transform potentials and voltages measured into apparent resistivities. The purpose of this transformation is to obtain a good visualization of how the behavior of the voltages observed over the study area differs from the behavior, for identical system parameters, over a hypothetical earth which is uniform in resistivity with depth. A common definition for D.C. resistivity is:

$$\frac{\rho_a}{\rho_1} = \frac{E(obs)}{E(un\rho_1)}$$

where ρ_a is the apparent resistivity and ρ_1 is the true resistivity of the top layer (overburden). $E(obs)$ and $E(un\rho_1)$ are the observed voltage and the computed voltage over for a uniform earth having resistivity ρ_1, respectively.

In the various systems of electrical resistivity measurements, different system parameters are varied to increase effective exploration depth: frequency in controlled source audiomagnetotellurics (CSAMT), electrode spacing in D.C., and time in transient electromagnetic induction (TDEM). Figure 3.4 shows two-layer apparent resistivity curves for different techniques. It is evident from all these curves that the geoelectric section (resistivity layering) can be visualized. When the resistivity of the second layer is greater than that of the upper layer, ρ_a increases when effective exploration depth is increased (or decreases when $\rho_2/\rho_1 < 1$). The definition of apparent resistivity therefore encompasses all of the different methods of electrical resistivity mapping. It is an important unifying factor.

2.0 Direct Current (D.C.) Resistivity Method

In the D.C. method of prospecting, current is injected into the earth by galvanic contacts (steel probes). The usual practice consists of
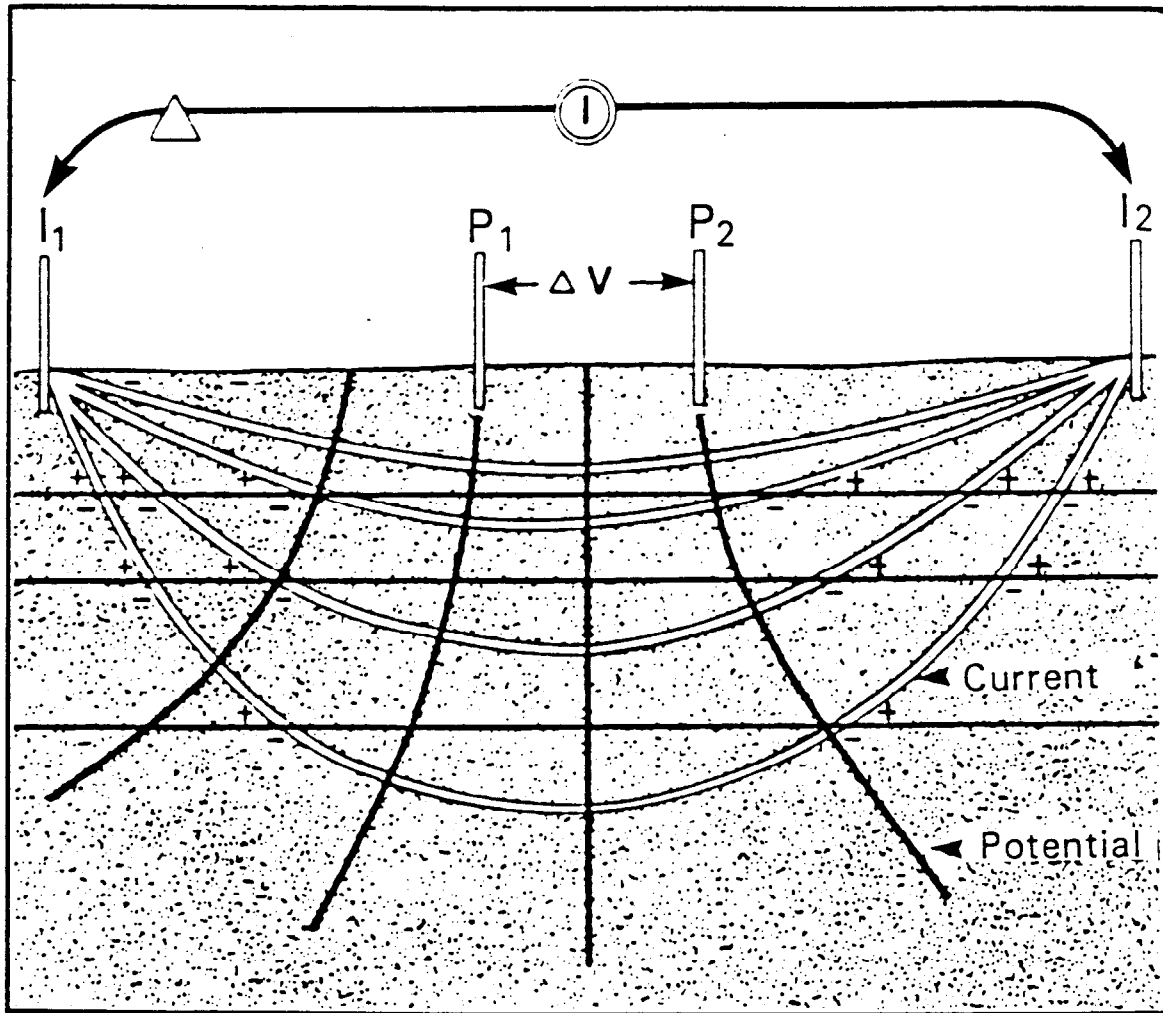
Figure 3.2.   Current flow within a layered medium (Electric charges arise at resistivity boundaries).
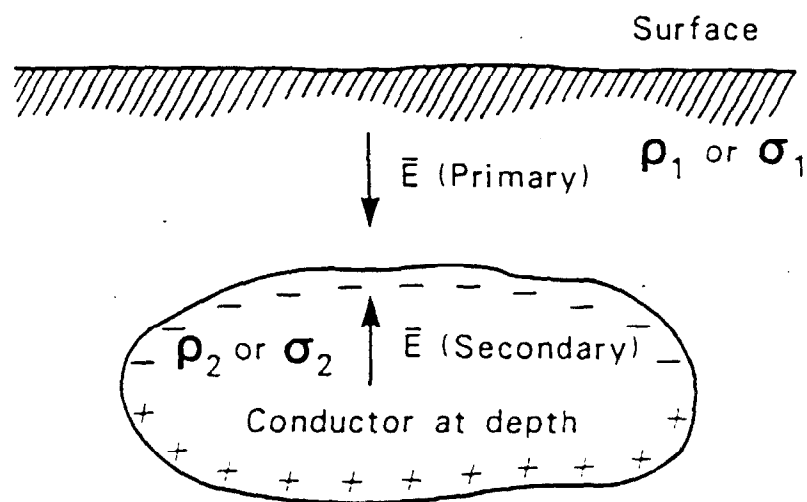
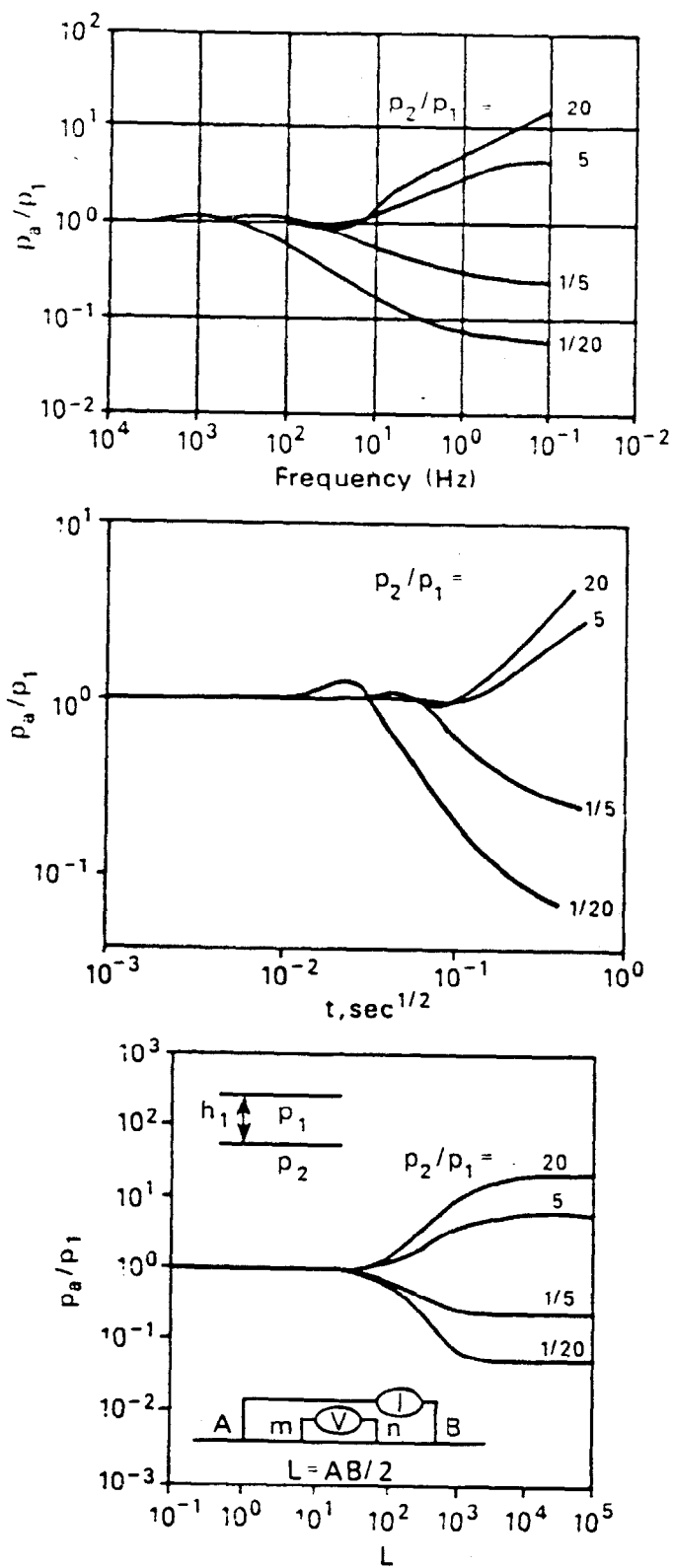Figure 3.3. Charge formation in response to an impressed electric field.

Figure 3.4.   Two-layer apparent resistivity curves for MT, TDEM, and DC.

42

driving current flow through the earth between two electrodes, I_1 and I_2 (Figure 3.2). The current flow causes potential differences to exist at different points along the surface. From the measurements of these potential differences the electrical resistivity of the earth can be derived.

Because the D.C. method is the oldest electrical technique and has a history of 60 years of practice and improvements, there are more treatises and case histories published for this method than for the other methods of electrical resistivity mapping. Probably the most complete discussion on the technique is by Van Nostrand and Cook, 1966.

The depth of exploration in the D.C. method is mainly a function of the spacing between the potential electrodes and current electrodes. The electrodes can be arranged in different arrays. Two common arrays are shown in Figure 3.5 (Schlumberger and Wenner). The distance between current and voltage electrodes is designated by L in the Schlumberger array shown in Figure 3.5. Figure 3.6 shows apparent resistivity curve; for a two-layered earth as a function of the L-spacing. For example, if the objective of an investigation were to detect the presence of a conductive layer with a resistivity ρ_2 under a resistive layer of resistivity ρ_1, and if $\rho_2/\rho_1 = 0.20$, then, at an L-spacing of about $2h_1$, the apparent resistivity ρ_a would be about 75 percent of the resistivity of the surface layer. This is about the limit of detection in the presence of normal geologic noise. Thus, exploration depth in the Schlumberger array is approximately one-fourth of the spacing between current electrodes (2L). The relatively large arrays (array length is approximately ten times depth of interest) required for depth investigations limit the D.C. method in its ability to resolve lateral variations at depth. A third array, however, the dipole-dipole array, has slightly better lateral resolution at depth. Examples of the use of vertical soundings and horizontal profiling are given in Chapter 4, Section 4.2.

3.0 Electromagnetic Induction Methods

3.1 General

In electromagnetic induction, eddy currents are induced in the earth by a time-varying magnetic field. This primary magnetic field is generated by a local source, most often a coil of wire or a grounded line through which a time-varying electrical current is driven. Figure 3.7 illustrates several geometries used by commercially available systems. All these systems have in common a relatively small separation between transmitter and receiver. In fact, the separation distance between transmitter and receiver is about equal to the effective exploration depth (for flat-lying conductors over a layered earth).

Figure 3.7 also illustrates common current waveforms driven through the transmitter loop. In one type of system, the alternating current driven through the transmitter loop has a harmonic frequency waveform. The transmitter continuously emits a primary magnetic field. In other types of systems, the current waveform has a 50 percent duty cycle.

43
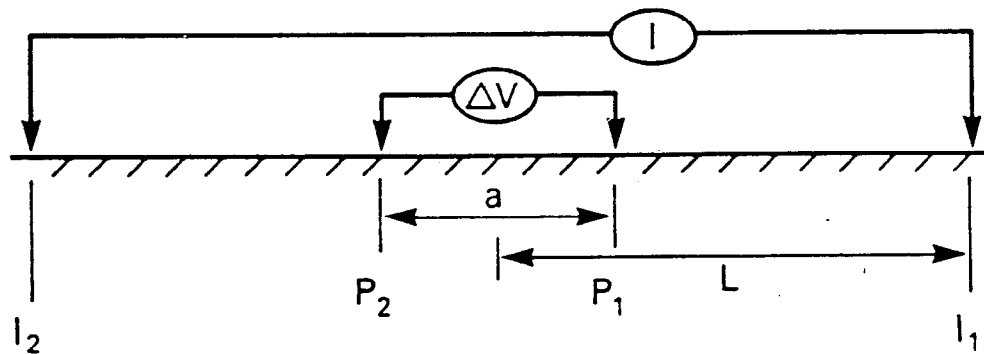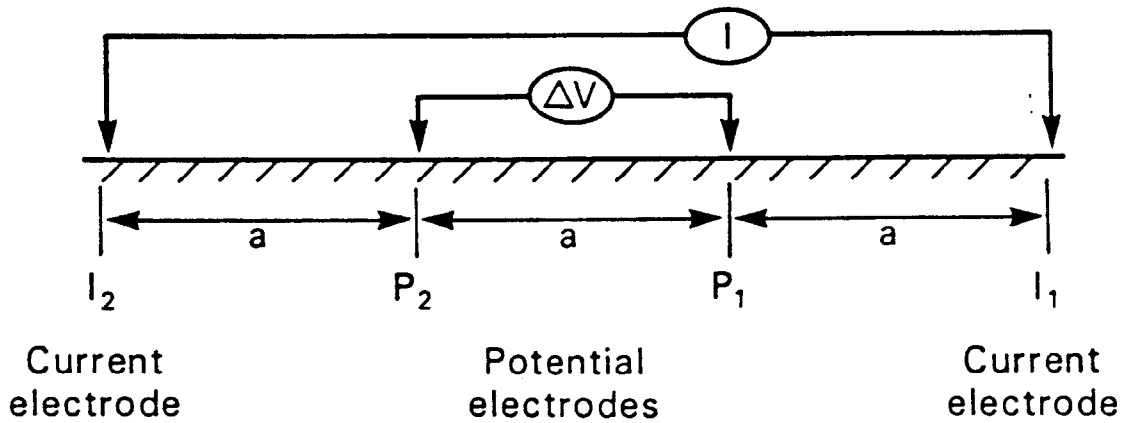
Figure 3.5. Schematics of Wenner and Schlumberger arrays.
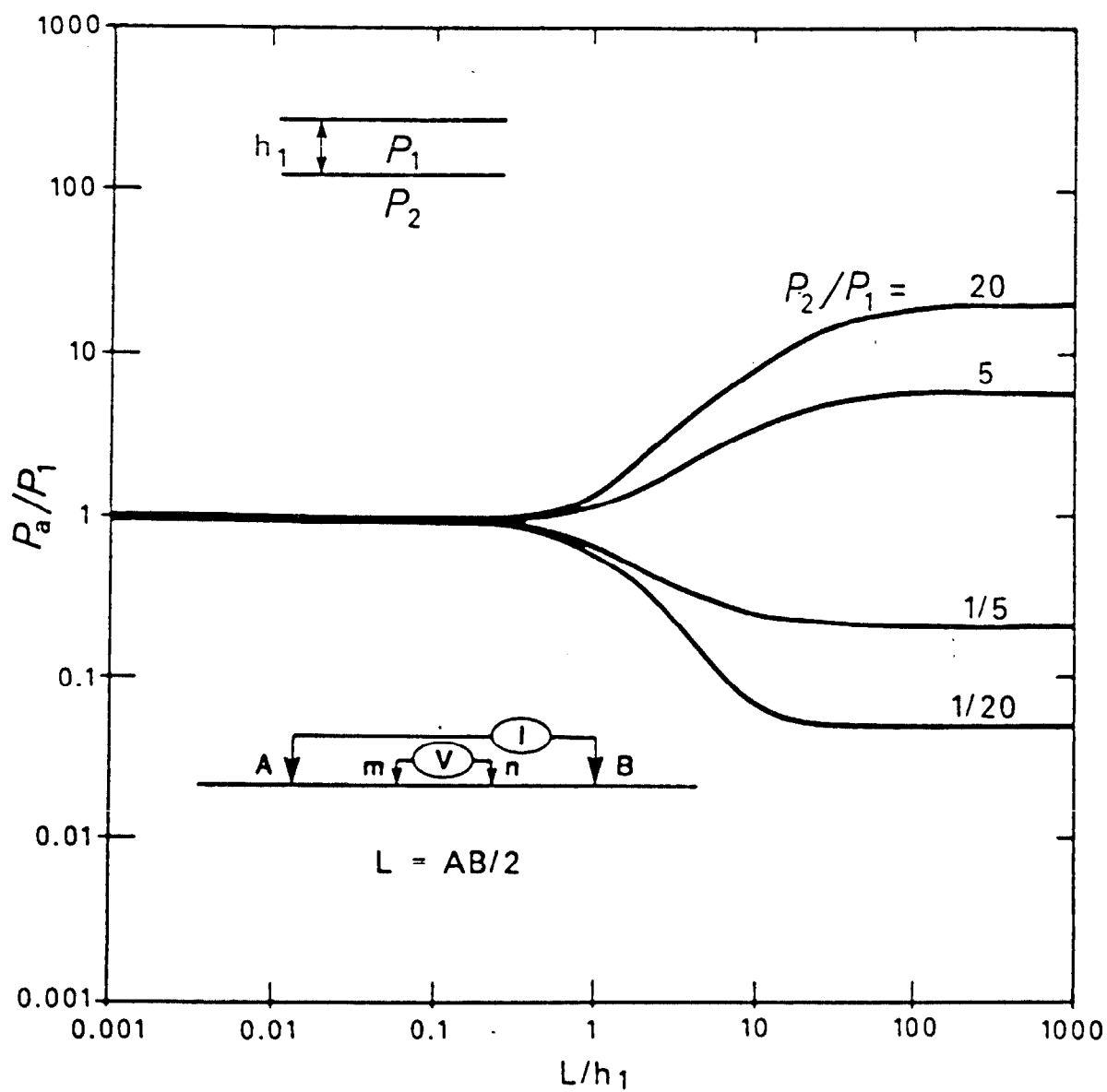
3.6. Schlumberger array two-layer master curves of apparent resistivity versus electrode spacing.
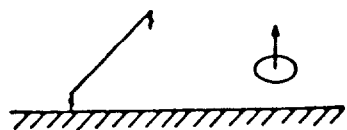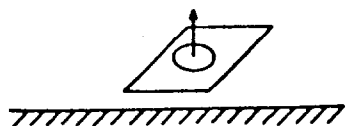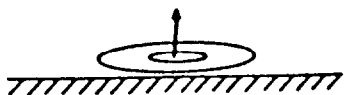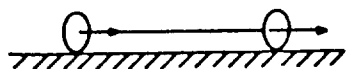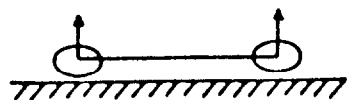
Transmitter Receiver Geometry	Current Waveform	Examples (Frequency separation and coil orientation may be varied)
	sinusoid	Geonics EM-31 Geonics EM-34 MAX-MIN II Slingram
	sinusoid	Geoprobe
		Geonics EM-37 Geonics EM-42 UTEM Sirotem
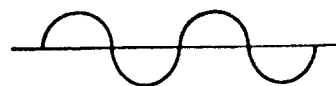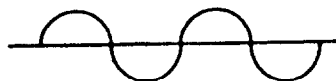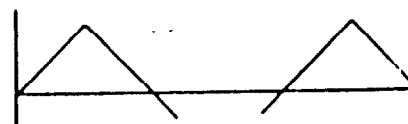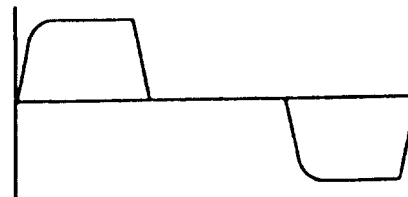
Figure 3.7. Waveforms and transmitter-receiver geometry for electromagnetic induction.

The eddy currents induced in the earth have similar geometry both for the alternating harmonic frequency and for the 50 percent duty cycle waveform. The eddy currents in a horizontally-layered earth consist of closed rings concentric about the transmitter. The pattern of current flow is the same for both horizontal loops (vertical magnetic dipoles) and vertical loops (horizontal magnetic dipoles). The eddy current intensity is a function of earth resistivity (Kaufman *et al.*, 1983).

3.2 Continuous Electromagnetic Induction

Figure 3.8 further illustrates the operation of the systems. An alternating current is driven through a transmitter coil, T_x. The time-varying magnetic field arising from the currents in the transmitter coil induces very small currents in the subsurface. These currents generate a secondary magnetic field, H_s, which is sensed together with the primary magnetic field, H_p, by a receiver coil. The receiver coil is separated some distance from the transmitter coil. These systems were originally developed to detect anomalies caused by highly conductive ore bodies. Rigorous interpretation of data from layered-earth situations is difficult. In a rigorous and complete solution, the secondary field is related by a complicated function to earth resistivity, intercoil spacing (s), and operating frequency (f). However, it has been shown that for certain ranges of frequencies and intercoil spacings, the secondary field is related to earth conductivity by approximations which are relatively simple functions (Kaufman and Keller, 1983). These simplifications are incorporated in the design of the Geonics EM31 and EM34 terrain conductivity meters. The physical concepts of their operation are briefly discussed below.

The secondary magnetic field H_s can be separated into two components: (1) the component H_{sq} in quadrature (out-of-phase) with the primary magnetic field H_p, and (2) a component H_{si} in phase with H_p. Thus, the total magnetic field, H_T, at the receiver can be written as:

$$\frac{H_T}{H_p} = (1 - \frac{H_{SI}}{H_p}) + i \frac{H_{SQ}}{H_p} \qquad (i)$$

where subscripts I and Q refer to in-phase and quadrature components, respectively, and $i = \sqrt{-1}$.

Typically, values for (H_{SI}/H_p) and (H_{SQ}/H_p) for the EM31 and EM34 are on the order of 10^{-4}. It is, therefore, very difficult to measure the first term in Equation (i) accurately because the small value of (H_{SI}/H_p) caused by currents in the earth must be measured in the presence of a value 10^4 times larger which is caused by currents in the transmitter. For that reason, only the term (H_{SQ}/H_p) is used to measure earth conductivity. That term generally can be determined with an accuracy of 1 part in 10^4.

A well known characteristic of a homogeneous half-space is the electrical skin depth δ, which is defined as the distance in the half-space that a propagating place wave has travelled when its amplitude has been attenuated to 1/e of the amplitude at the surface. The skin depth is given
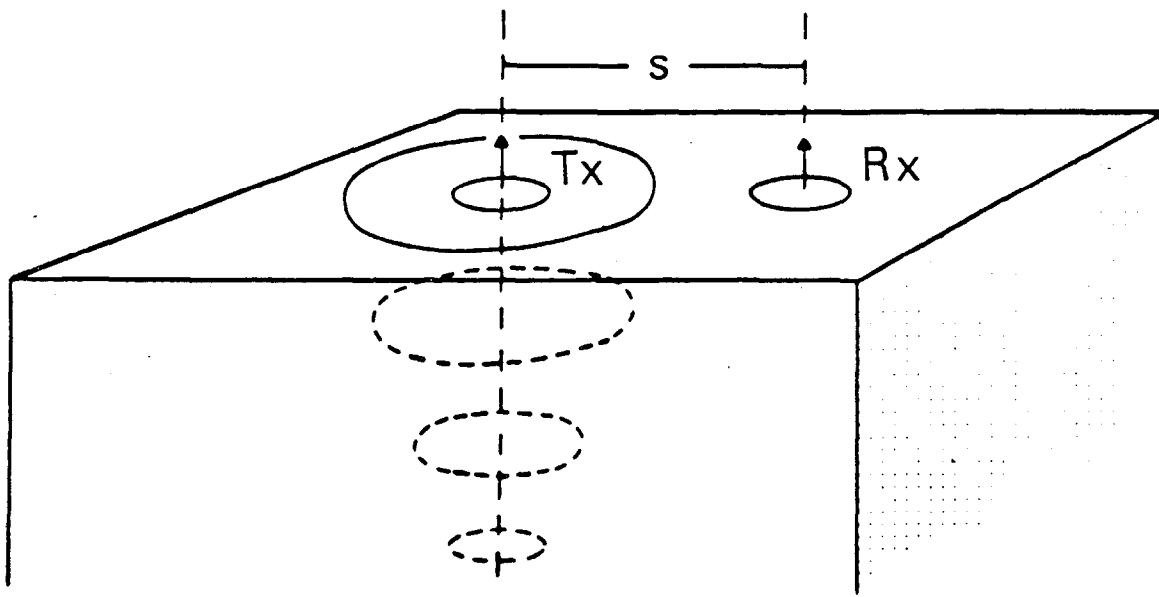
Figure 3.8. Operation of electromagnetic induction in a layered earth.

by

$$\delta = \sqrt{2/\omega\mu_o\sigma}$$

where

ω = $2\pi f$

f = frequency

μ_0 = permeability of free space

s = intercoil spacing (meters)

The ratio s/δ, the intercoil spacing (s) divided by the skin depth δ, is defined as the induction number B, whereupon

$$B = s/\delta = \sqrt{\omega\mu_o\sigma s^2/2}$$

Now if B is much less than unity (i.e., $s/\delta \ll 1$, the low induction number region) it is a simple matter to show that the field ratio reduces to the simple expression

$$\frac{H_{sa}}{H_p} = \frac{iB^2}{2} = \frac{i\omega\mu_o\sigma s^2}{4} \qquad (ii)$$

where $i = \sqrt{-1}$.

The magnitude of the secondary magnetic field is now directly proportional to the ground conductivity and the phase of the secondary magnetic field leads the primary magnetic field by 90°.

To make B much less than unity we see that we must make s very much less than δ and thus

$$\omega \ll \frac{2}{\mu_o\sigma s^2} \qquad (iia)$$

That is, having decided on a value for s (which fixes the effective depth of penetration under the condition B $\ll 1$), the maximum probable ground conductivity is estimated and the operating frequency is chosen so that equation (iia) is always satisfied.

The apparent conductivity which the instrument reads is then defined by

$$\sigma_a = \frac{4}{\omega \mu_o s^2 H_p} H_{SQ} \quad \text{quadrature component} \tag{iib}$$

Equation iib gives the apparent conductivity under the low induction number approximation. Furthermore,

$$\frac{H_{SI}}{H_p} = -1 - \frac{2\sqrt{2}}{15} (\sigma \mu_0 \omega s^2)^{3/2} \tag{iii}$$

Thus, (H_{SQ}/H_p) is linearly related to earth conductivity, and (H_{SI}/H_p) is related to the 3/2-power of earth conductivity. It is clearly unfortunate that it is very difficult in practice to measure (H_{SI}/H_p) because it would be a more sensitive measure of earth conductivity.

Operation of instruments at low induction numbers are is only convenient because of the simple relationship between (H_{SQ}/H_p) and earth conductivity but also because operation at low induction numbers simplifies interpretation. Consider the horizontally-layered earth pictured in Figure 3.9. The transmitter will induce eddy currents in all layers. In general, there will be interaction (magnetic coupling) between the layers, so that the contribution of a layer to the secondary magnetic field is complex. However, for systems operating at low induction numbers, this interaction is negligible, and the contribution of each layer can readily be evaluated. In fact, it has been shown that the electromotive force (emf) measured at the receiver on the surface which is caused by (H_{SQ}/H_p) can be written as:

$$\text{emf} = \Sigma \text{emf}_i \tag{iv}$$

where emf_i is the contribution of the i-th layer. The contribution of the i-th layer can be written as:

$$\text{emf}_i = \sigma_i R_z(i) \tag{v}$$

where

$\sigma_1 \quad h_1$

$\sigma_2 \quad h_2$

$\sigma_L \quad h_L$
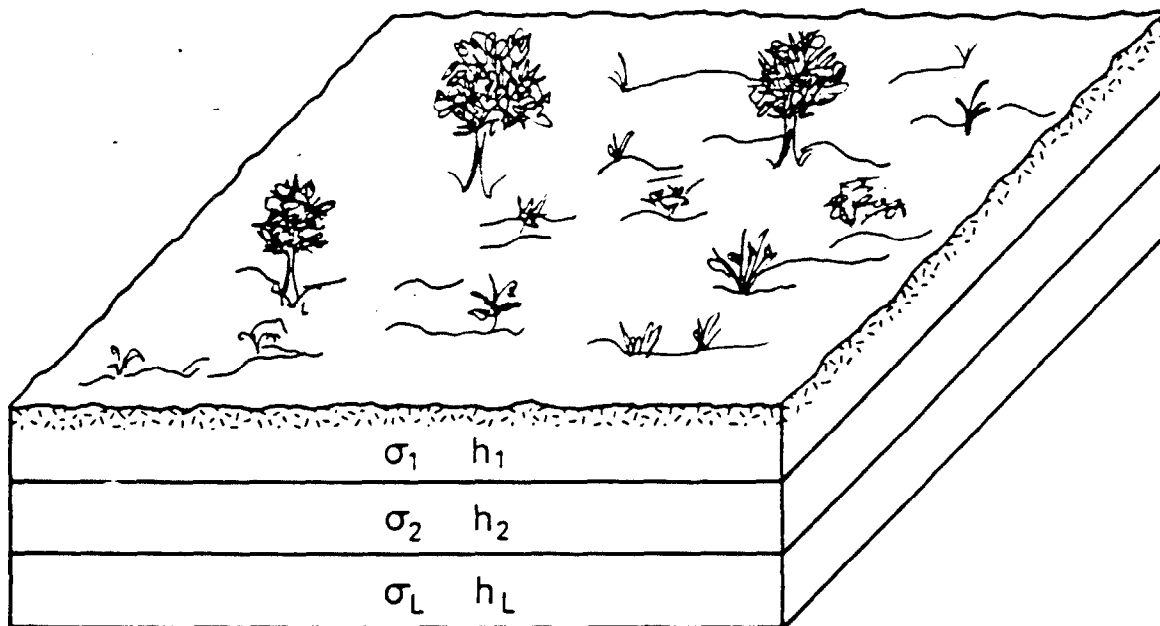
Figure 3.9.   Schematic of horizontally-layered earth.

σ_i = conductivity of the i-th layer

$R_z(i)$ = geoelectric factor of the i-th layer

The geoelectric factor, $R_z(i)$, is a function of the depth and thickness of the i-th layer. The function R_z is readily available in mathematical and graphical form. Figure 3.10 shows R(i) for both horizontal (R_H) and vertical (R_V) magnetic dipoles.

Commercially available systems operating on the principles outlined above are now widely used in ground-water investigations. In general, their effective depth of exploration is limited to about 30 meters (100 feet). Their advantages, limitations, and applications are discussed in Chapter 4, Section 2.1.

3.3 Transient Electromagnetic Systems

In this section, transient electromagnetic induction systems using 50 percent duty cycle waveforms are considered. Transient or time-domain electromagnetic induction (TDEM) is a magnetic induction method, and in many aspects its principles are similar to frequency-domain electromagnetic induction profiling with the EM-31 and EM-34. A TDEM system consists of a transmitter and a receiver. A common array, known as central loop configuration, is shown in Figure 3.11. The transmitter is a square loop of insulated wire laid on the earth surface. A multi-turn air coil wound on a rigid mandrel (about 1 meter diameter) is employed in the center as a receiver. The dimensions of the transmitter loops are a function of the required exploration depth; in practice these dimensions have been varied from 50m x 50m for about 100m exploration depth to 500m x 500m for exploration depths in excess of 1000m. The array is moved for each sounding, as shown in Figure 3.11.

A common current waveform driven through the transmitter loop is shown in Figure 3.12a. The waveform consists of equal periods of time-on and time-off. A primary magnetic field is associated with the current driven through the transmitter loop (Kaufman and Keller, 1983). During the rapid current turn-off ramp, this primary magnetic field is time-variant, and in accordance with Faraday's Law, there will be electromagnetic induction during the current ramp turn-off (Figure 3.12b). The electromagnetic induction causes eddy currents to flow in the subsurface. The intensity of these eddy currents at a certain time and depth is mainly a function of earth resistivity; this fact is the basis for using TDEM to derive subsurface resistivity layering.

In a horizontally-layered earth, the eddy currents are horizontal closed rings concentric about the center of the transmitter loop. A schematic illustration of eddy current distribution is shown in Figures 3.13a and 3.13b. Immediately after turn-off, the currents are concentrated near the surface (Figure 3.13a). With increasing time, currents are induced at greater depth, and Figure 3.13b illustrates the eddy current distribution at later times when currents have migrated. Thus, in a horizontally-layered earth, there is no vertical component of current flow.
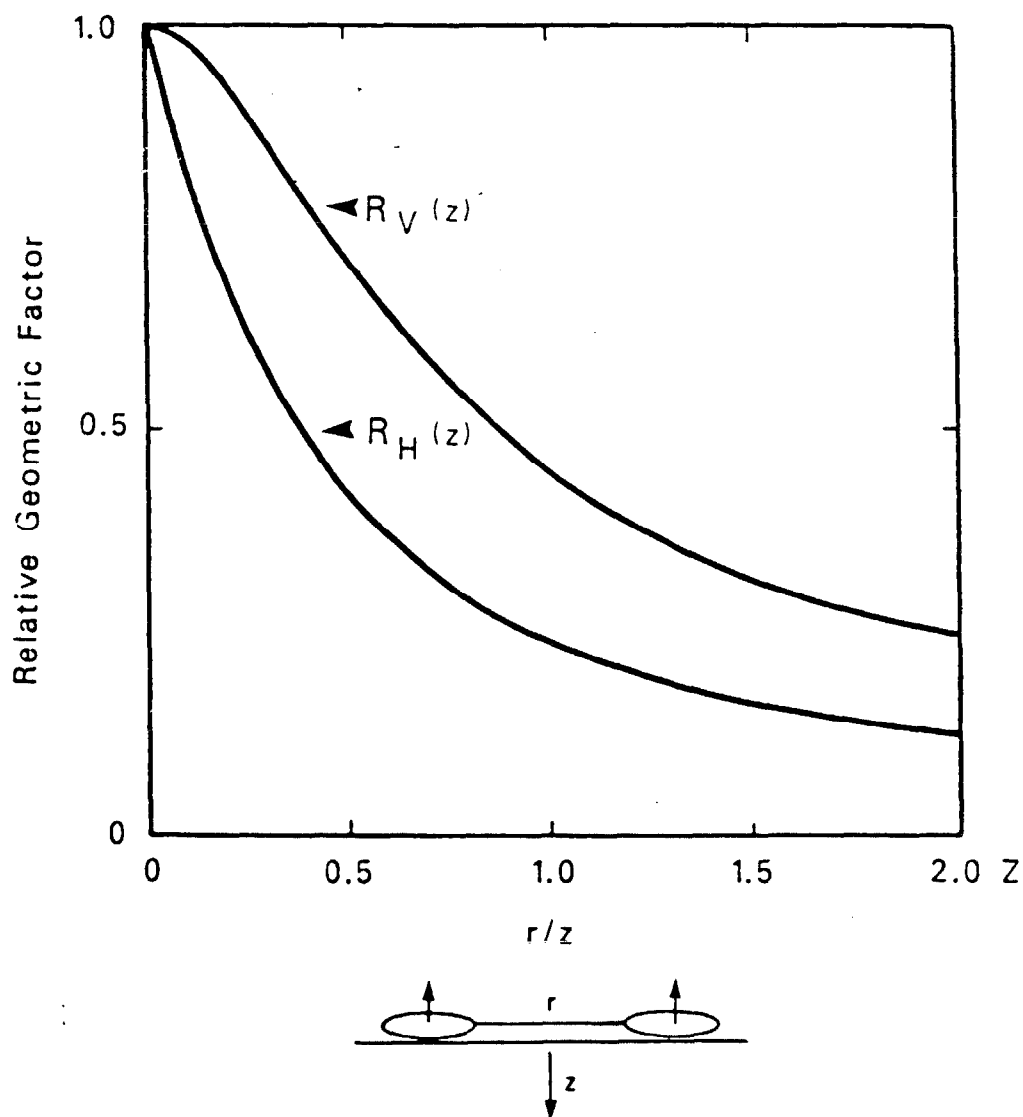
Figure 3.10. Electromagnetic induction response versus depth for horizontal and vertical dipoles.
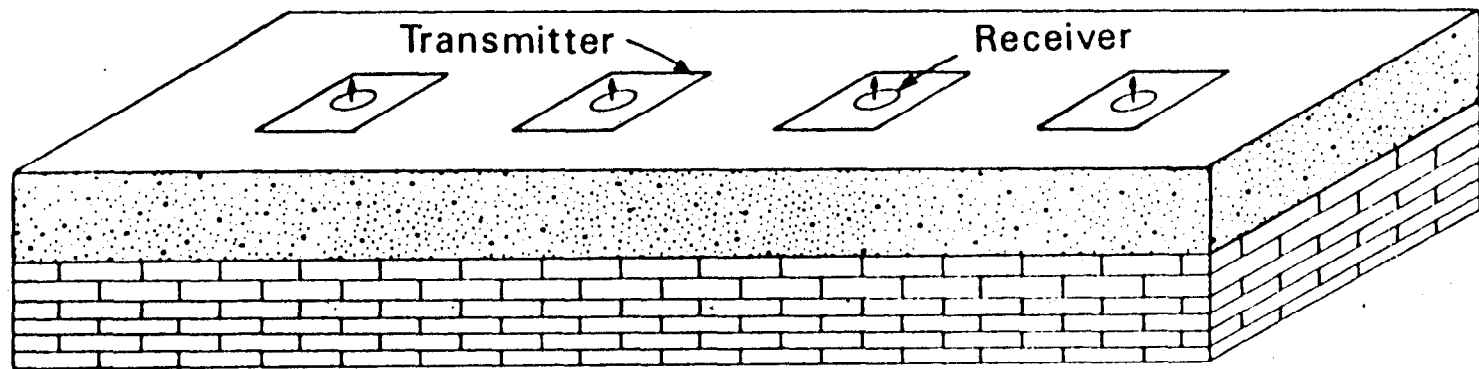
Figure 3.11.   Transmitter-receiver array used in TDEM soundings (the array is moved for each sounding).
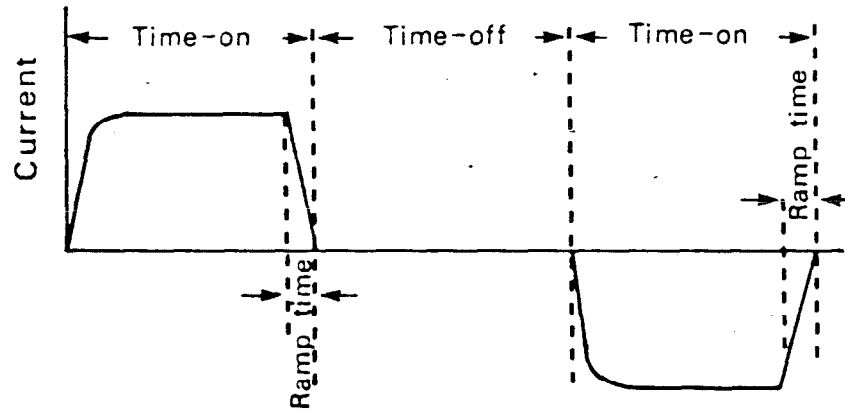
a) Current in transmitter loop
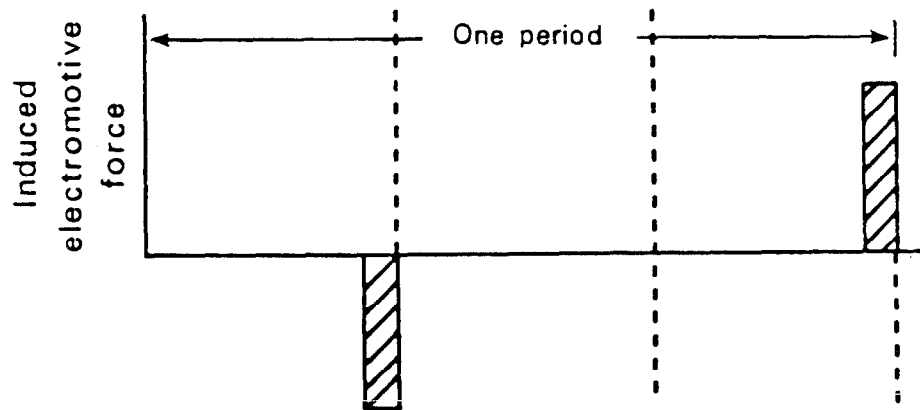
b) Induced electromotive force caused by current turn-off
(EMF caused by turn-on not used.)
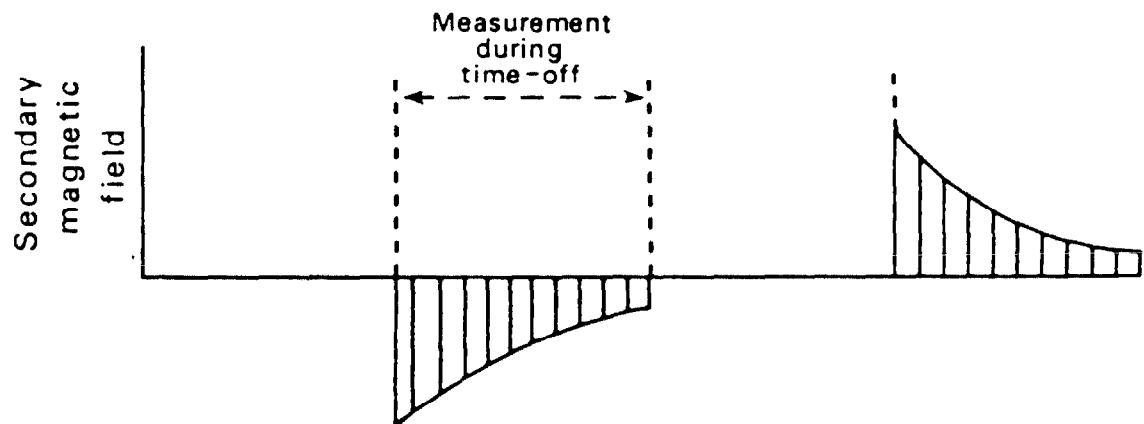
c) Secondary magnetic field caused by eddy currents

Figure 3.12.   TDEM waveforms.
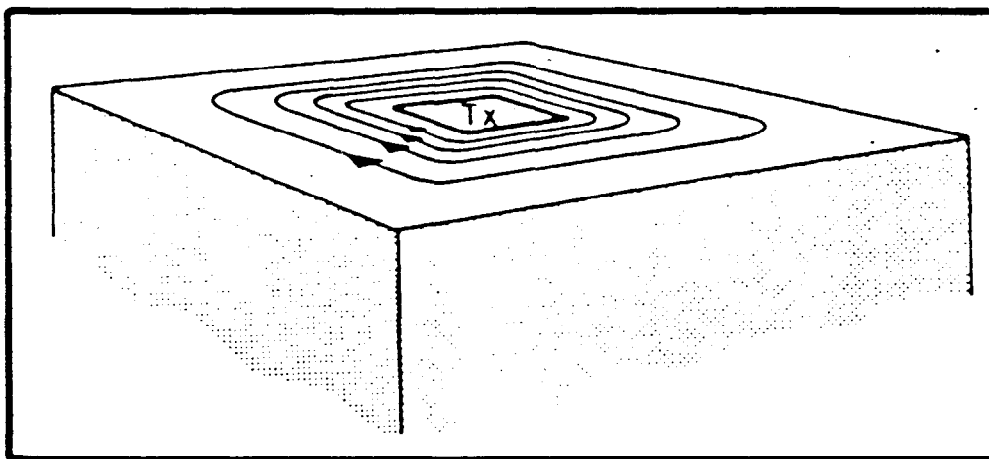
(a)
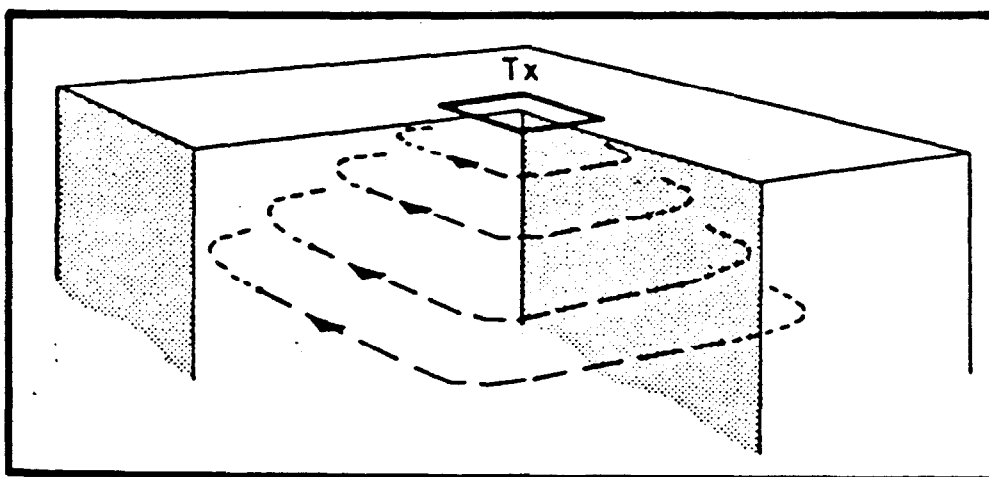
(b)

Figure 3.13. TDEM eddy current propagation in a homogeneous earth.

The time-varying eddy currents in turn cause a time-variant secondary magnetic field (Figure 3.12c) which is measured as an electromotive force (emf) in the receiver coil as a function of time.

Because a visualization of eddy current behavior and distribution is critical to understanding TDEM soundings, one other display is given. Figure 3.14 shows schematically the distribution of eddy current intensity as a function of depth at several times. This figure shows that:

a) At an early time, t_o, currents are concentrated in the upper layers. Consequently, a measurement of the emf at early time will be sensitive primarily to the electrical resistivity of the upper layers.

b) With increasing time the current intensity migrates to greater depth. At later times the emf measured by the receiver will progressively be more influenced by the resistivities of deeper layers.

c) Thus, exploration depth is mainly a function of time rather than of transmitter-receiver separation [as is the case for direct current soundings and frequency-domain EM measurements (EM-31 and EM-34)].

d) After a certain time, e.g., t_3, most of the current density in the near surface layers is small. In fact, for a one-dimensional model, the intensity of eddy currents at late time is independent of near surface conductivities. This means that the electrical resistivities of near surface layers have less influence on the measured emf at later times; measurements at later times have become transparent to surface layers (Newman et al., 1986). This is of practical importance since it reduces sensitivity to surface variations in resistivity, often the main cause of poor data quality in other electrical prospecting methods. Field measurements have shown, however, that cultural effects, e.g., pipes near the surface, affect the late time response.

Finally, Figure 3.15 is included to provide an approximate visualization to correlate exploration depth to time of measurement. It shows the distance from the center of the transmitter loop to the location of maximum current intensity as a function of time. The rate of current migration can be seen to be a strong function of earth resistivity. In resistive earth, currents migrate quickly away from the center; in conductive earth, this migration is much slower.

The secondary magnetic field caused by the eddy currents in the earth have vertical and horizontal components that vary with time and along the surface. Although in principle the resistivity layering can be derived from both horizontal and vertical fields at any place inside or outside the transmitter loop, it is common to use only the emf caused by the vertical magnetic field in the center of the loop.
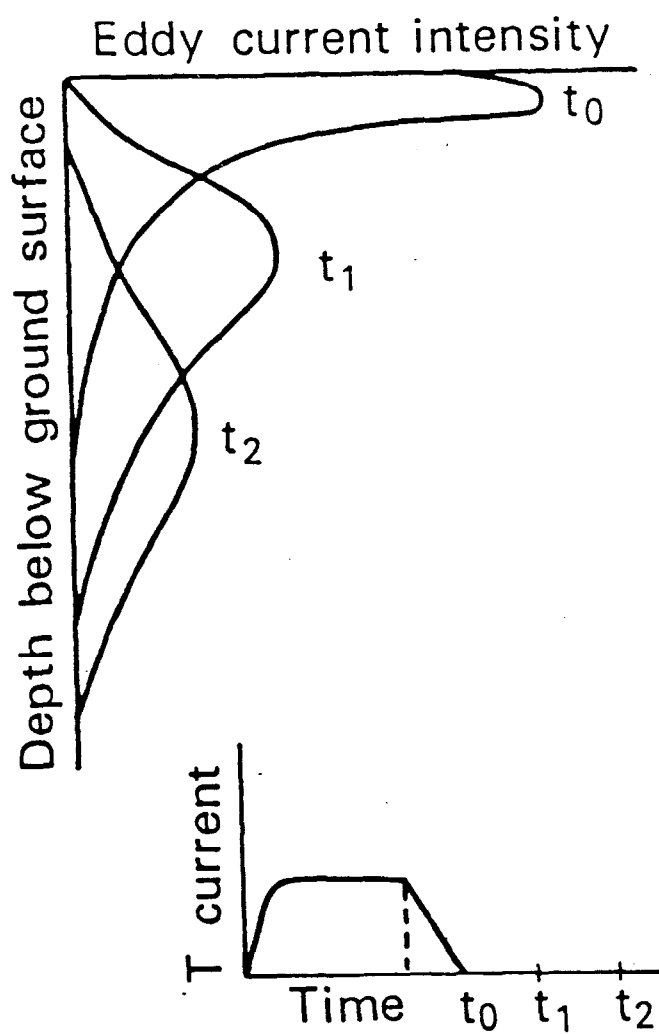
Figure 3.14. Eddy current intensity as a function of depth below the surface.
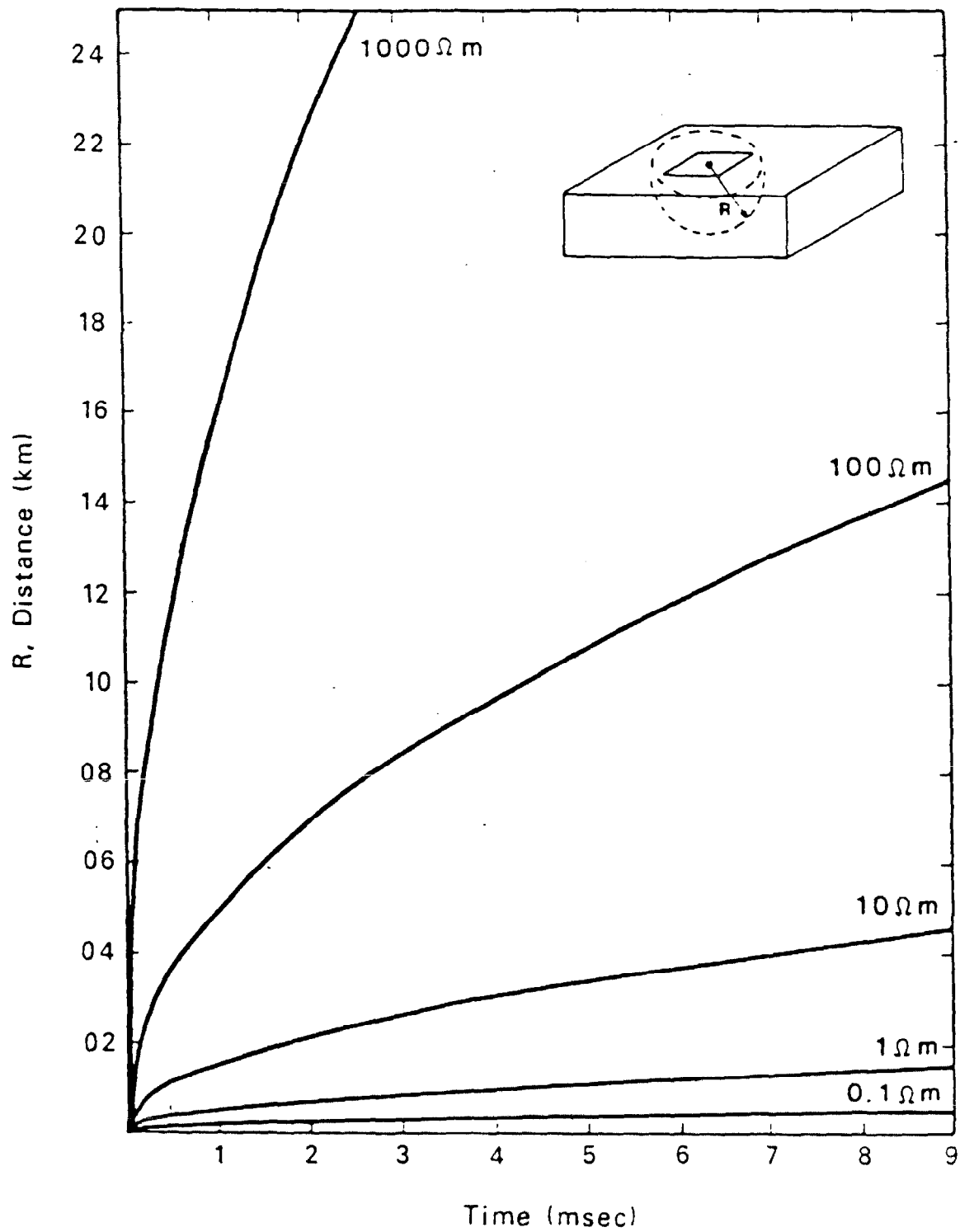
Figure 3.15. Migration of the location of maximum eddy current intensity as a function of time.

Thus, in TDEM the time rate of change of the vertical magnetic field is measured in the center of the loop. That field falls off rapidly with time, generally decreasing by four orders of magnitude over the time range measured. One transient decay recorded over a few tens of milliseconds contains information about resistivity layering over a significant depth range. It is common to "stack" or to average several hundred transient decays to improve signal-to-noise ratio. This stacking of transient decays generally allows operation in urban environments in the presence of 60 Hz noise. Stacking of several hundred transient decays requires a few seconds, and multiple data sets are, therefore, quickly and easily obtained.

Another transmitter-receiver array used in TDEM consists of a grounded line transmitter and a receiver offset often several kilometers from the grounded line.

There are several operational advantages to using measurements from the center of the loop to derive resistivity layering. These advantages can be understood from Figure 3.16 which shows the behavior of the vertical (z) and horizontal (x) components in profiles in the center of the loop. Figure 3.16 also shows that the profile of the z-component is relatively flat about the center. Thus, errors in surveying the center are generally negligible. Some distance away from the center, the z-component can change rapidly with distance, and it will be necessary to survey the location carefully. Figure 3.16 shows that the horizontal component is zero in the center of the loop. Unwanted interference by horizontal components in vertical field measurements caused by receiver misalignment is minimized. Center loop measurements therefore allow quality control in data acquisition which would be much more difficult to realize at other receiver positions. In fact, TDEM measurements in the center of a loop can be acquired with a high degree of accuracy and repeatability with minimum surveying requirements and other quality control procedures. Several data sets can be recorded within a short time period to ascertain repeatability.

The processing of TDEM data proceeds in ways similar to those used in other electrical prospecting methods. The emf measured as a function of time is converted to an apparent resistivity. Figure 3.17 compares a two-layer apparent resistivity curve from a Schlumberger D.C. sounding with a similar curve from a TDEM sounding. In the Schlumberger sounding, exploration depth is increased by increasing the L-spacing; at large L-spacings, the apparent resistivity ρ_a approaches the true resistivity of the lower layer, ρ_2, at later times. In TDEM, exploration depth is mainly a function of time, and ρ_a approaches ρ_1 at early time and approaches ρ_2 at later times. The spacing between transmitter and receiver remains unchanged. In TDEM as in Schlumberger soundings the apparent resistivities are entered into inversion programs which find a solution for the resistivity layering that best fits the observed apparent resistivity curve. These programs run on minicomputers, and inversions are generally performed in the field for quick data turn-around and for quality control.
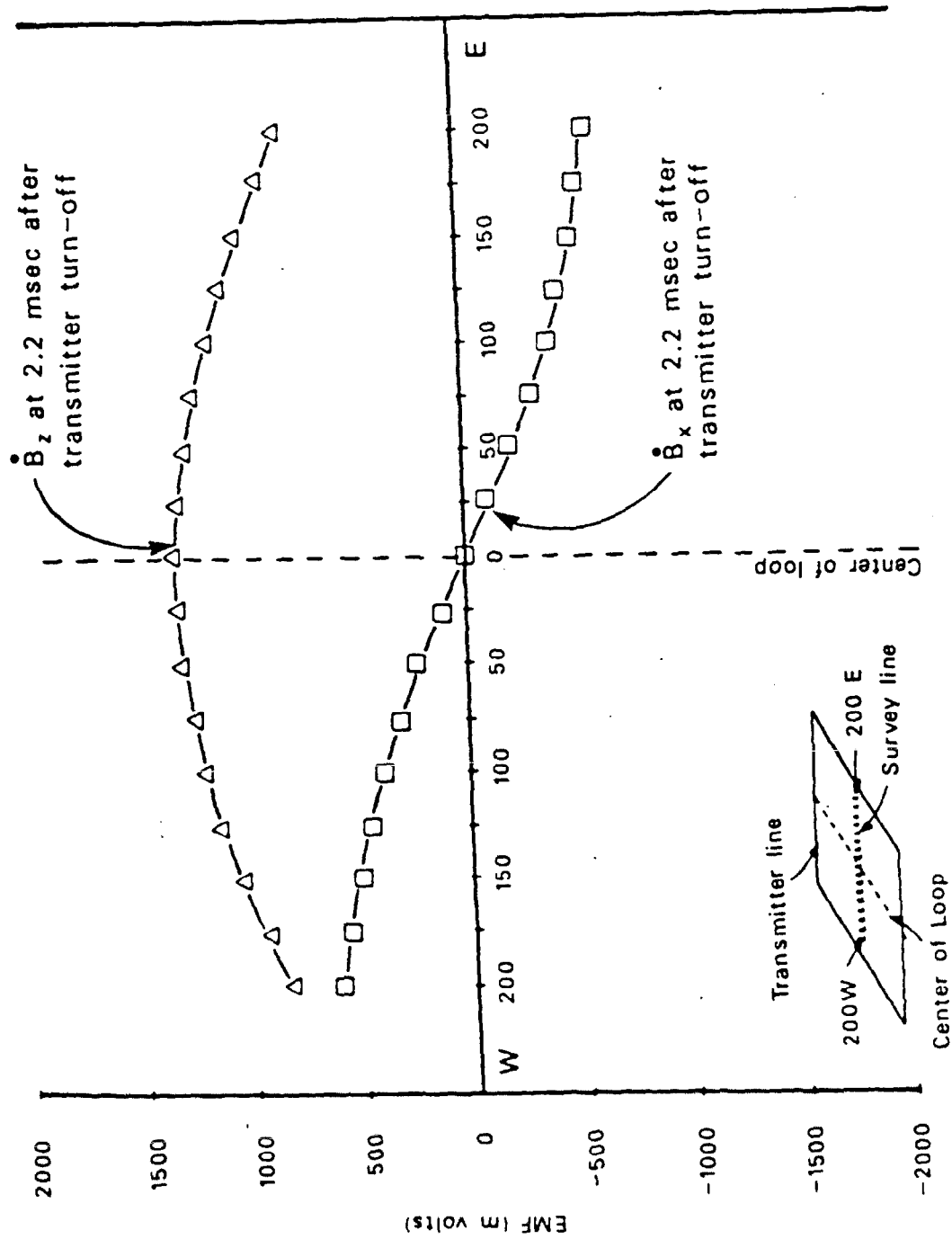
Figure 3.16. Behavior of EMF due to vertical magnetic field ($\dot{B}_z$) and horizontal field ($\dot{B}_x$) on a profile through the center of the transmitter loop.

61
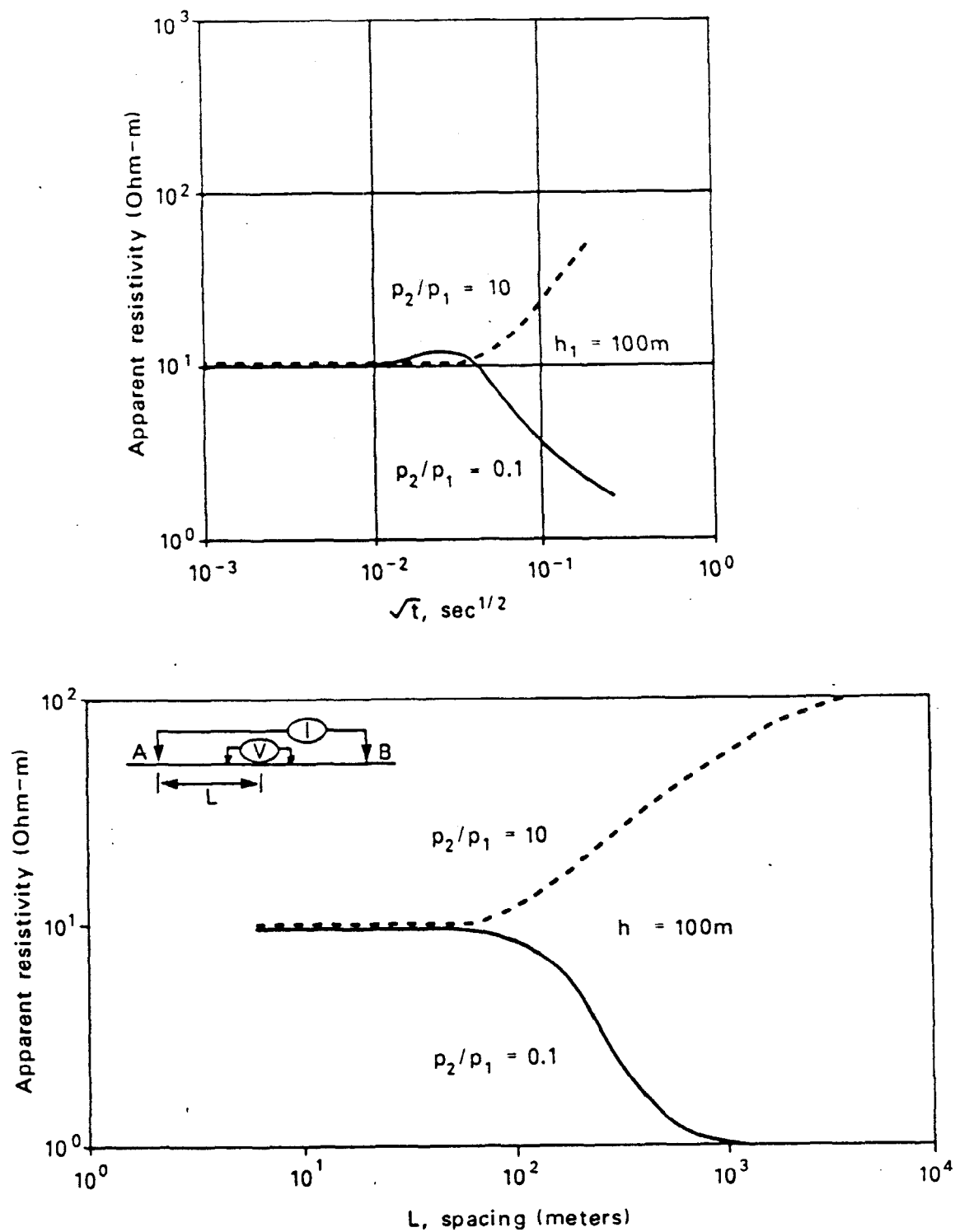
Figure 3.17. Computed two-layer apparent resistivity curves over resistive $(p_2/p_1 = 10)$, and a conductive $(p_2/p_1 = 0.1)$ lower layer. In the model, p_1 is 10 ohm-m, and h_1 is 100 m
a) Schlumberger Sounding
b) TDEM sounding

4.0 MagnetoTelluric (MT), Audio-MagnetoTelluric (AMT), and Controlled-Source Audio-MagnetoTelluric (CSAMT) Methods

Several techniques can be grouped under these methods. They go under the names of very low frequency (VLF)-radiohm, Controlled Source Audio Magnetolellurics (CSAMT), MagnetoTellurics (MT), and Audio-MagnetoTellurics (AMT) (Strangway *et al.*, 1973; Hoekstra 1978).

These systems have in common a general behavior of fields used in the measurements. Common to all of these methods is a distant source for the electromagnetic field. Figure 3.18 schematically illustrates the sources of the various methods. In VLF-radiohm the sources are radio stations used by the navies of the world operating in the VLF band (10 kHz to 30 kHz). In CSAMT the sources are grounded line transmitters installed a considerable distance from the measurement location. In MT the sources are natural geomagnetic activity and thunderstorms. The operational frequency bands of these methods are also shown in Figure 3.18.

The methods which have thus far seen most use in ground-water exploration are the two methods using controlled-sources, VLF and CSAMT. An important reason is that use of controlled sources does not require the extensive signal processing required in the use of natural sources (MT, AMT). The electromagnetic field emitted from the distant controlled source has three field components at the surface of a horizontally-layered earth, at a location far away from the source: the vertical and horizontal components of the electric field, E_z and E_x, respectively, and a horizontal magnetic field, H_y. Over a horizontally-layered earth, there is no vertical component of the magnetic field.

The wave propagates nearly vertically into the earth, and in the earth the wave has two field components, E_x and H_y (Figure 3.19). These components are attenuated in the earth and are reflected from discontinuities in electrical resistivity. At the surface, the quantity (E_x/H_y) is measured. This quantity is called surface impedance, Z, and is related to the electrical resistivity of a homogeneous earth by:

$$Z = \frac{E_x}{H_y} = (\omega\mu\rho)^{1/2} e^{-i\pi/4}$$

where:

ω = angular frequency in radians/second;

μ = magnetic susceptibility, in henrys/meter;

ρ = resistivity in ohm-meters;

$i = \sqrt{-1}$.

For a heterogeneous earth, apparent resistivity is defined on the basis of $|Z|$ by

Figure 3.18. Signal sources for magnetotelluric methods.
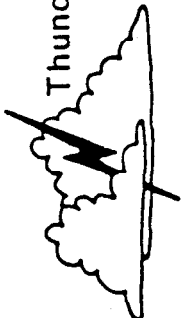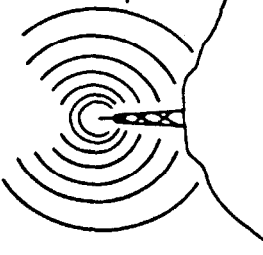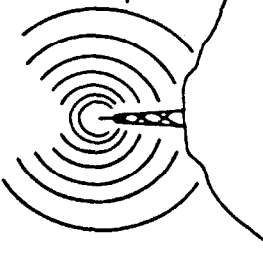
Method	Source of Electromagnetic Waves	Frequency Range
Magnetotelluric	Thunder Storm	10^{-3} Hz to 300 Hz
Controlled-Source Audio Magnetotelluric		1 Hz to 10 KHz
Very Low Frequency	Radio Transmitter	10 KHz to 30 KHz
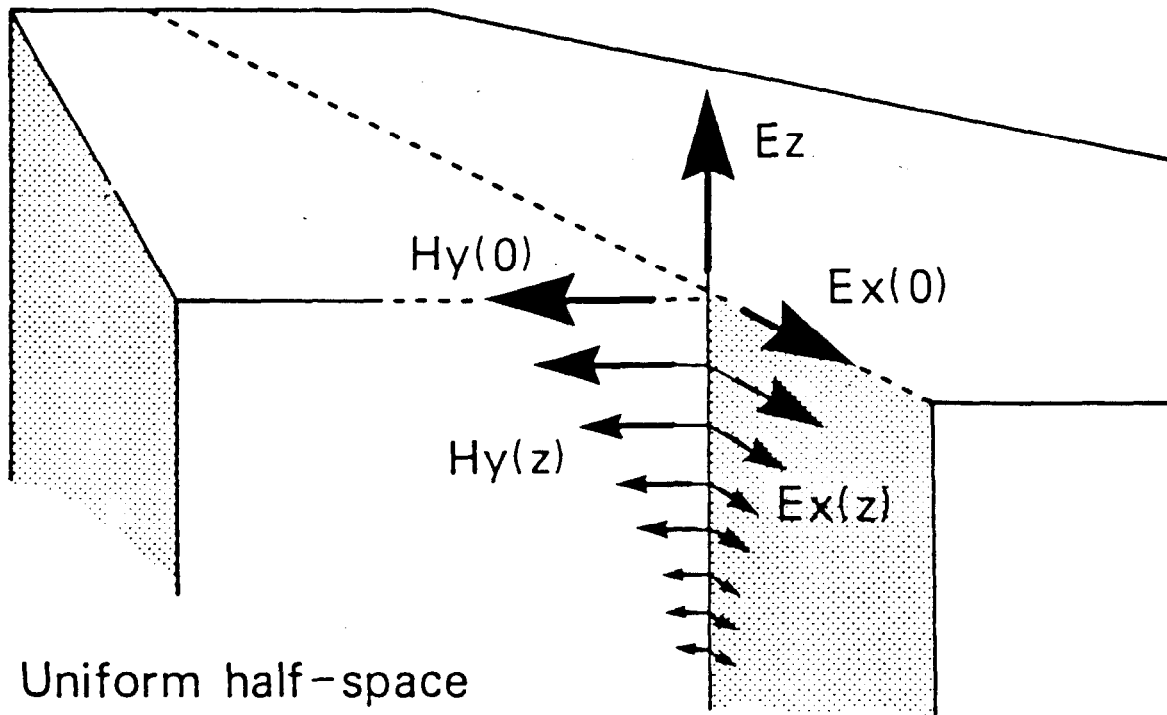
Figure 3.19. Propagation of electric and magnetic fields in magnetotelluric
methods.

$$\rho_a = \frac{|Z|^2}{\omega\mu}$$

The simple definition of apparent resistivity and surface impedance is valid for a horizontally-stratified earth. In the presence of lateral resistivity changes, the surface impedance, Z, must be described by a tensor, and the interpretation of field data becomes complex. Even though the source of the waves is distant, the evidence is that a measurement of ρ_a derived from (E_x/H_y) is a local determination of earth resistivity. The components E_x and H_y are influenced by many factors such as path of propagation between source (transmitter) and measurement station and atmospheric effects. However, these non-local factors influence both E_x and H_y equally. The dominant effect is in E_x due to the local subsurface electrical resistivities, while H_y is only slightly affected by the properties of the subsurface in the absence of lateral resistivity variations. The influence of non-local factors is eliminated in measuring the ratio (E_x/H_y).

It is important as background for later discussions to realize that in a horizontally-layered medium, the current flows in horizontal sheets. There is no vertical component of current flow, and, therefore, no charges are induced at the interface between horizontal layers of different resistivities.

The wave propagating into the earth is attenuated. This attenuation determines to a large extent the effective exploration depth. It is common to correlate exploration depth with the *skin depth* of a plane electromagnetic wave travelling into the earth. Effective exploration depth is usually about one-half to two-thirds of the skin depth. Skin depth is defined as the distance which causes an attenuation in amplitude of $1/e$ (e = 2.7183). Skin depth is related to the resistivity of the earth and frequency by:

$$d = (\frac{2\rho}{\mu\omega})^{1/2}$$

where

δ = skin depth in meters.

In Figure 3.20, δ is given as a function of frequency. It is evident that soundings to different depths of exploration can be obtained by measuring at different frequencies. This commonly is done in CSAMT by stepping the source and the receiver synchronously through a range of discrete frequencies. Since the natural noise spectrum caused by geomagnetic storms also contains energy over a large frequency range, a sounding can also be made in MT. However, a major computational step is involved in decomposing the spectrum measured as a function of time to a frequency-domain spectrum. The cost in acquiring and processing MT data generally prohibits its use in ground-water investigations. Moreover, the
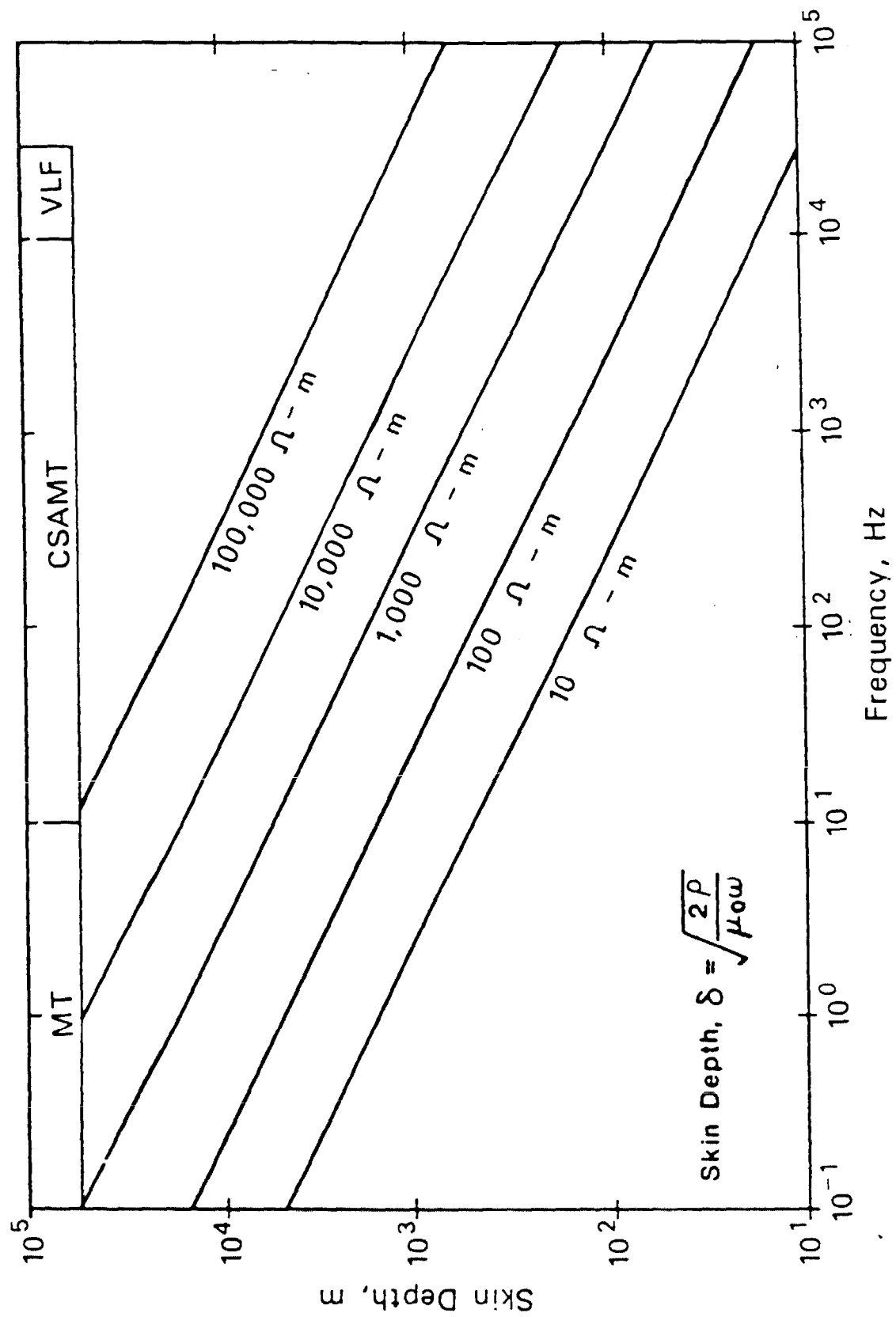
Figure 3.20. Skin depth of electromagnetic plane waves as a function of frequency and earth resistivity.

upper frequency range used in MT measurements is about 200 Hz to 300 Hz, generally too low for effective use in ground-water investigations. CSAMT data acquisition and processing do not measure the surface impedance as a tensor and therefore cannot deal effectively with lateral resistivity variations. However, lateral resistivity variations can be estimated by measuring at a large number of stations.

5.0 Induced Polarization Method

The principles of all the previous methods for measuring the electrical properties of the subsurface are based on Ohm's Law, as given by

$$R = (V/I)$$
where
R = resistance (ohms)

V = potential difference (volts), and

I = electrical current (amperes)

This equation implies that the impression of a current, I, instantly results in a potential difference, V.

There are, however, subsurface conditions where there is a significant time lag between the impressed current and the resulting potential difference. This phenomenon is called induced polarization (IP) and is further illustrated in Figure 3.21. Figure 3.21 shows that the potential difference V_p, arising from an impressed current I terminated at time t_o, drops instantaneously to a value V_s but subsequently decays gradually to zero. The ratio (V_s/V_p) is called the chargeability, M, and is an important quantity measured in induced polarization.

The main objective of IP surveys has been the detection of disseminated sulfide minerals. The magnitude of IP response generally increases with the amount of mineralization. Also, extensive surveys have been conducted to detect "halos" of disseminated sulfides that may or may not exist above oil deposits.

Although the presence of disseminated sulfides is a dominant cause of IP effects, there are several other important causes (Olhoeft, 1985) such as processes associated with ion exchange in clay minerals, oxidation-reduction reactions, and clay-organic reactions (Ogilvy et al., 1972). Therefore, these causes must be taken into consideration in the data interpretation.

IP effects are measured by experimental arrays similar to those used in D.C. resistivity measurements. Many different arrays are in use (Figure 3.22). They all have in common the fact that effective exploration depth is approximately one-fourth of the distance between current and voltage electrodes. For investigating the spreading of contamination at the injection horizon of injection wells (typically 2,000 feet or greater), large arrays would be required. Such large arrays have been used in Figure

68

Square wave current waveform

Voltage drop
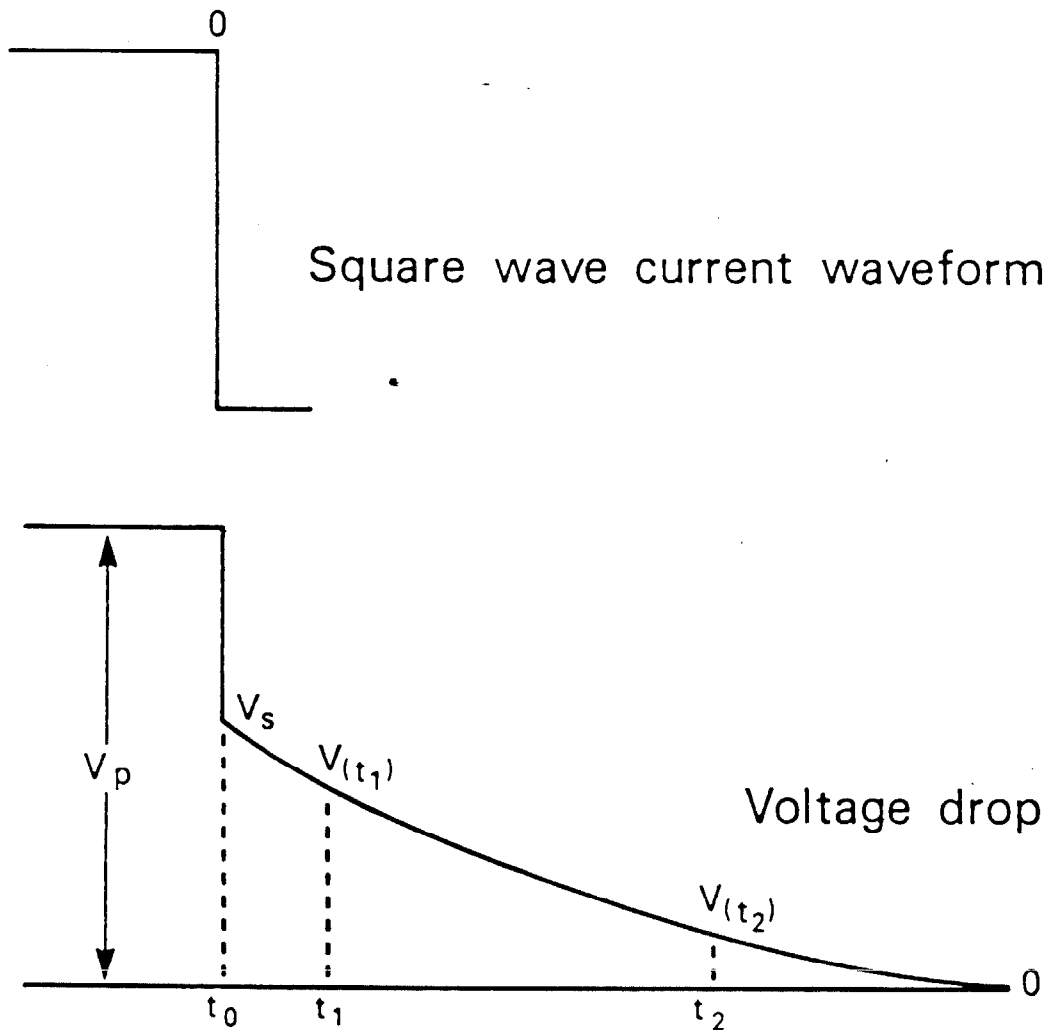
Figure 3.21. Induced polarization effect: Transmitter current and voltage waveforms in induced polarization.

Pole-Dipole
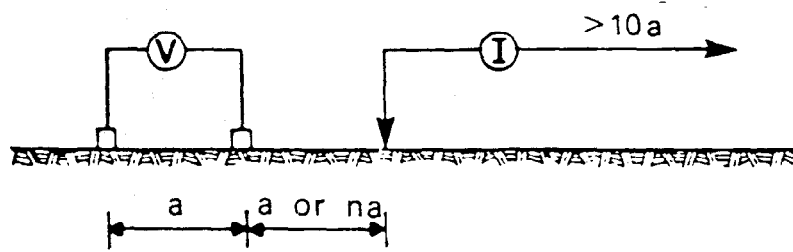
Pole-Pole
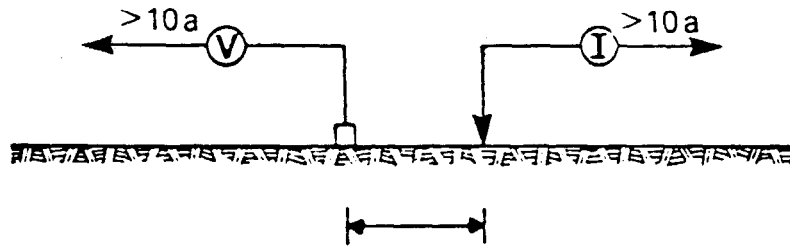
Schlumberger
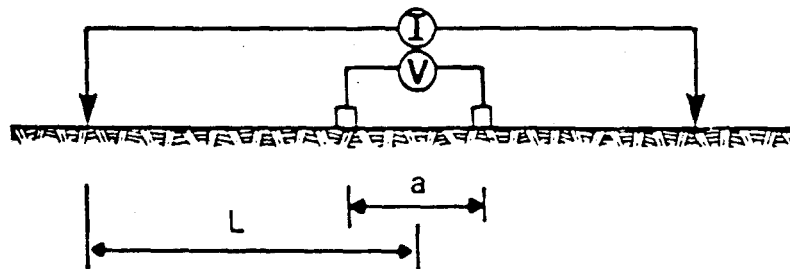
Wenner
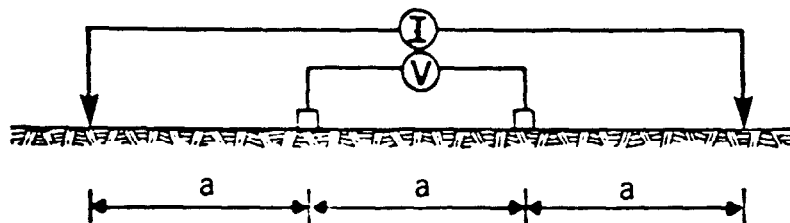
Figure 3.22. Commonly used array types for DC resistivity and IP.

70

geothermal exploration but are considered impractical in investigations over oil and gas fields. The size of the field and the presence of culture (pipelines, power lines) limit the area and size-of the array which can be used.

IP data can be acquired in time domain or in frequency domain. Figure 3.23 shows transmitter current waveform for time-domain operation; a synchronous receiver measures the resulting voltage waveform. Typically, the receiver measures the ratio of voltages at one or more centered intervals of time (V_1, V_2, V_3). The decay time in IP is on the order of a second and, therefore, much larger than decay times used in TDEM soundings.

In freqency domain IP, square waves are used, and the transmitter and receiver are sequentially stepped through a range of frequencies. In summary, IP is in operation similar to resistivity measurements. The difference is that in IP, in addition to resistivity, information is obtained about the time lag between impressed current and the resulting potential difference. The acquisition of field data is similar.

The IP method is expected to have very limited applications to investigations of contamination from injection wells. The reasons for this are as follows:

a)   IP measurements, like D.C. resistivity measurements, require large arrays (6,000 to 8,000 feet) to investigate contamination at the depths of injection horizons.

b)   It is unlikely that significant changes in IP are associated with brine contamination. IP effects may be associated with organic liquids.

c)   Injection wells are typically located in areas with significant cultural interferences (power lines, pipe lines, fences), and determining IP effects with any accuracy in such areas will generally be very difficult.

d)   For investigating brine leakage, no additional information is expected to be derived from measurements of IP compared to those which are obtained with D.C. resistivity.

e)   IP measurements require careful decoupling of EM effects caused by pipe lines, fences, and power lines. In operations near producing oil fields, this may also be a serious limitation.
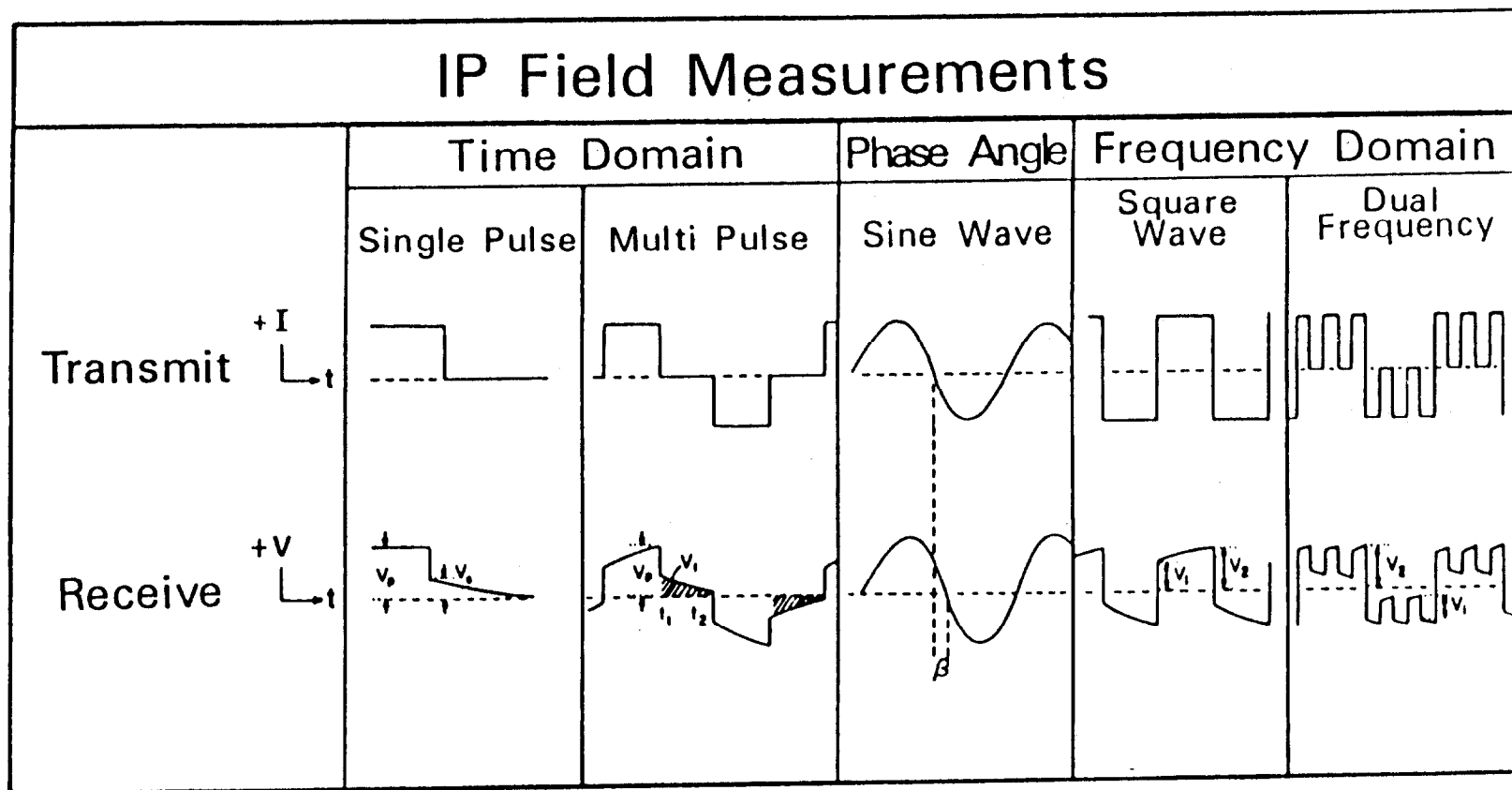
Figure 3.23.   Transmitter current and receiver voltage waveforms in IP field measurements.

IV.   APPLICATIONS AND CASE HISTORIES

In Chapter 3 the physical principles of several geophysical methods were discussed. All of these methods have, at one time or another, been applied to investigations of ground-water contamination. However, in the majority of these previous investigations, the contamination was detected at shallow depths. There are few case histories dealing with leakage from injection horizons or from wells at depths of several thousand feet where injection frequently occurs. The quality of information obtained and the settings in which each technique may be applied differ with different methods. The various electrical exploration tools are far from equivalent.

The success of geophysical surveys is critically dependent on the clear definition of exploration objectives. Geophysics is no panacea; it can accomplish certain tasks but not others. In the best of circumstances, it can map the target of interest to a certain degree of accuracy. It might well be that the required accuracy is greater than the accuracy obtainable with surface geophysics. In such cases the use of geophysics must be rejected.

There may often be more than one exploration objective; for example, the mapping of contamination in two different aquifers at different depths may be desired. Experience has shown that two exploration objectives can seldom be achieved with one set of survey specifications. Better results are often obtained by surveying for one objective at a time.

The objectives of surveys using electrical geophysical methods can best be stated in terms of geoelectric sections. A geoelectric section displays the variation in electrical resistivity laterally and vertically across a vertical plane passed through some line on the surface. Examples of geoelectric sections are shown in Figures 4.1a and 4.1b where the variation in resistivity is caused by lithology and brine leakage from a disposal well. The detectability of the contamination will vary with different sections and methods. Detectability can often be evaluated from modeling investigations.

To evaluate the applicability of various electrical methods to certain exploration objectives, evaluation criteria are required. The important criteria are as follows:

o lateral resolution

o vertical resolution

o sensitivity to geologic noise

o survey productivity (cost, ease of operation, personnel qualifications)
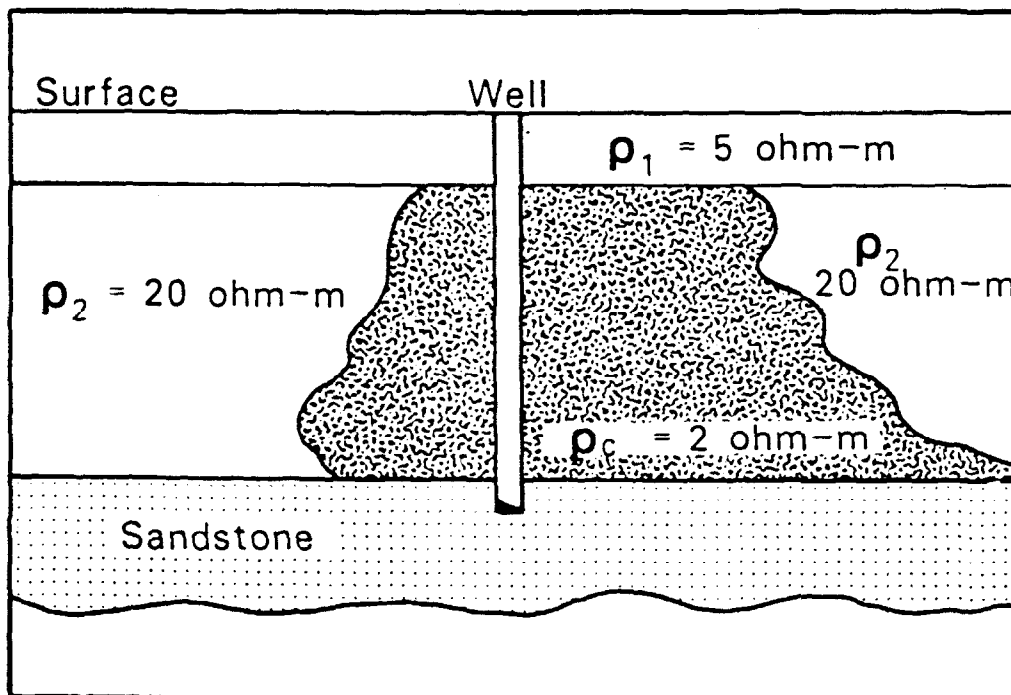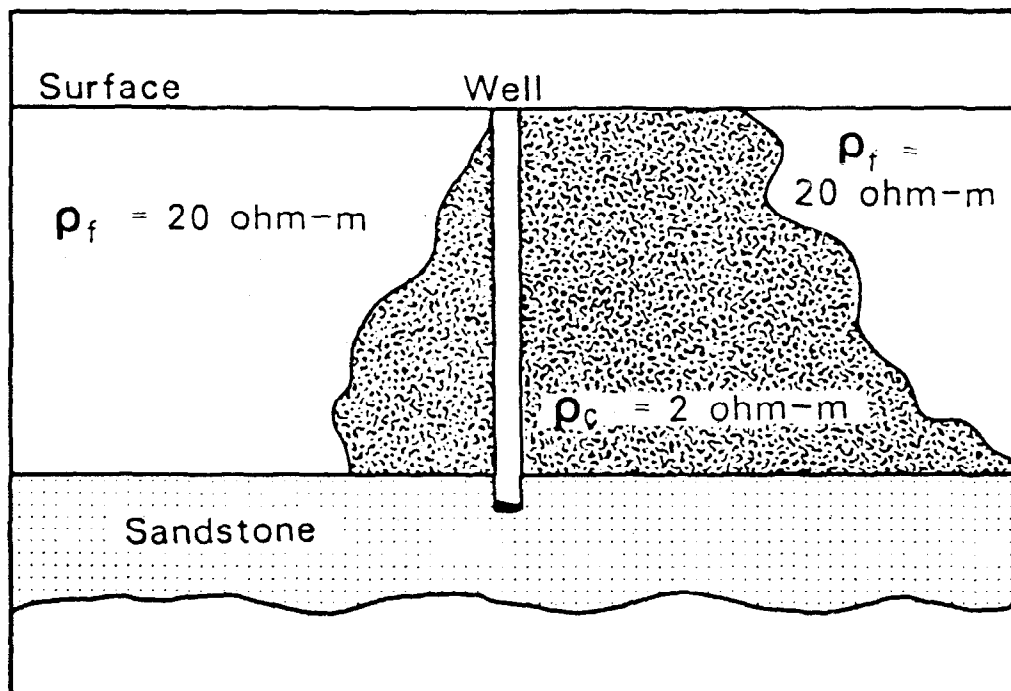
Figure 4.1. Examples of hypothetical geoelectric sections which could be associated with injection wells.

74

The first three criteria can be evaluated from physical principles discussed in Chapter 3. The fourth criterion is dependent not only on the particular geophysical method in question but also on site-specific factors: terrain, vegetation, and cultural interferences such as power lines, fences, pipelines, and nearby radio-frequency transmitting stations.

1.0 Criteria for Evaluation of Electrical Methods

1.1 Lateral Resolution

Lateral resolution is defined as the accuracy to which lateral changes in electrical resistivity can be mapped and interpreted. For example, in the geoelectric section of Figure 4.1a and 4.1b, the distance which the brine contamination has progressed horizontally is important. Moreover, the concentration of brine in the ground water can be expected to decrease gradually with increasing distance from the well. An ability to assess this gradual decrease would be beneficial; this ability is related to the lateral resolution of resistivity mapping.

The lateral resolution of different electrical methods is mainly determined by such factors as:

o   the separation between source (transmitter) and receiver

o   the components of the electromagnetic field which are measured
    (There is a difference between the lateral resolution of methods
    which measure electric fields or a ratio of electric and magnetic
    fields, and the resolution of methods which measure only magnetic
    field components.)

o   desired depth of exploration

While it is often possible to observe lateral resistivity changes in the data, it is more difficult to determine the geoelectric section where rapid lateral changes exist. This is again related to a strong tendency to interpret data by one-dimensional models. Cost-effective 2- and 3-dimensional models are still not common in electrical prospecting.

1.2 Vertical Resolution

Vertical resolution is defined as the accuracy with which vertical changes in resistivity with depth can be resolved. Vertical resolution is mainly determined by two factors:

o   the relationship between the electrical resistivity of the
    subsurface and the measured voltages or electromotive forces. In
    Table 4.1, this relationship is summarized for several
    electromagnetic methods. The TDEM method with small
    transmitter-receiver separation has the highest sensitivity to
    earth resistivities. This high sensitivity is generally realized
    in soundings in the center of the transmitter loop.

TABLE 4.1. Relationship Between Resistivity and Measured EMF (or voltage) for Various Electrical Survey Methods

Electrical Method	Relationship
Direct Current	$\rho = KV$
MT; CSAMT; VLF	$\rho = K(emf)^{1/2}$
Frequency Domain EM (low induction numbers)	$\rho = K(emf)$
Time Domain EM (late stage, small transmitter-receiver separation)	$\rho = K(emf)^{-3/2}$
Time Domain EM (early stage, small transmitter-receiver separation)	$\rho = K(emf)$

The constants denoted by K are different values for each method.

o   the accuracy to which the field can be measured. Accuracy is partly determined by minimum detectable signal and by geologic noise.

1.3 Sensitivity to Geologic Noise

Geologic noise is defined as changes in signal which are caused by geologic conditions and which obscure the exploration objectives or targets. Very often, geologic noise is the limiting factor in electrical and electromagnetic surveys. The schematic geological and geoelectric section of Figure 4.2 illustrates the nature of geologic noise. This section is a simplification of the geologic setting of the Floridian aquifer system. The limestone aquifer is overlain by Pleistocene deposits of sands, clays, and organic material of various thicknesses.

The Floridian aquifer is believed to have been infiltrated at one time by saline water during high sea levels. Since the lowering of the sea level, saltwater is gradually being replaced by freshwater. However, a freshwater-saltwater interface occurs at some depth in the Floridian aquifer, and the thickness between the top of the limestone and the freshwater-saltwater interface represents the quantity of potable water. An objective of electrical geophysical surveys could be the mapping of that freshwater-saltwater interface. Geologic noise in this geologic setting would be introduced by variations in soil types and thickness of sediments above the freshwater-saltwater interface.

Another objective of geophysical surveys could be the delineation of recharge areas. Recharge into the Floridian aquifer is likely to occur where the Pleistocene sediments are dominantly coarse-grained or absent. When the geophysical objective is to map the soil types and thickness of the overburden, geologic noise could be introduced by variation in the freshwater-saltwater interface, particularly when it would occur relatively near the surface.

Geologic noise is, thus, a function of the exploration objective. By clearly defining the exploration objective and the sources of geologic noise, optimum geophysical tools can be selected to reduce that noise to the maximum possible extent.

2.0 Electromagnetic Induction Methods

Electromagnetic induction methods as discussed here include both continuous or frequency-domain EM systems and transient or time-domain
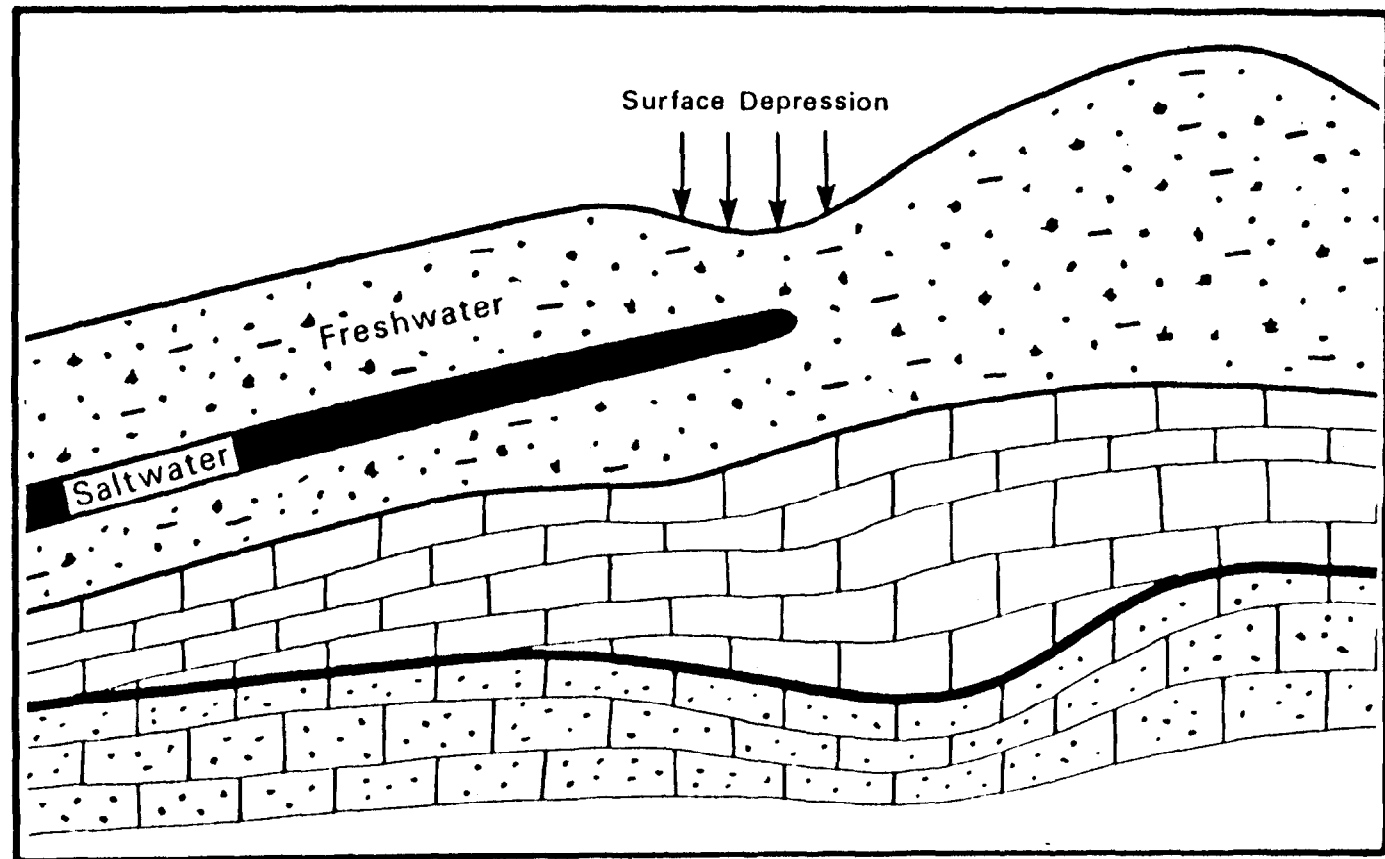
Figure 4.2. Geologic noise obscuring the mapping of a freshwater-saltwater interface. Geologic noise is caused by heterogeneity of the layer thickness.

(TDEM) systems. Applications of frequency-domain systems to injection well problems have been limited to cases where leaks in the upper reaches of the well systems create contamination targets at shallow depths or where surface brine pits have left near-surface saline targets. TDEM has also been useful in defining large areas of contamination at considerable depths.

2.1 Frequency-Domain Methods

2.1.1 . Instrumentation

The most common configuration of frequency-domain systems consists of two air coils separated by discrete distances; one coil functions as a transmitter and the other functions as a receiver. A cable typically connects the transmitter and receiver and provides synchronization. The first series of these instruments were used in the mining industry (Slingram, Max-Min). In these instruments both in-phase and quadrature phase components are measured. It was discussed in Chapter III that the in-phase component which is caused by earth eddy currents must be measured in the presence of a primary magnetic field caused by currents in the transmitter. This is accomplished by electronically subtracting the contribution of the primary field from the measured in-phase emf. Since this primary field (at a constant frequency) is only a function of distance, this can be done for each discrete distance. This requires that these distances must be accurately chained in field work. Since the primary magnetic field is proportional to $(1/r^3)$ where r is the transmitter-receiver separation, this chaining must be accurate to 0.3 percent to obtain an accuracy of 1 percent in the measured in-phase component. However, in-phase components with amplitudes of 1 percent of the primary field or greater are generally only observed over mineral ore at the frequencies employed. Measurement of earth conductivities using in-phase currents would require 0.001 percent accuracy in measuring the in-phase current to achieve 1 percent accuracy in measured apparent conductivities. For this reason, the quadrature-phase component is generally used in ground-water investigations where the contrast between target and background is usually less pronounced than in minerals exploration. The in-phase component or amplitude can be used when spacing, frequency, and conductivity are such that the induction numbers are not small.

Another problem in applying the systems used in mining to ground-water investigations is the difficulty of interpretation. In general, the relationship between measured emf and subsurface resistivity layering is complex and inconvenient for routine interpretations. Interpretation procedures and the relationship between measured emf and earth conductivity can be considerably simplified by operating over certain ranges of transmitter-receiver separation and frequency called low induction numbers. The EM-31 and EM-34 are designed to operate at low induction numbers.

The exploration depth of frequency-domain systems is mainly a function of transmitter-receiver separation. A practical limit for maximum exploration depth for the EM34 is about 30 meters, although highly

conductive anomalies can be detected at greater depth.   Increasing
exploration depth requires increasing transmitter-receiver separation and
transmitter output power.

The limited exploration depth (about 30 meters) of these
frequency-domain systems restricts their use in injection well leakage
investigations where targets will usually be more deeply buried. The method
can perhaps be used to detect leakage at shallow depths but would be
incapable of detecting targets at the depth of typical injection horizons,
several thousand feet. A more likely class of targets for frequency-domain
systems would be leakage from temporary holding ponds.

Commercially available instrumentation for frequency-domain methods is
listed in Table 4.2.   In ground-water contamination investigations, the
main instruments used are the Geonics EM-31 and the EM-34-3.   The
configurations of the EM-31 and the EM 34-3 are sketched in Figures 4.3 and
4.4.   An important reason for their popularity is their operation at low
induction numbers (Chapter III, section 3.2), resulting in a linear
relationship between apparent conductivity and the emf caused by the
quadrature field, which in turn allows the use of simple interpretation
procedures.   In the EM-31, a rigid fiberglass boom connects the transmitter
and receiver, and an electronic bucking voltage cancels the primary field.
In the EM 34-3, the transmitter and receiver are connected by a cable.   The
bucking voltage, equal to the primary field, is used to determine exact
transmitter-receiver separations.

The other instruments listed in Table 4.2 are mainly used in mineral
exploration to detect conductive ore targets. These instruments generally
do not operate at low induction numbers and require complicated functions
to relate instrument response to earth conductivity.

2.1.2   Operational Advantages and Disadvantages

Frequency domain systems have their application in detecting leakage
from injection wells which is manifested in the upper 30 meters beneath the
surface. For such shallow targets, frequency-domain EM and D.C. resistivity
are the principal electrical methods. However, there is little or no
application for these methods for targets at the depth of injection of
waste fluids (several thousand feet).

Table 4.2. Commercially Available Frequency-Domain EM Systems

System	Waveform	Frequency of Frequency of	Transmitter-Receiver Separation	Component Measured	Approximate Effective Depth of Exploration (meters)	Comments
Geonics EM-31	sinusoid	9800 Hz	3.66	quadrature	7	In-phase component electronically cancelled; main area of application in shallow conductivity mapping.
Geonics EM-34-3	sinusoid	6400 Hz 1600 Hz 400 Hz	10 m 20 m 40 m	quadrature quadrature quadrature	8 16 32	Bucking voltage, equal to the primary field, is used to determine exact separation.
Max-Min	sinusoid	222 - 3555 Hz	8 m - 250 m	in-phase quadrature	180	Distances must be slope-chained.
Syntex Genie	sinusoid	37 - 3037 Hz	6 m - 300 m (effective to 200 m)	in-phase, quadrature, amplitude dip	120	Distances are electronically determined; no interconnecting cable necessary between transmitter and receiver.

81

Rx

Tx

Receiver

Transmitter
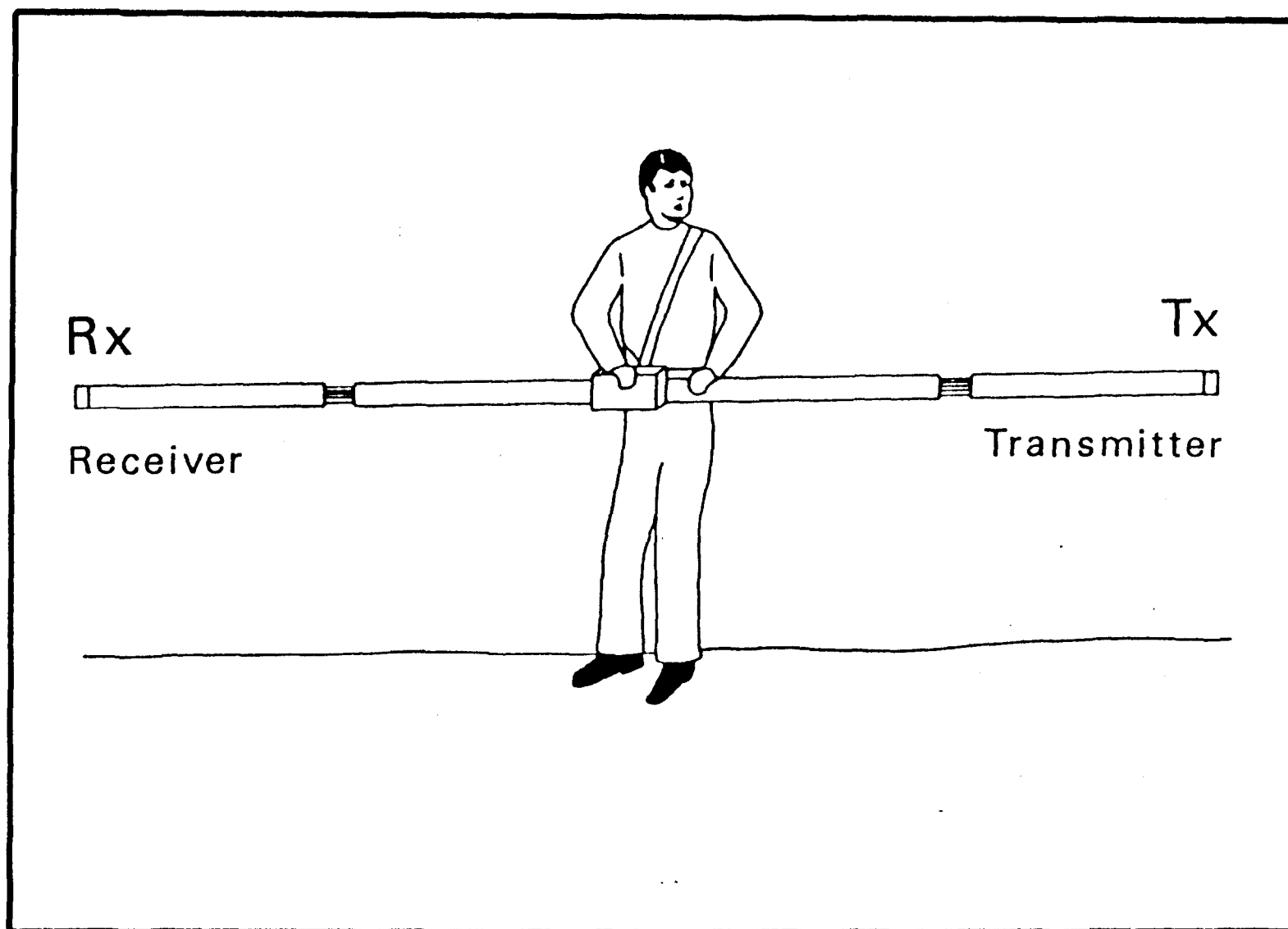
Figure 4.3. Geonics EM-31 conductivity meter vertical dipole mode.
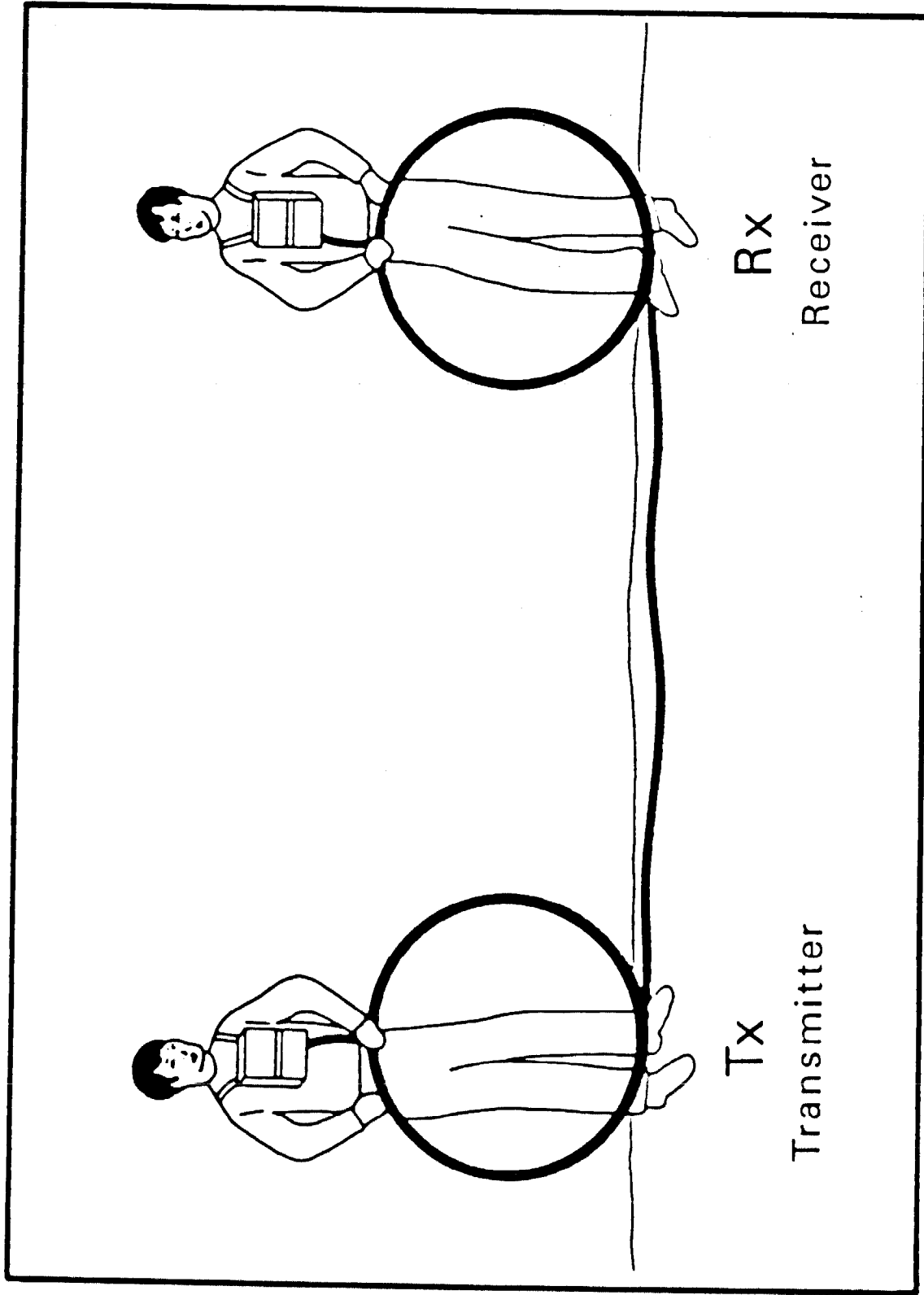
Figure 4.4. Geonics EM-34-3 conductivity meter horizontal dipole mode.

Tx
Transmitter

Rx
Receiver

83

Effective depth of exploration for EM is also about equal to the intercoil spacing (See Table 4.3). There are substantial differences in the lateral resolutions of the different arrays, however.

For detection and mapping of shallow ground-water contamination, there are some inherent operational advantages in the use of the Geonics EM-31 and EM-34:

o   no galvanic contact with the ground is required. Measurements can be made over highly resistive upper layers, such as frozen ground, dry sand surfaces, and asphalt.

o   the instrumentation is lightweight and portable so that high survey productivities can be achieved.

o   the distance between transmitter and receiver need not be chained. The in-phase component is used to derive the correct distance.

Disadvantages are:

o   the eddy current intensity in the earth and the resulting emf decreases with increasing earth resistivity. It is difficult to measure earth conductivities less than 0.001 mho/m (resistivities> 1000 ohm-m). In practice this is not a major drawback in ground-water studies.

o   with commercial instrumentation the method is mainly applicable to profiling: measuring lateral or areal variation at certain effective exploration depths. Surveying at several effective exploration depths yields some information about resistivity variation as a function of depth, but the few data points in the vertical direction make the interpretation of resistivity layering difficult.

2.1.3   Lateral Resolution

The lateral resolution of the EM methods compares favorably with the direct current method. To achieve the same detectability with D.C. resistivity, by using the Wenner array, as with EM with a two-layered earth would require an a-spacing of about $2h_1$ or a total electrode spread of $4h_1$. Although there is not a one-to-one correlation between the array size and the lateral resolution of the array, D.C. resistivity methods tend to have a somewhat lower lateral resolution than EM methods. The dipole-dipole array provides slightly better lateral resolution than the Wenner array.

TABLE 4.3 APPROXIMATE EFFECTIVE DEPTH OF INVESTIGATIONS FOR
GEONICS EM-31 AND EM-34

Instrument	Frequency of Operation	Transmitter-Receiver Separation	Dipole Orientation	Effective Exploration Depth, Ft.
EM 31	9.8 khz	3.66m (11.7 ft.)	Verticle	19
	9.8 khz	3.66m (11.7 ft.)	Horizontal	9.5
EM 34-3	6.4 khz	10m (32 ft.)	Horizontal	24
	1.6 khz	20m (64 ft.)	Horizontal	48
	0.4 khz	40m (128 ft.)	Horizontal	96

2.1.4   Geologic Noise

Frequency-domain EM instruments are chiefly used for profiling. They are used to measure lateral variations in earth conductivity within a certain depth interval (fixed intercoil spacing). The methods are employed to cover a large area quickly, and by far the greatest limitation to data quality is sensitivity to geologic noise.

The degree of geologic noise is highly dependent on the geologic setting and is one of the survey parameters most difficult to predict. Variation in subsurface composition is often greatest in the upper 30 meters. This is the zone where rapid changes are most likely to occur in soil types, water content, and organic content.

Sources of geologic noise can often be distinguished from the exploration target if:

o   the amplitude of the noise is less than the amplitude of the response from the exploration target; or

o   the spatial spectrum of the target includes different frequencies than the spectrum of the noise

The cause for the relatively high sensitivity of EM to geologic noise can perhaps be best understood from Figure 4.5. Figure 4.5 shows eddy current intensity as a function of depth for horizontal, co-planar dipoles. The intensity of eddy currents is high near the surface and decreases with depth. For that reason variation in thicknesses and conductivities of near-surface layers will have a proportionally greater influence on instrument response than layers at greater depth.

2.1.5   Case Histories: Fixed-Frequency Electromagnetic Induction

The use of the Geonics EM-31 and EM-34 for injection well investigations is restricted by the limited exploration depth (<30 meters). They may be employed for detecting leakage from injection wells where the leaks are manifested near the surface or for investigating contamination emanating from temporary surface holding ponds. Two case histories have been selected to illustrate the application of these devices to shallow targets. Neither case history is from an injection well, but both illustrate the use of the EM-31 and EM-34 for detection and mapping of shallow, conductive contamination.
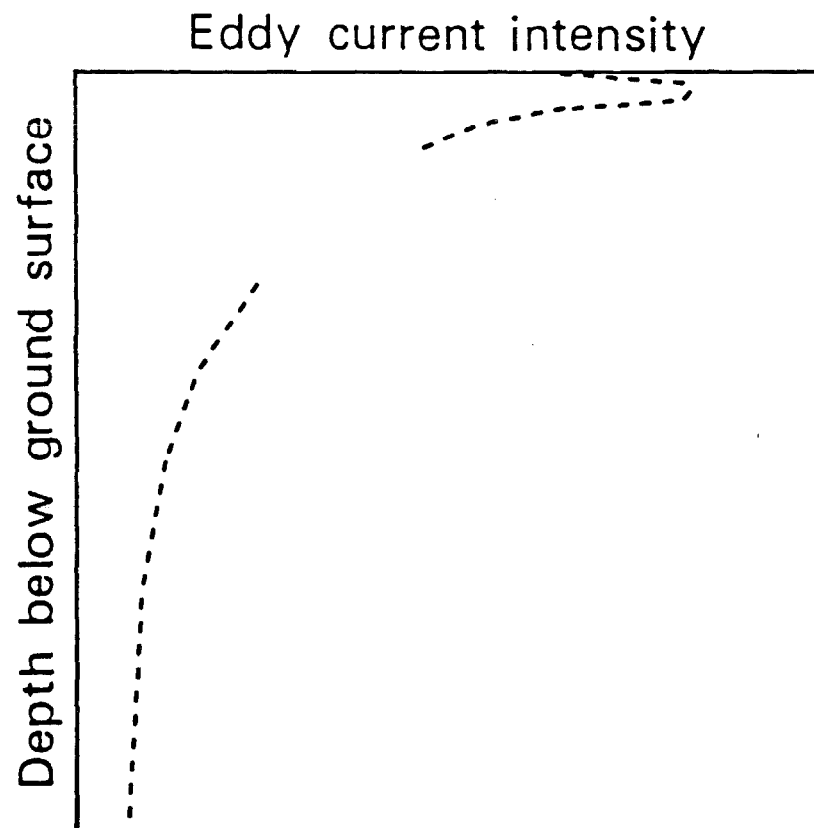
Figure 4.5. Eddy current intensity as a function of depth for electromagnetic induction (horizontal, co-planar dipoles).

2.1.5a   Henderson, Nevada .

Reference:

"Study of Subsurface Contamination with Geophysical Monitoring Methods at Henders:n, Nevada," E.G. Walther, D. LaBrecque, and D.D. Weber, Lockheed Engineering and Management Services Company, Inc., and R.B. Evans and J.J. van Ee, EMSL-LV, EPA, Proceedings of the National Conference on Management of Uncontrolled Hazardous Waste Sites, 1983, Washington, D.C.

Figure 4.6 shows the layout of the industrial complex and a survey line along which measurements were made with an EM-31 which was oriented in the vertical dipole position. The objective of the survey was to detect contamination leakage plumes. The field observations are shown in a profile in Figure 4.7. The plume is identified by an increase in conductivity above 100 millimhos/meter. When conductivities exceed about 70 mmho/m, a correction for non-linearity must be applied to observations with the EM-31. Figure 4.7 shows measured and corrected apparent conductivities. It is evident that the contamination along the profile is above background. Noise in the data is caused by cultural interferences (fences, highways), but the signal caused by the plume is several times greater than the interference signal.

2.1.5b   Falmouth, Massachusetts

Reference:

Olhoeft, Gary R., and D.R. Capron, "The Use of Geophysics in Hazardous Waste Investigations," Open File Report, U.S. Geological Survey, Denver, CO, 1986.

The second case history involves an EM-34 survey near Falmouth, Massachusetts, conducted to detect ground-water contamination from a sewage lagoon. The near-surface geology of the site consists of clean sands and gravels (glacial outwash) several hundred feet thick. The water table occurs at a depth of about 20 feet. The topography is rolling sand dunes with elevation differences of about 50 feet.

Since the objective of the investigation was to map ground-water contamination, the apparent conductivity of the ground water was to be determined. The relatively dry sands above the water table have very low electrical conductivity.

Figure 4.8 shows the influence of topography along a profile with topographic relief. The relatively small changes in conductivity of the ground water are masked by topographic relief. Topographic relief in this case is the source of geologic noise; unless the survey data are corrected
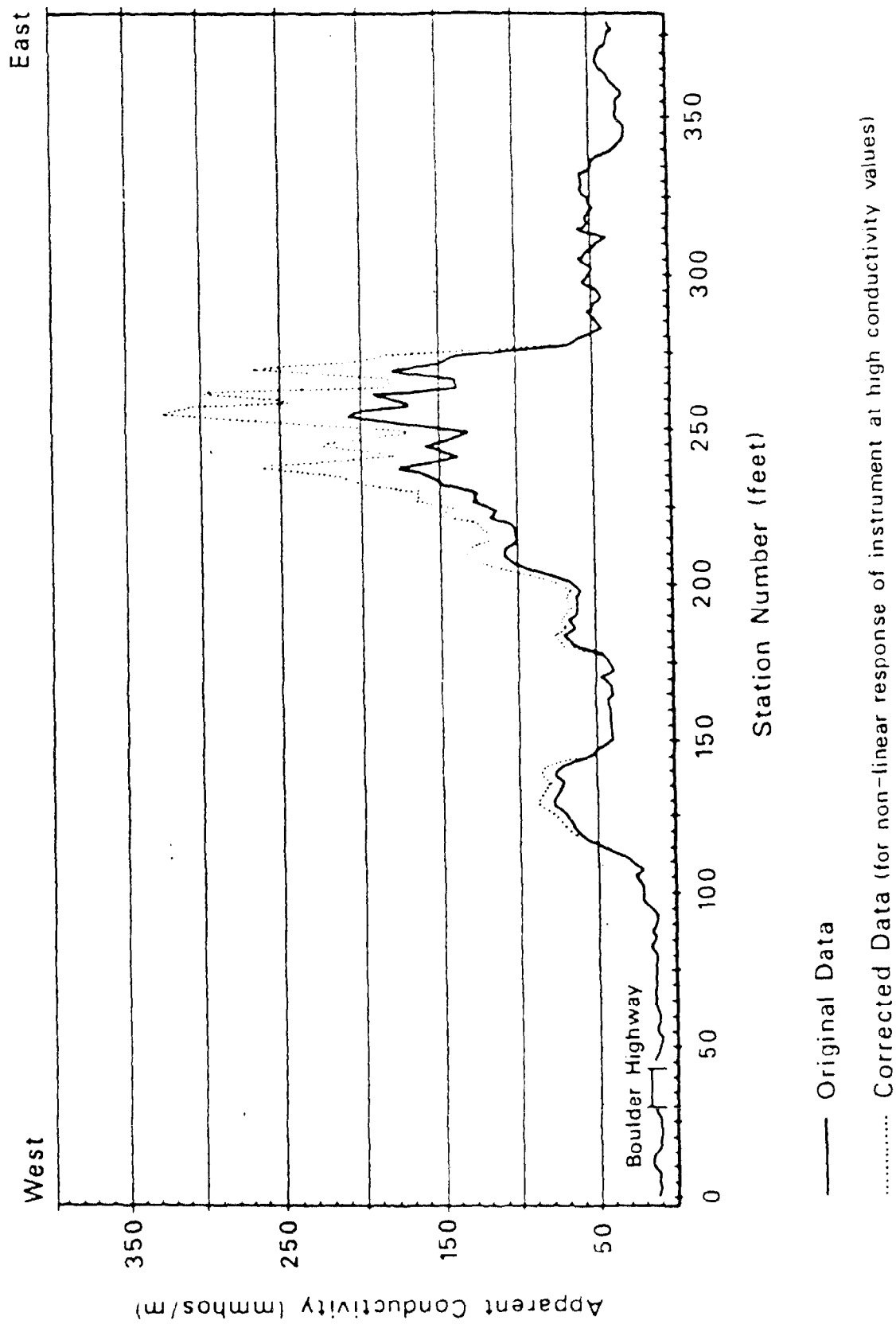
Figure 4.7. Apparent conductivity values from Geonics EM-31 along survey line in Henderson, Nevada.

—— Original Data

·········· Corrected Data (for non-linear response of instrument at high conductivity values)
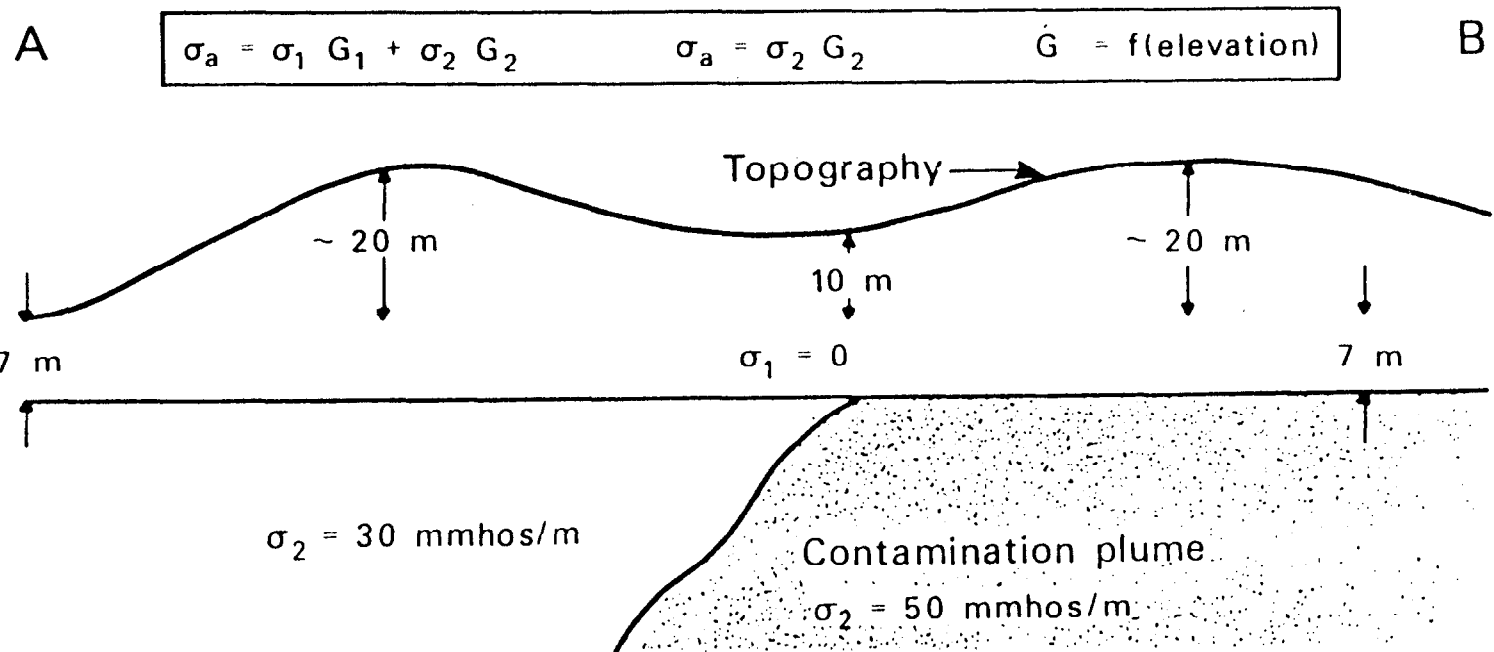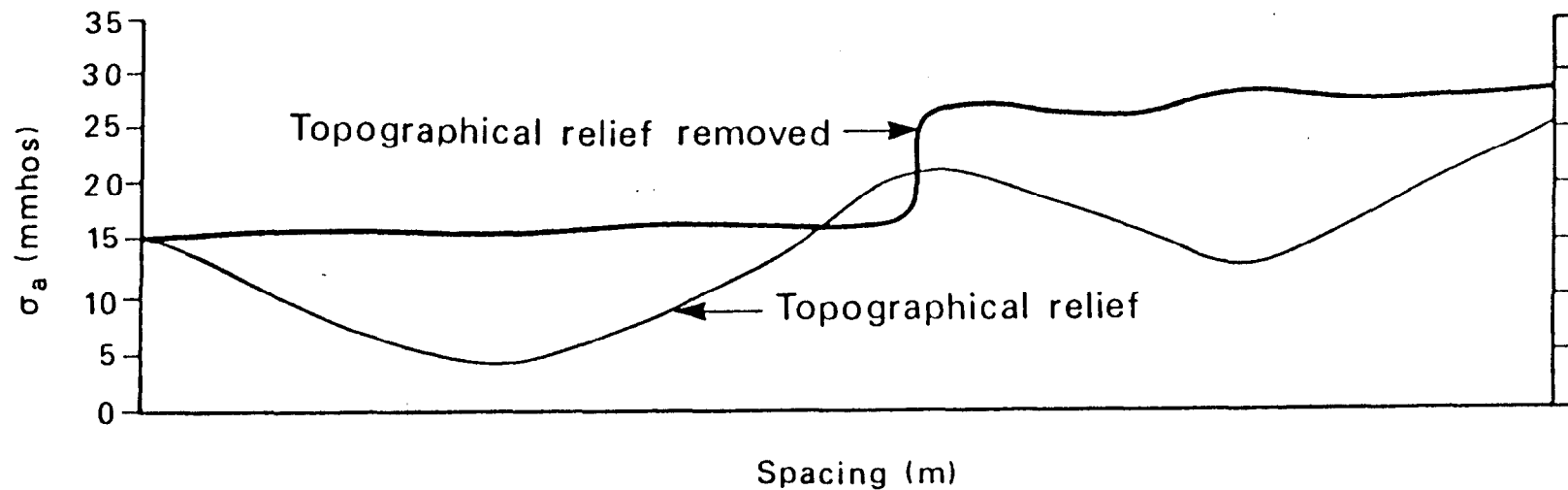
Figure 4.8. Effect of topography on apparent conductivity values from EM-34 survey near Falmouth, Massachusetts.

for topography, the contaminant plume cannot be delineated from the profile data.

Also shown in this figure is the EM profile corrected for topographic relief. The changes in ground-water contamination are now measurable. A map showing the survey line and the outline of the contaminant plume is shown in Figure 4.9.

The two case histories illustrate the applications and limitations of the fixed-frequency EM methods for ground-water and brine leakage investigations. These limitations are as follows:

o   limited exploration depth (<75 feet); and

o   relatively high sensitivity to geologic noise.

In some situations the data may be corrected for geologic noise; the Falmouth site was such a situation. In other cases, the signals caused by contamination may greatly exceed noise, as was the case with the Henderson site. In general, it appears that more manipulation of the data (noise reduction) would improve the use of the method. The major advantages of the method are its low cost, rapid data collection, and ease of operation. The principal disadvantage of fixed-frequency EM for investigating injection wells is the limited exploration depth.

2.2 Time Domain (TDEM) Soundings

2.2.1   Instrumentation

The instrumentation available for TDEM soundings is listed in Table 4.4. TDEM equipment is primarily used for two purposes:

o   to detect highly conductive zones associated with mineral ores, and

o   to perform soundings (that is, to determine subsurface resistivity layering).

In Table 4.4 a judgment has been made about the performance of the equipment for soundings. There is little information available in the literature to back up that judgment.

2.2.2   Operational Advantages and Disadvantages

The advantages of TDEM soundings are as follows:

o   no galvanic contacts (probes) are required. This is particularly attractive for the relatively deep exploration targets associated with injection wells.

92
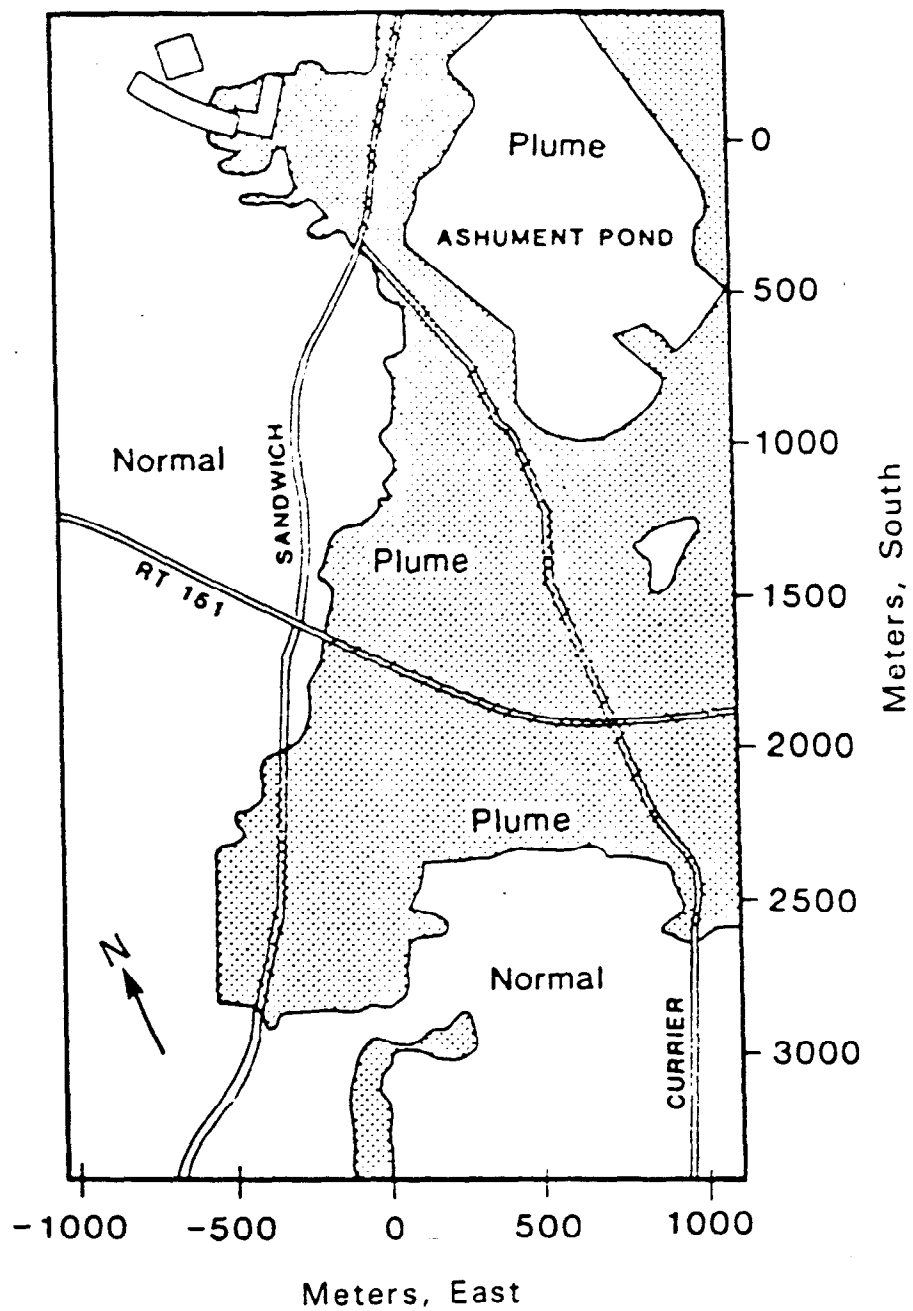
Figure 4.9.   Sewage plume as outlined by survey with Geonics EM-34 near
Falmouth, Massachusetts.

93

TABLE 4.4 CHARACTᴇᴿISTICS OF TRANSIENT SOUNDING SYSTEMS

System	Current Waveform	Maximum Current	Turn-off Time for 450m x 450m Loop	Measurement Time Range	Comments
Geonics EM-42	bipolar 50% duty cycle	40A	200μs	890μs - 3.3	separate receiver and transmitter; computer-controlled digital acquisition
Geonics EM 37-3	bipolar 50% duty	40A	400μs	89μs - 79ms	separate receiver and transmitter; data logger available
Mineral Control Instrumentation Pty., Ltd., SIROTEM	bipolar 50% duty cycle	10A or 20A	100μs	50μs - 161ms	single unit for single loop operation; built-in logger; quite portable
Zonge GDP-12	bipolar 50% duty cycle	27A or 43A	ns*	120μs - 900ms	separate receiver and transmitter; built-in data logger
Lamontagne UTEM-II	triangular	6A	ns	25μs - 25ms	separate receiver and transmitter; built-in data logger

ns* (not specified)

94

o   measurements require limited space and can be conducted in an environment with high ambient electrical noise (powerlines and radio stations)

o   procedures for data acquisition are highly automated

The disadvantages of TDEM soundings are:

o   the method generally cannot be applied to exploration in the upper 50 feet

o   equipment is expensive, and equipment operation and interpretations are complex and require highly-trained technical personnel

2.2.3   Lateral Resolution

TDEM soundings map subsurface resistivity layering with good lateral resolution.   The physical reasons for high lateral resolution are as follows:

o   exploration depth is mainly a function of time rather than spacing between source and receiver

o   a local source for the electromagnetic field is used

Although hard data are not available, lateral resolution is approximately equal to exploration depth.   Thus, for a target at an exploration depth of 1,000 feet, a measurement is probably representative of an area within a 500-foot radius of the measurement site.

2.2.4   Sensitivity to Geologic Noise

TDEM soundings have a lower sensitivity to geologic noise than any other method.   This fact can be conceptually explained from Figure 4.10 where the eddy current intensity as a function of depth is schematically illustrated at different times after turn-off.   With increasing time the maximum current intensity occurs at increasingly greater depth;   for example, at time t_2 the current intensity in the upper layers is small.   A measurement at time t_2 will, therefore, be relatively insensitive to near-surface layers.   The geologic noise from the upper layers will be small in measurements at later times. High data quality can be realized with TDEM because of the low influence of geologic noise; this is one of the major advantages of TDEM. Some of the case histories are used to illustrate this point.
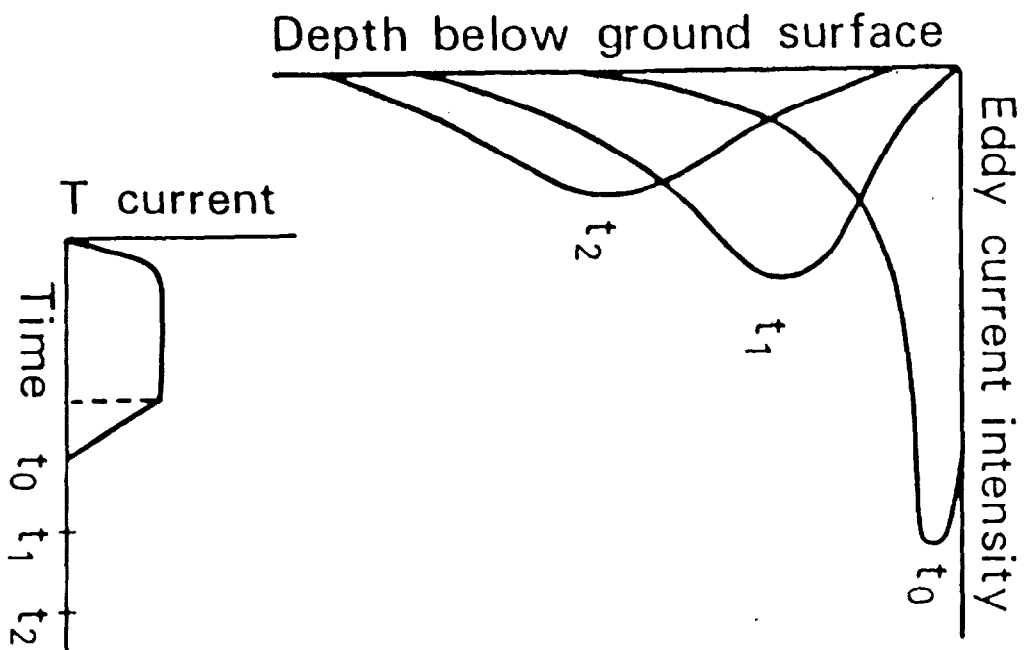
Figure 4.10. TDEM eddy current intensity as a function of depth.

96

2.2.5   Case Histories: Time Domain Methods

TDEM has been used for exploration targets at depths varying from 15 meters to about 3,000 meters. This is clearly the depth of interest in investigations of problems related to leakage from injection wells or to migration at the injection horizon. Two published case histories are reviewed, one with a mapping target at about 500 meters depth and another where contamination from injected fluids was evident at shallow depths.

2.2.5a   TDEM Survey in Haskell County, Oklahoma

Reference:

Wightman, W.E., A.A. Kaufman, and P. Hoekstra, "Mapping Gas-Water Contacts in Shallow Producing Formations with Transient EM," presented at 53rd Annual Meeting, Society of Exploration Geophysics, Las Vegas, Nevada (1983).

In Class II injection wells, the produced brines are often reinjected into the pay zone. In this case history, the objective was to map the extent of the producing zone and the contact between hydrocarbon saturation and brine saturation in this zone; this is an objective closely related to well siting and completion.

Figure 4.11 shows a geologic section of the study area with four induction logs. These logs show that where the producing horizon is saturated with brine, formation resistivities of 2 to 3 ohm-meters are encountered; where the producing horizon is saturated with hydrocarbons, formation resistivities in excess of 50 ohm-meters are found. The formation resistivities above and below the producing horizons vary between 15 ohm-meters and 30 ohm-meters.

Thus, in traversing the contact between hydrocarbon and brine saturation, a large change in resistivity occurs in a relatively thin layer (20 meters) at a depth of about 500 meters. It is common in all electrical methods to express the electrical property of a thin layer by its conductance, the ratio of its thickness to its resistivity. Thus, the pay zone sa'urated might have a conductance of about 10 mhos when saturated with brine and a conductance of less than 1 mho when saturated with hydrocarbons.

The first step in the investigation was to make an evaluation with computer modeling of the feasibility of detecting the contact between the brine and the hydrocarbons by TDEM from the surface. For that purpose the geoelectric section of Figure 4.11 is simplified to the model shown in Figure 4.12, consisting of a thin layer embedded in a half-space with a
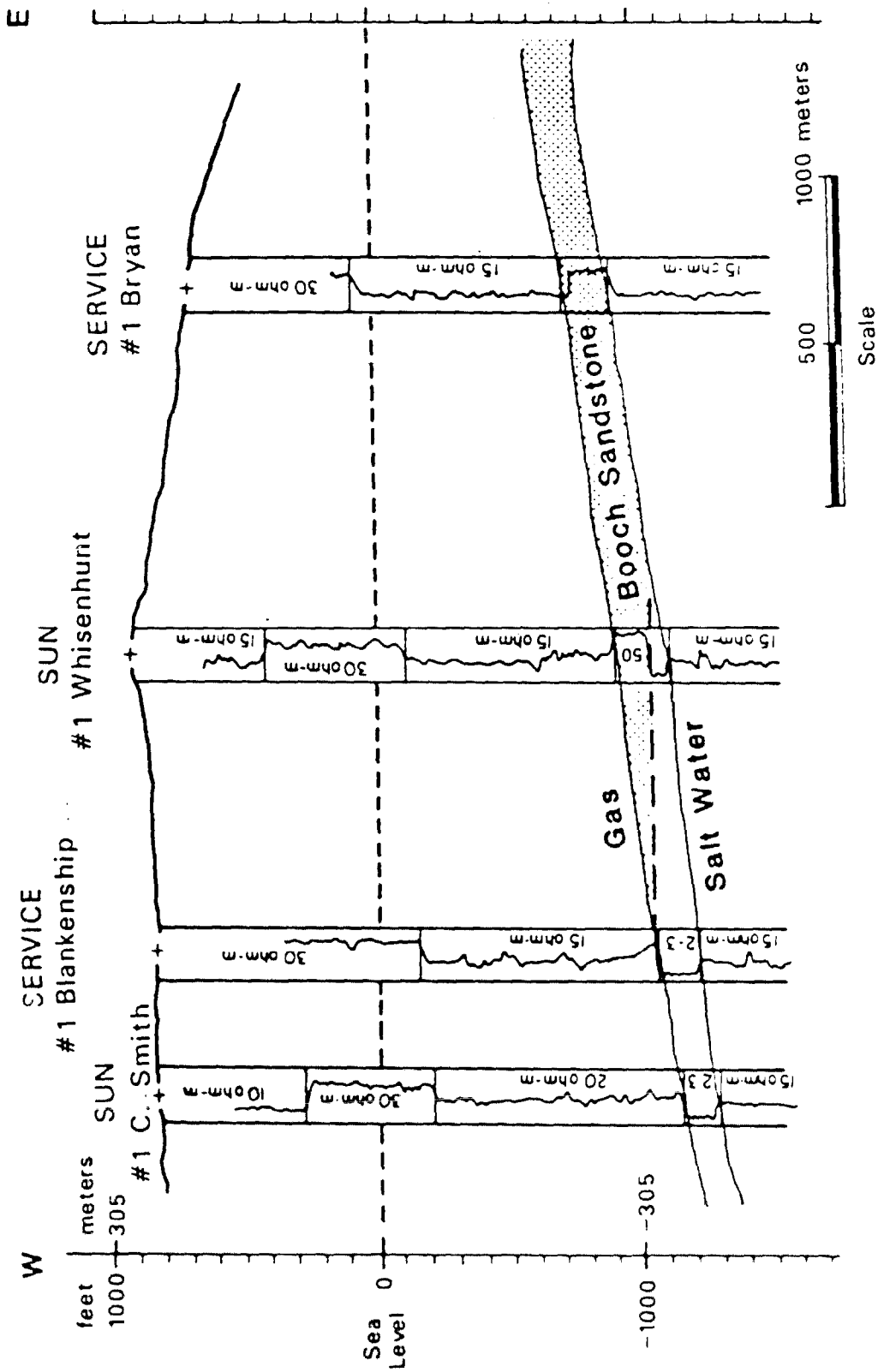
Figure 4.11. Geologic cross-section and borehole induction logs, Haskell County, Oklahoma.
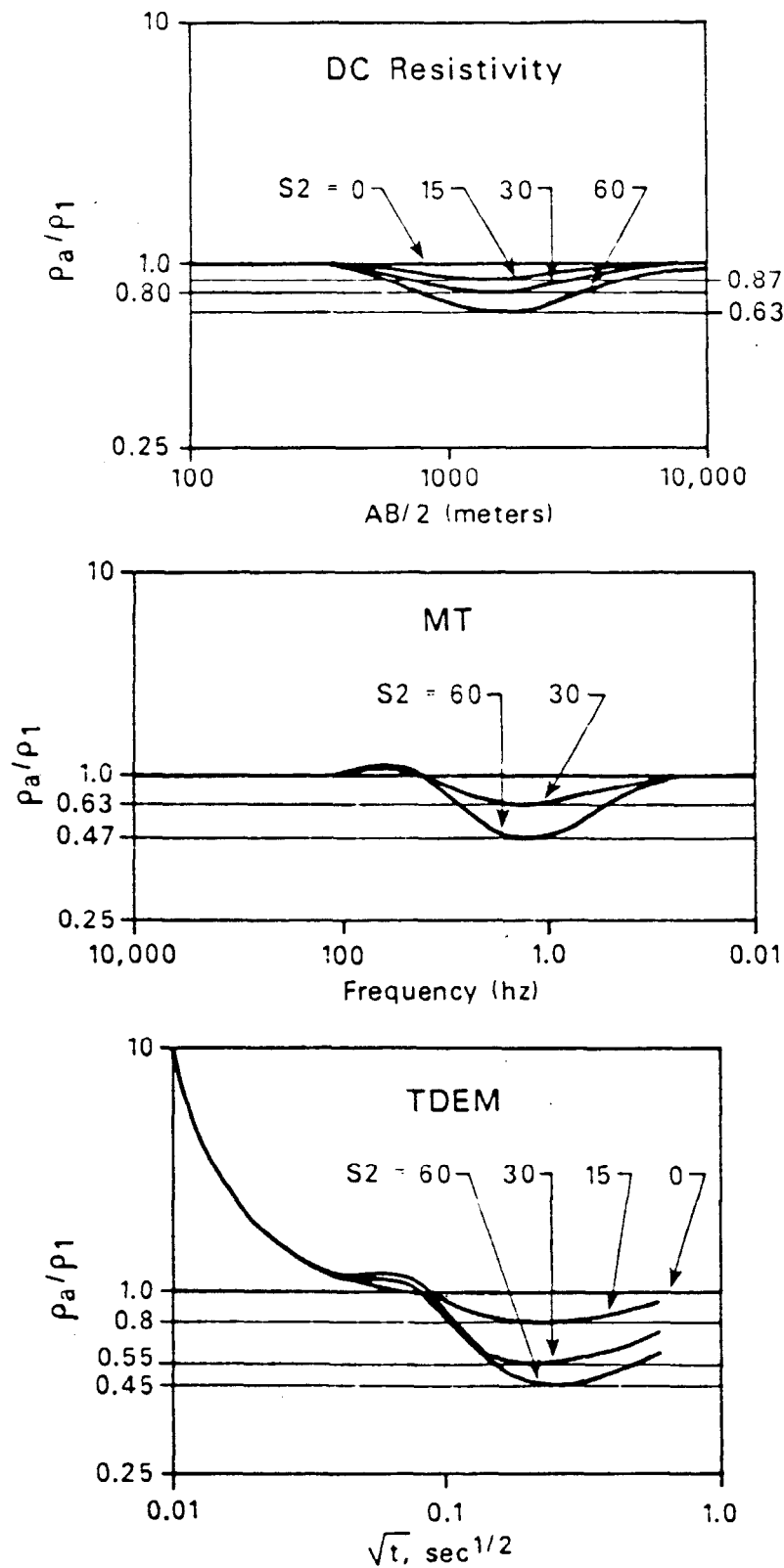
Figure 4.12: Computer modeling studies of detectability of thin pay zone with TDEM, Mt, and DC Resistivity.

uniform resistivity of 20 ohm-meters. The conductance of the thin layer is varied in the model. In Figure 4.12 the results of computer modeling studies for three electrical methods are shown (TDEM, MT, and D.C.). The model curves show that there is a range of time, frequency, and spacing where the change in conductance in the producing zone causes a decrease in apparent resistivities. Two important conclusions can be derived from these models:

o The change in apparent resistivity for the TDEM and MT methods is considerably larger than for the D.C. method. Table 4.5 lists the maximum decrease in apparent resistivity caused by changes in the conductance.

o Impractically large electrode separations are required in D.C. soundings to measure the decrease in apparent resistivity. For TDEM soundings, measurements are made within a 500-meter square loop.

The layout of the TDEM survey and the locations of drilled wells are shown in Figure 4.13. Square loops 500 meters on a side were laid across the gas field, and measurements were made in the loop centers. Typical apparent resistivity curves over locations with gas saturation, brine saturation, and over dry holes (low porosity) are superimposed on Figure 4.13. The characteristic decrease caused by brine is clearly visible in the curves of Loops No. 1, 4, and 10 in Figure 4.13. From the behavior of the curves of the various soundings, a contour map of producing horizons was made, outlining areas where either gas or brine saturation occurred or where porosity of the normally high porosity sandstone layer was reduced. This map was consistent with logs from four available wells and agreed with logs from wells which were subsequently drilled.

Similar case histories are available from the Russian literature. An example from the Siberian Basin is shown in Figure 4.14. As the oil-water contact is traversed, the apparent resistivity curve changes shape (Rabinovich, 1973).

The implications of these case histories for investigations of injection wells appear to be the following:

o TDEM soundings can determine the depth and water quality of high porosity layers in sedimentary basins.

o TDEM soundings have been used to determine the areal extent of these high porosity, brine-saturated layers.

TABLE 4.5 MAXIMUM DECREASE IN APPARENT RESISTIVITY AND MEASURED
VOLTAGE CAUSED BY ACTUAL INCREASES IN CONDUCTANCE FOR
TDEM, MT, AND DC

Conductance	Maximum Decrease in	For Various Methods	
	TDEM	MT	DC
15	20%	19%	13%
30	45%	37%	20%
60	55%	53%	36%
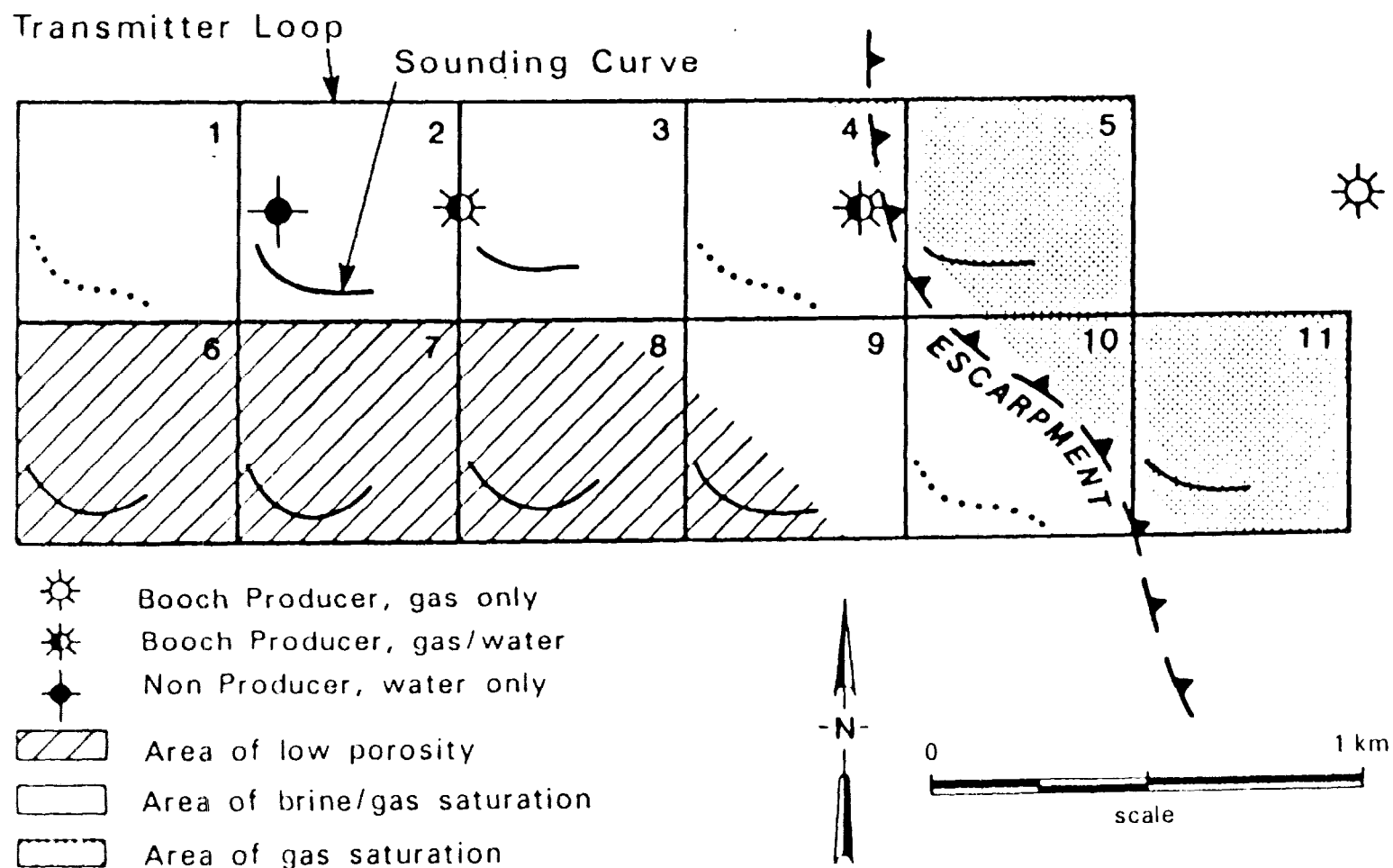
Figure 4.13. Layout of TDEM survey and locations of drilled wells, Haskell County, Oklahoma, showing typical TDEM apparent resistivity curves over locations with gas saturation, brine saturation, and dry holes.
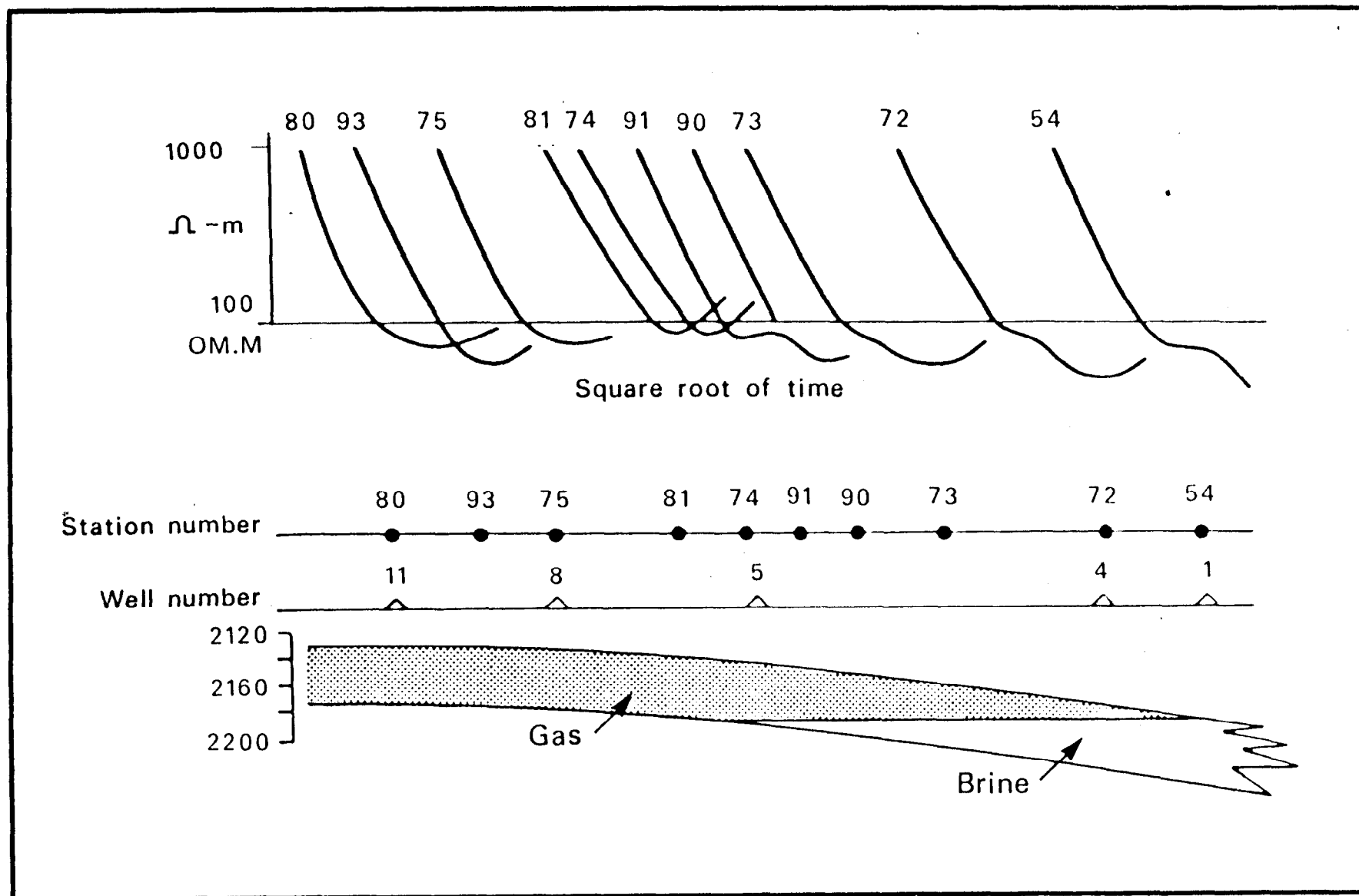
Figure 4.14.   TDEM apparent resistivity curves along survey line in Siberian Basin, showing oil-water contact. Distance from station 80 to 54 is 16 km.

2.2.5b   TDEM Survey in Osage County, Oklahoma

Reference:

Fitterman, D.V., P.V. Raab, and F.C. Frischknecht. "Detection of Brine Contamination from Injection Wells Using Transient Electromagnetic Soundings," EPA, pre-issue copy, January, 1986.

   TDEM test surveys were conducted to determine brine leakage from injection wells in Osage County, Oklahoma. In the test area vegetation damage was a visual surface indicator of brine contamination.

   The producing horizons are sandstone layers in the upper Pennsylvania sediments, and brine is reinjected into these producing horizons. The producing horizons occur at various depths ranging from 200 feet to 1,000 feet. In some parts of Oklahoma, such as Texas County, large fresh water aquifers such as the Ogallala Formation occur above injection horizons, and the possibility for contamination exists. The Ogallala Formation is, however, absent in Osage County.

   For the TDEM survey, coincident loop soundings were used with 76-meter or 152-meter loops. Figure 4.15 is a plan view of the loops and of nearby test wells.

   A typical geoelectric section derived from the TDEM soundings is shown in Figure 4.16. In the vicinity of Well #1W, a substantial decrease in resistivity (about a factor of 3) is observed. The decrease in resistivity was interpreted to occur near the surface. The bottom contact of the low resistivity zone was not derived.

   This case history showed brine contamination from the injection well to be localized. This is an example where the validity of one-dimensional interpretation may have to be determined. TDEM surveys were capable of detecting the presence of brines at depths of several hundred feet and were also capable of mapping, at least near the surface, the areal extent of the contamination.

3.0 CSAMT Method

3.1 Instrumentation

3.1.1   Operational Advantages and Disadvantages

   Advantages are as follows:

o   Many receiving stations can be serviced by the same CSAMT source. This reduces survey line setup time.
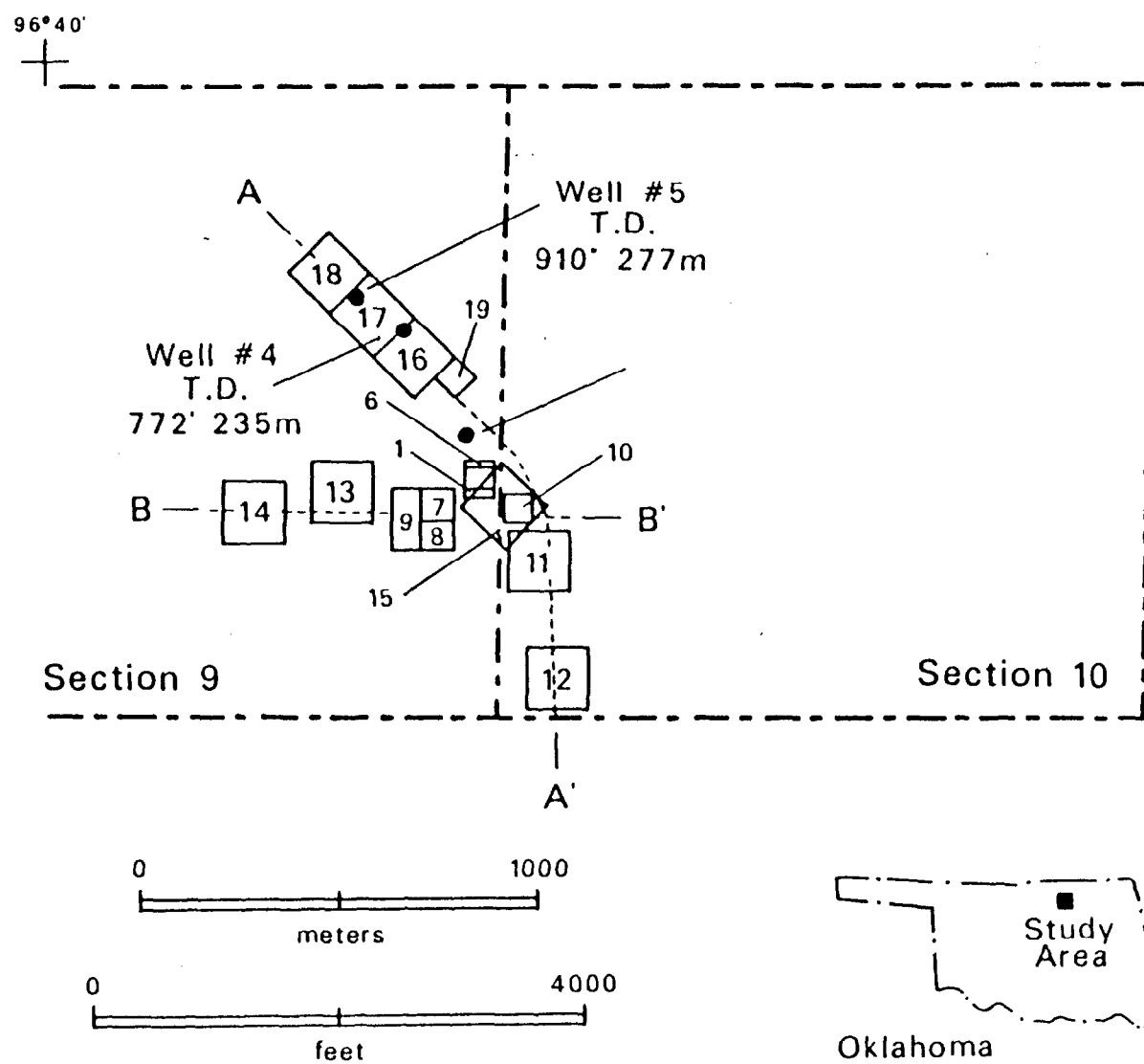
Figure 4.15. Plan view of TDEM loops and nearby test wells, Osage County, Oklahoma.
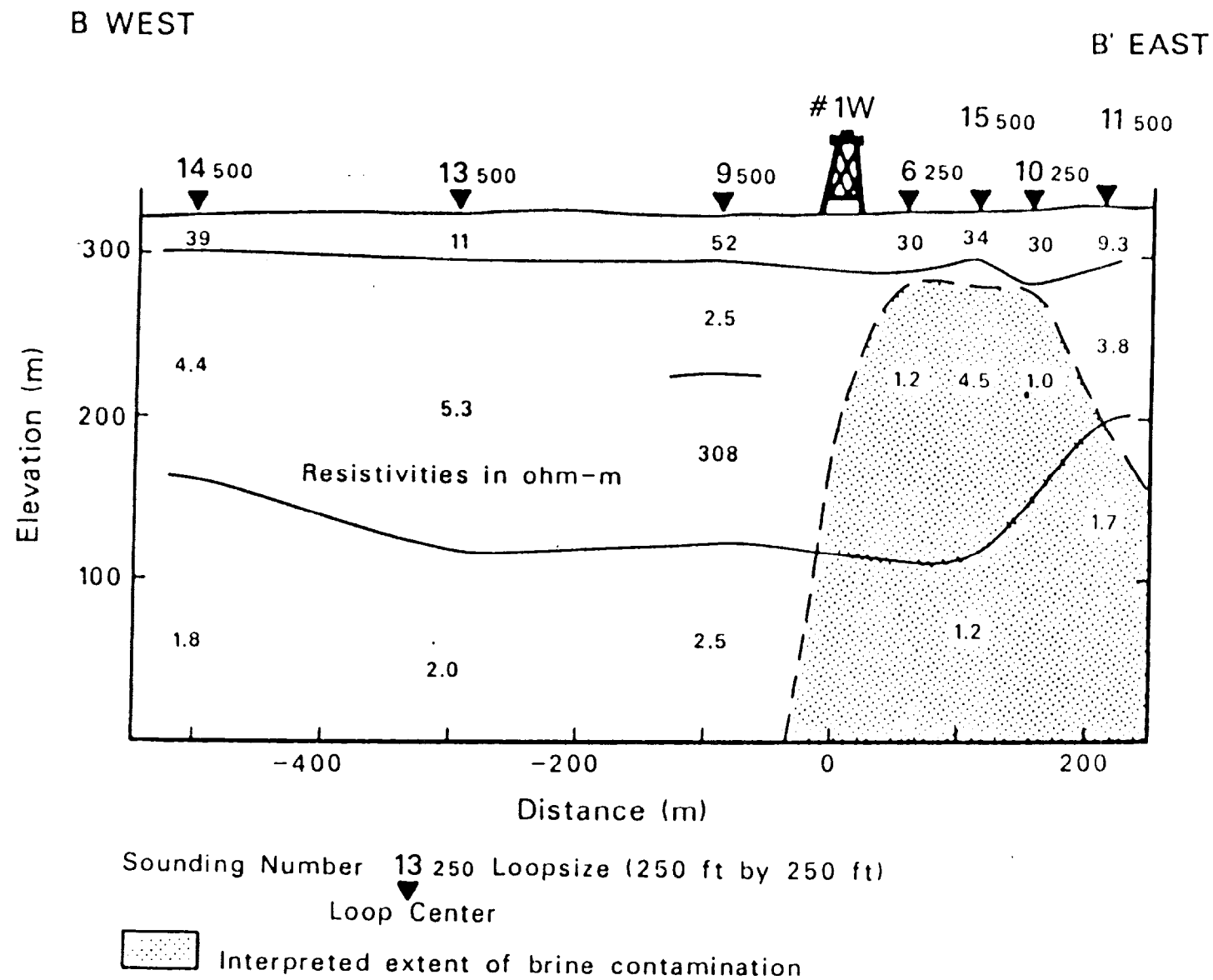
Figure 4.16.   Typical geoelectric cross-section derived from TDEM soundings, Osage County, Oklahoma.

o   Data collection is rapid.

Disadvantages of the method are as follows:

o   The method is highly sensitive to geologic noise, and lateral variation in resistivity can have a major influence on soundings.

o   In CSAMT, the source must be located several kilometers from the receiver (measurement site). This may create problems in obtaining access to needed sites.

o   Common data acquisition procedures in CSAMT involve obtaining data with only one orientation of electrical dipoles. As a result, the full tensor of the surface impedance is not measured and surface impedance is treated as a scalar quantity.

3.1.2   Geologic Noise

The method is highly sensitive to geologic noise. An important reason for this high sensitivity is that a ratio of an electric field to a magnetic field is measured. The electric field is greatly affected by near-surface resistivity variations. At boundaries between regions of different electrical resistivity, electrical charges form. Because of the usual variability of surface layer composition, the surface layer is likely to have many such boundaries. These local charge formations distort the electrical field and cause high sensitivity of the method to geologic noise.

3.1.3   Lateral Resolution

Lateral resolution for mapping of features exposed near the surface can be very high. Interpretation of the depth of targets may be very difficult, however. The physical reasons are illustrated in Figure 4.17; electrical charges form at the boundaries of lateral discontinuities in resistivity and in turn greatly alter the local electric fields. Consequently, apparent lateral resolution may be very high if a receiving station is located near the discontinuity, as would be the case for Station A in Figure 4.17. On the other hand, it will also cause distortion in a sounding at B. In general the effect of electric charges will extend both vertically and laterally. Although an anomaly may be measured at A, it may not be possible to determine reliably the depth of the cause of the anomaly.

Electrical charges form when electrical currents cross boundaries of different resistivities. The formation of charges is, therefore, also highly dependent on the direction of the electrical field, as illustrated in Figure 4.17. This phenomenon often results in different apparent resistivity curves based on the direction of measurement of electric fields (or the orientation of survey lines).

107
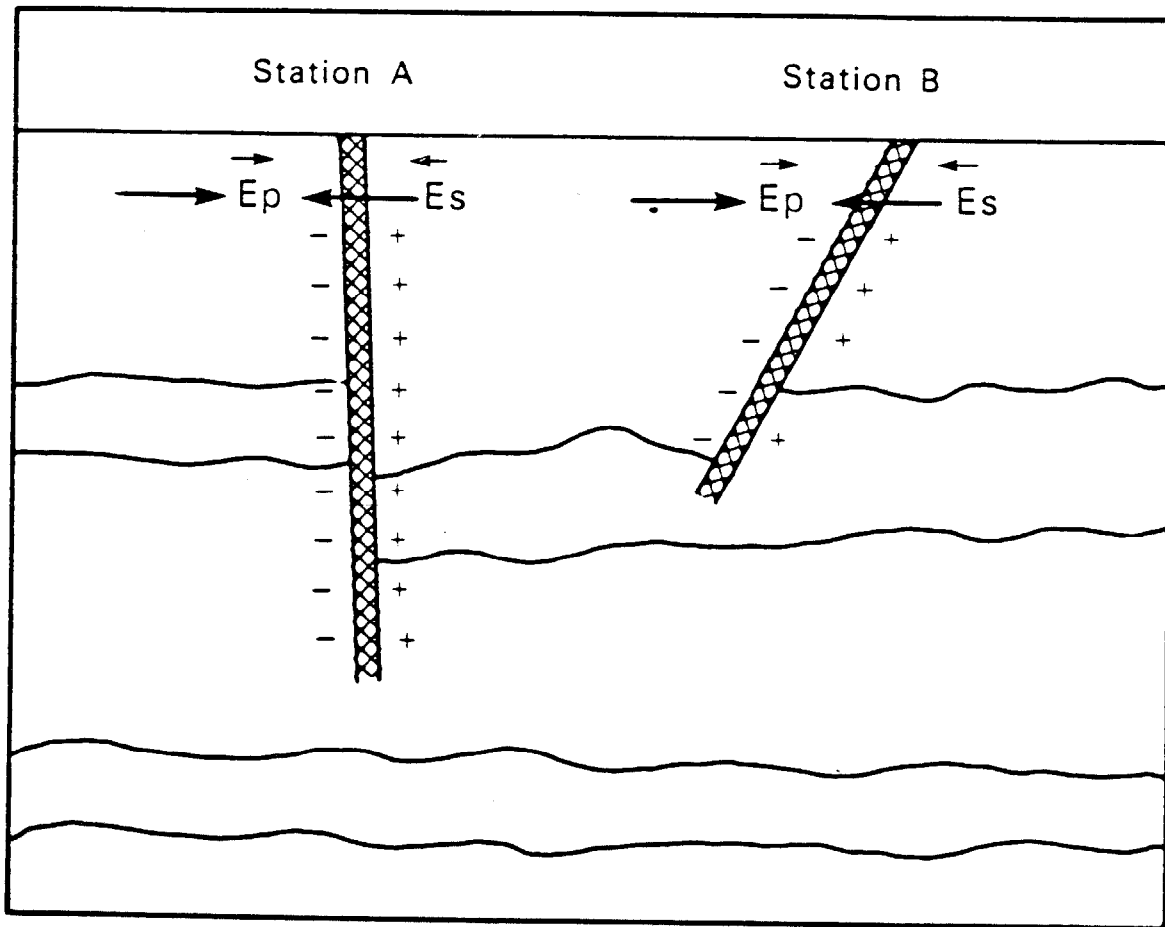
Figure 4.17. CSAMT geologic noise created by charge formation along discontinuities.

3.2   Case History: CSAMT Survey of Brine Contamination in Lincoln County, Oklahoma

Reference:

Syed, T., K.L. Zonge, S. Figgins, and A.R. Anzzolin, "Application of the Controlled Source Audio Magnetotellurics (CSAMT) Survey to Delineate Zones of Ground-Water Contamination: A Case History," presented at the Second National Conference and Exposition on Surface and Borehole Geophysical Methods in Ground-Water Investigations, National Water Well Association, Fort Worth, TX, February 12-14, 1985.

A CSAMT survey was conducted in Lincoln County in east-central Oklahoma. Oil production in the study area began in the 1930's. Water injection for secondary and saltwater disposal purposes began in the 1950's, and the cumulative volume of water injected through August 1982 was approximately 75 million barrels.

The major objective of the ground-water contamination study included the identification of high chloride concentrations in upper aquifers and an investigation of the possibility that the source of these high chloride concentrations could be oil field brines. CSAMT was part of an overall exploration program consisting of drilling, ground-water sampling. Although the hydrocarbon formations occur at depths of about 3,000 feet, the freshwater/saltwater interface occurs at shallow depths from 150 feet to 450 feet. This was the interface mapped by CSAMT; the survey did not determine whether the near-surface brines originated at deeper horizons.

A schematic survey layout is given in Figure 4.18. A transmitter dipole length of 5,000 feet was used and was positioned approximately 3 to 4 miles from the survey area. In the survey area, measurements were made at intervals of 200 feet along the survey lines. The direction of the electric field measurement was parallel to the survey lines. At each measurement station, scalar apparent resistivities were determined at discrete frequencies over a range from about 5,000 Hz to 22 Hz. The data were presented in vertical and horizontal pseudo-sections where the apparent resistivities measured along profiles are displayed and contoured. An example of a vertical pseudo-section is given in Figure 4.19. Typical background resistivities in the area are on the order of 10 ohm-meters, so that skin depth at 5000 Hz is about 20 meters, and at 22 Hz skin depth is about 340 meters.

The vertical pseudo-section of Figure 4.20 illustrates quite well some of the problems in CSAMT interpretation. At Station -4.0, a near-vertical anomaly of low resistivity, limited to this one station, is observed.
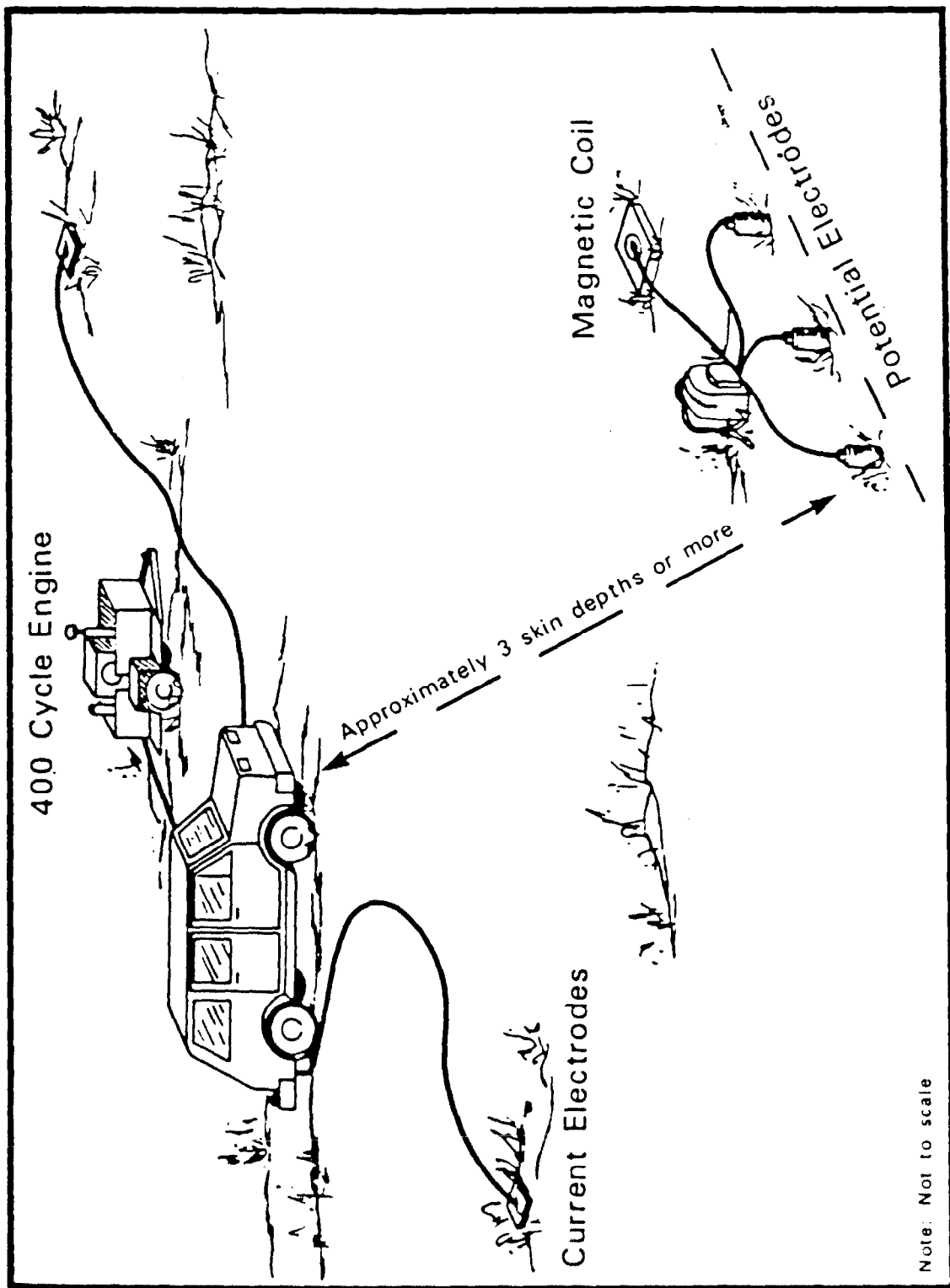
Figure 4.18. Schematic layout for CSAMT survey.
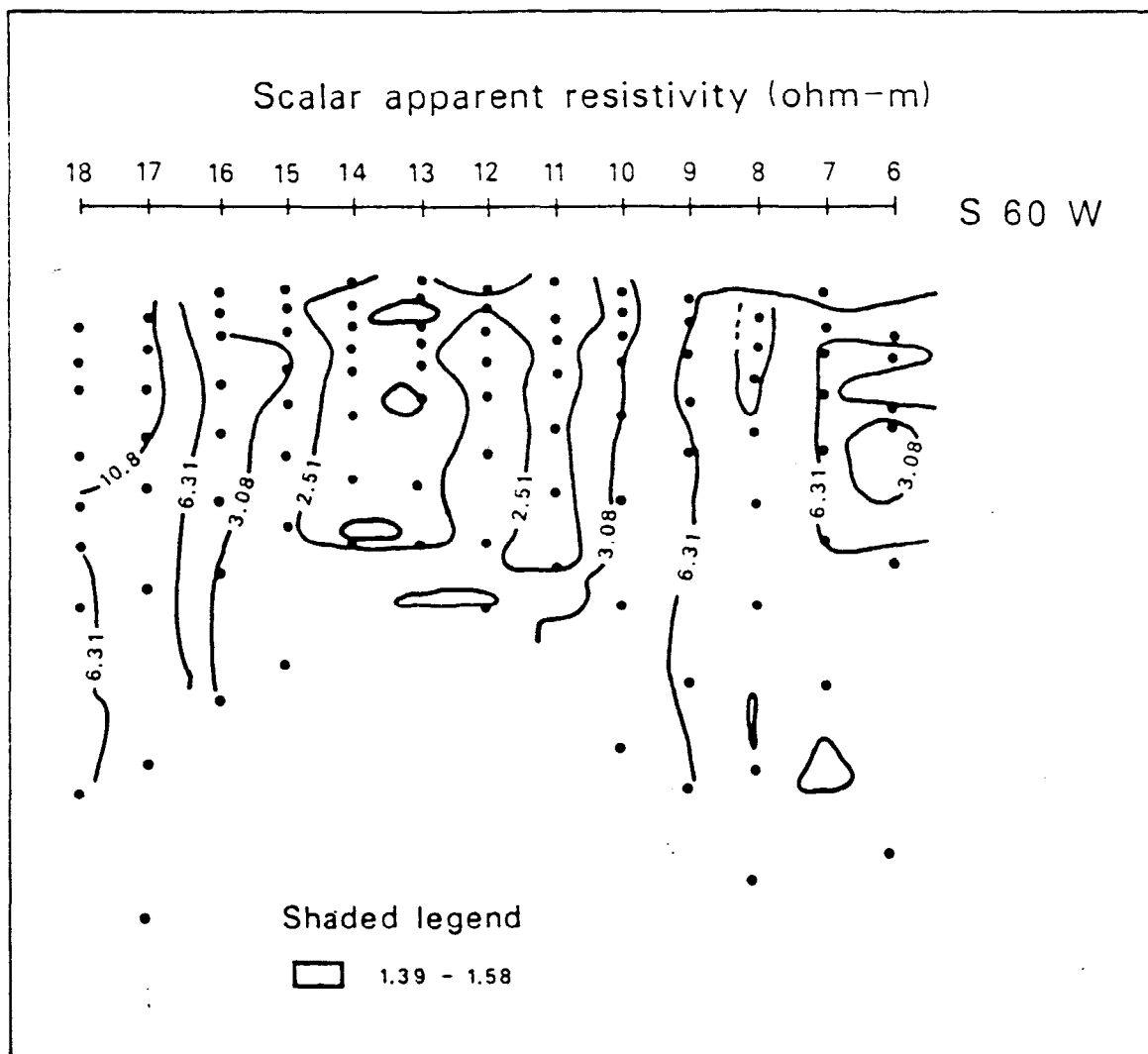
Figure 4.19. CSAMT Psuedo-section, Lincoln County, Oklahoma.

111

Scalar apparent resistivity (ohm-m)

S 60 W   1   0   -1   -2   -3   -4   -5   N 60 E

Contour labels: 2.51, 3.16, 3.98, 5.01, 3.98, 3.98, 5.01, 6.31, 7.94, 6.31, 10.0, 3.98, 3.16, 2.51, 3.16

Shaded legend
1.69 - 2.00
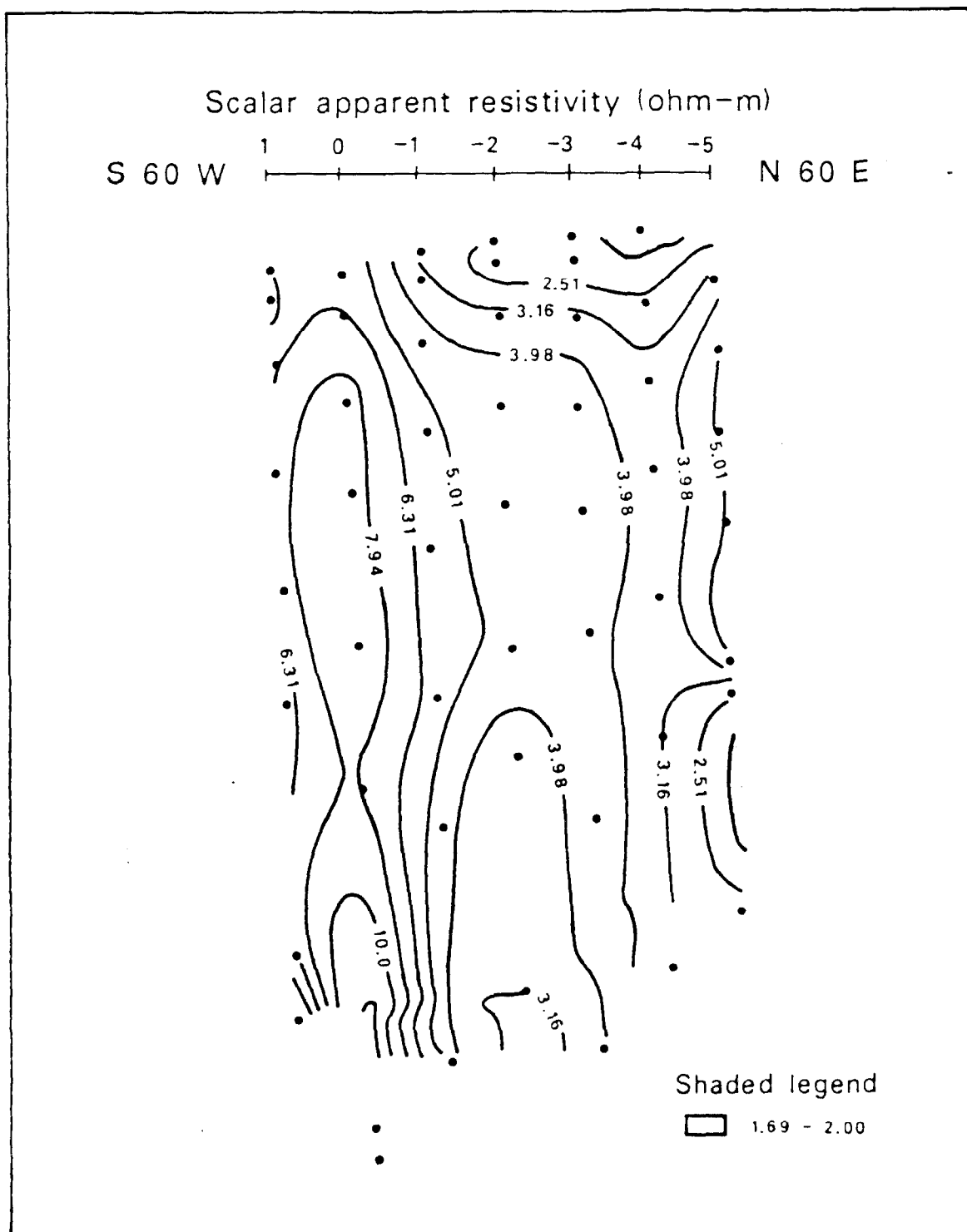
Figure 4.20. CSAMT vertical pseudo-section, Line 8, resistivity versus depth.

Particularly at lower frequencies, the data approached background values at Stations -3.0 and -5.0. Only at higher frequencies (shallow exploration depths) is the anomaly of wider lateral extent. It is very likely that CSAMT only mapped shallow brine occurrences in this example, and very little information about resistivity layering as a function of depth was obtained

4.0 Direct Current (D.C.) Method

4.1 Instrumentation

Extensive instrumentation is available for D.C. methods, and this fact reflects the 60-year history of the method. Table 4.6 gives a partial list of available equipment.

4.1.1 Operational Advantages and Disadvantages

Advantages of the D.C. methods are as follows:

o The equipment is inexpensive and does not require extensive personnel training.

o Interpretation procedures are well-developed. Forward modeling curves (the Mooney Master Curves) for a layered earth and for two- and three-dimensional situations are published and are readily available.

o Forward and inverse modeling computer programs are readily available.

o The method can be used for both depth soundings (determining resistivity strata or layers) and profiling (determining lateral variations in resistivity).

Disadvantages of the D.C. method are as follows:

o Large transmitter-receiver arrays are required to achieve the exploration depths associated with injection wells.

o Contacts with the ground (electrodes) are required.

4.1.2 Lateral Resolution

Lateral resolution of the method is poor, mainly because of the large arrays required for deeply-buried targets. In a typical Wenner or Schlumberger array, the spacing between current and voltage electrodes is approximately four times the required exploration depth. For mapping lateral resistivity variation the dipole-dipole array can provide great detail. However, two or three dimensional model computer calculations are required to interpret these data and near-surface lateral conductivity variations will still dominate and possibly mask the deeper structures.

113

Table 4.6. Partial List of Commercially Available D.C. Equipment

Manufacturer	Model	Output Quantity Displayed	Range	Sensitivity	Accuracy
Bison	2350B	$2\pi(V/I)$	0-10 ohms	1% of full scale	± 2%
Bodenseewerk	GGA-30	V,I	0-1000 mV	10 μV	± 1 μV
Phoenix	RV-1	V,I	0-10 V	0.5% of full scale	± 1 %
GISCO	RSPIP-10	$2\pi(V/I)$	0-2 megohms	0.1% of full scale	± 1%
Scintrex	RSP-6	V,I	0-1000 mV	0.2 mV	± 0.5%

4.1.3   Vertical Resolution

Vertical resolution is often limited by geologic noise in the data. The fact that the electrodes are spaced over distances several times the required exploration depth and the fact that they are moved for each discrete depth measurement, can introduce much noise in a data set.

4.1.4   Sensitivity to Geologic Noise

The method is highly sensitive to near-surface geologic noise. The reason is that inhomogeneities in resistivity near the voltage electrodes have a large effect on the measurement. Voltage electrodes must be moved frequently in a vertical sounding, and this introduces another source of noise. Noise which is caused by near-surface resistivity variation can also be severe in profiling applications.

4.2 Case Histories: D.C. Methods

Reference:

Reed, P.C., K. Cartwright, and D. Osby. "Electrical Earth Resistivity Surveys Near Brine Holding Ponds in Illinois," Illinois State Geological Survey, 1981.

A relatively large number of case histories describing the mapping of ground-water contamination with D.C. resistivity methods have been published. These investigations have usually dealt with shallow leakage from brine holding ponds rather than with contamination in deeper aquifers. There are at least two reasons for this different focus: first, such contamination sources have received greater attention historically; and second, D.C. methods are better suited to investigations of such shallow targets than they are to deeper targets.

A typical investigation using D.C. methods on a brine holding pond was reported by Reed et al. in Illinois. Before disposal of brines through reinjection into producing horizons became common practice, brine was placed into holding ponds. In Illinois, where annual precipitation exceeds evaporation, brine discharged into ponds may slowly enter ground water and eventually may be discharged into streams. The purpose of the study by Reed et al. was to test the usefulness of D.C. resistivity methods for mapping brine migration from ponds.

The investigators reported the results of surveys at four sites; one of these surveys is reviewed here. The ponds were constructed in an overburden of glacial till, consisting of sands, silts, and clays. A cross-section of the Woburn site is given in Figure 4.21, and the plan view is given in Figure 4.22.
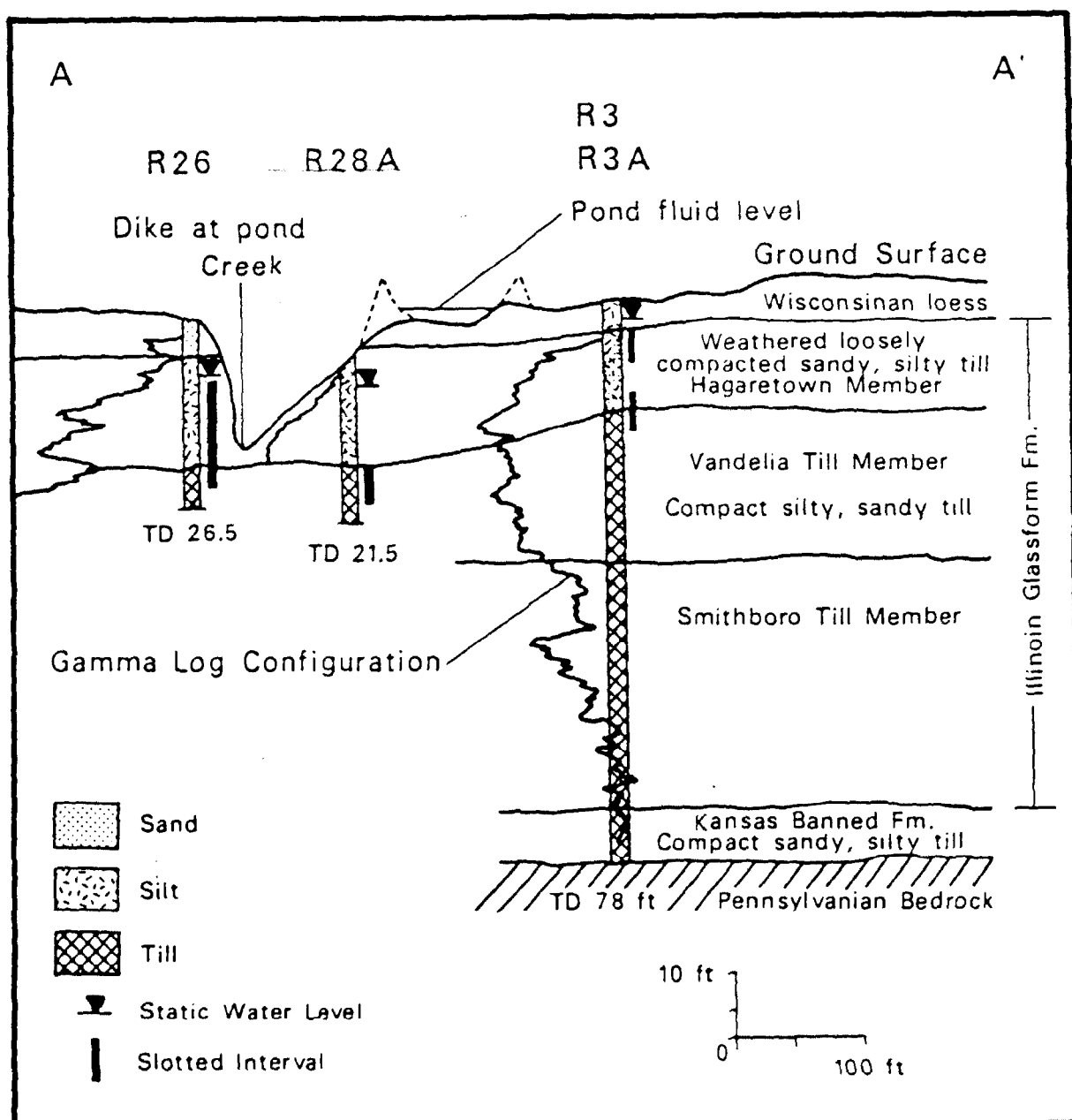
Figure 4.21. Geologic cross-section, Woburn, Illinois, consolidated oil field.
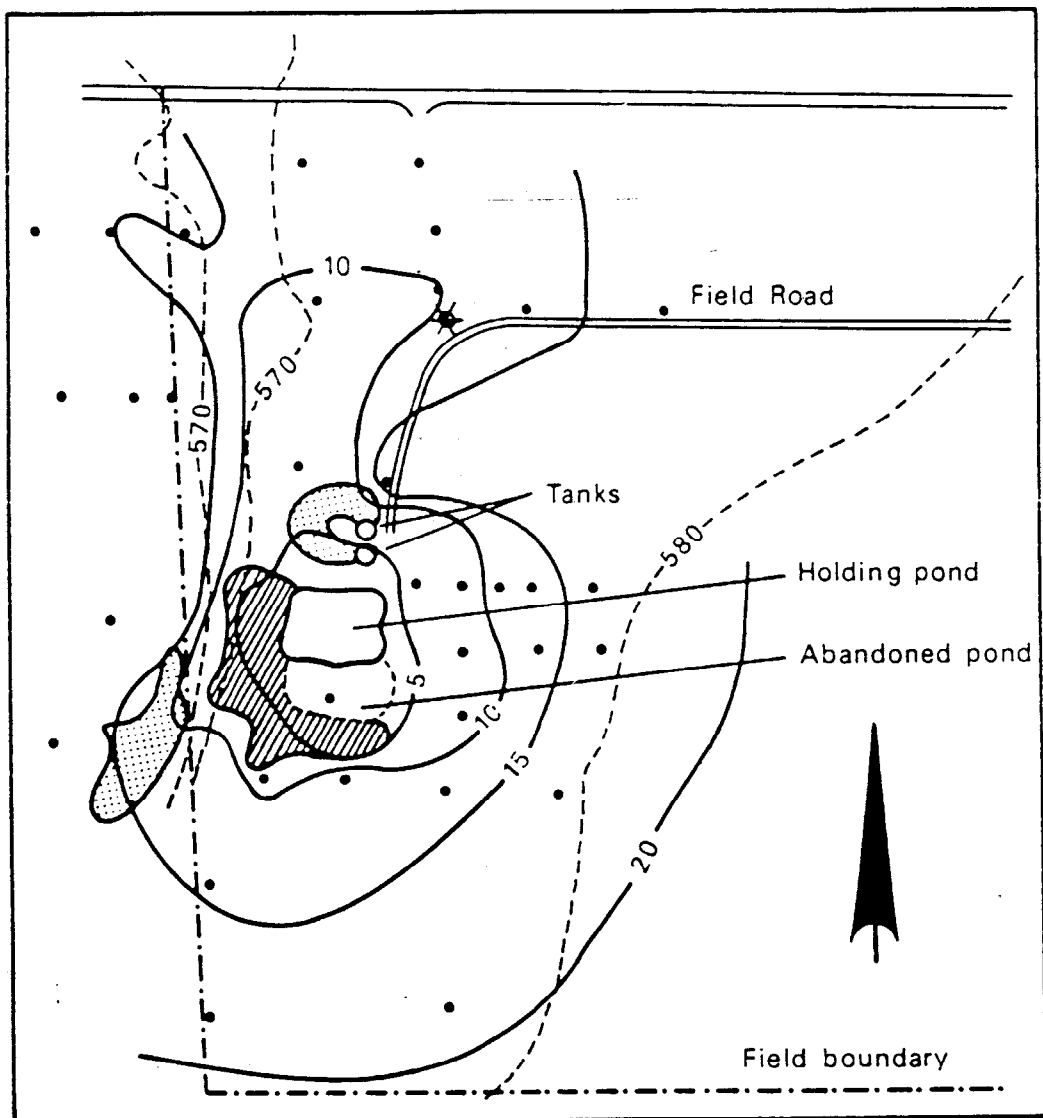
116

Figure 4.22. Plan view of Woburn Site, with apparent resistivity contours.

117

In Figure 4.23, apparent resistivity curves measured as a function of spacing for the Wenner array are shown. These data are typical of near-surface D.C. resistivity soundings in that the curves are distorted and would be difficult to interpret in terms of a horizontally-layered earth. However, a continuous decrease in resistivity is readily observed in going from sounding 11 to 12 to 28. The location map of Figure 4.22 gives the apparent resistivities at an "a"-spacing of 10 feet. This map shows that the brine contamination is more pronounced in a northern direction.

The depth of brine contamination was not evaluated in this investigation. Effective exploration depth of a Wenner array with 10-foot a-spacing is probably about 7 to 10 feet. The best way to determine depth of contamination is to invert the curves of apparent resistivity versus a-spacing. Where there are significant distortions from lateral variations in resistivity, inverse modeling may be difficult or impossible.

The use of D.C. methods for investigations of leakage from injection wells is expected to be limited. The method may be useful for measuring shallow contamination, but the large arrays required for mapping of deeper targets makes the method generally impractical for mapping injection well contamination. Another problem is created by the rapid decrease in brine contaminant concentration with increasing distance from the source; this creates rapid lateral variations in resistivity, making inverse modeling difficult.
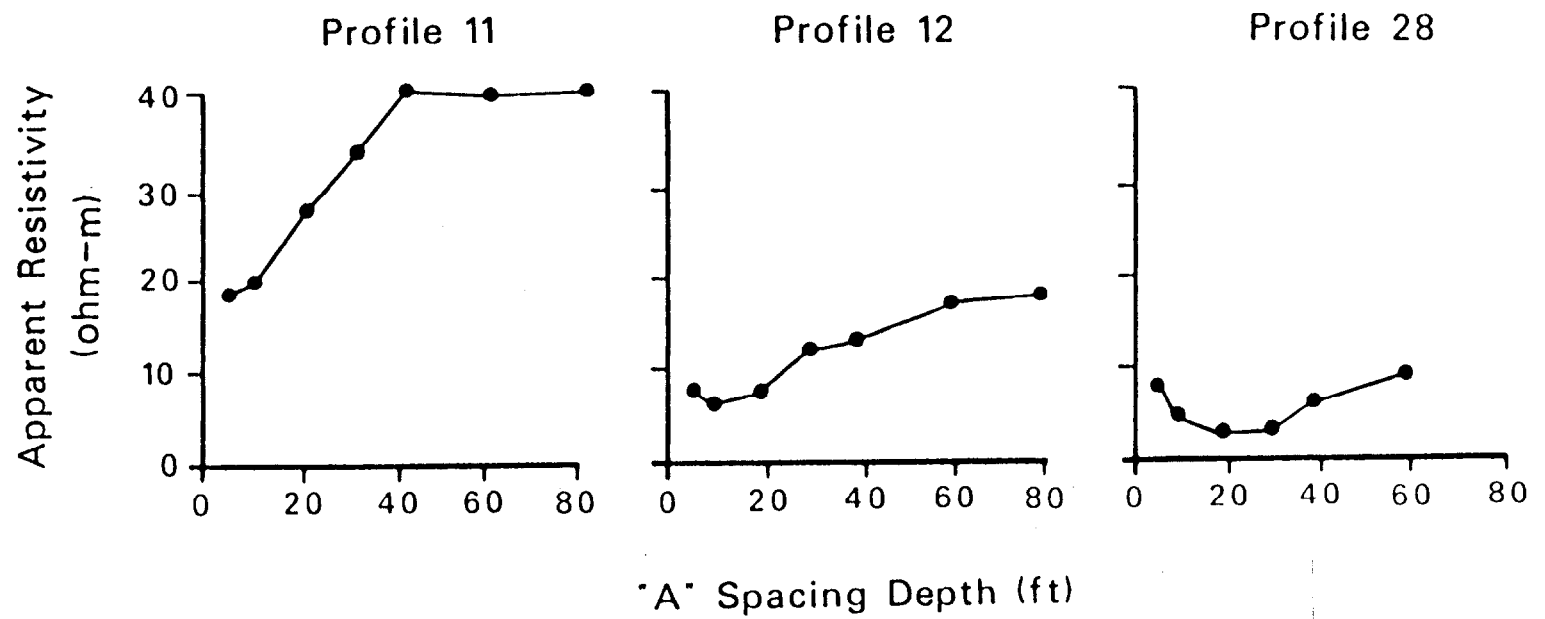
Figure 4.23.   Apparent resistivity depth soundings, Woburn, Illinois.

V.   SUMMARY AND CONCLUSIONS

Injected fluids present difficult electrical targets. Detection of target objects, formations, or strata by electrical geophysical techniques depends on the contrast in some electrical property between the target of interest and the material within which it is imbedded. Electrical conductivity is the principal property of interest for most electrical methods. While we do not fully understand the chemical interactions between contaminants and aquifer matrices, the conductivity of injected fluids is roughly proportional to their total dissolved solids content. Injection usually takes place at depths of a few thousand feet, beneath confining strata which are often highly conductive, such as shale. Often the injection zone already contains connate water high in total dissolved solids and hence of high conductivity. In such situations, with properly constructed and operated injection wells, surface electrical methods probably will not be very useful for directly monitoring injected fluids because the contrast between the injected fluids and the connate water of the injected stratum, as well as with the conductive overburden, would not be great.

However, in cases where wells are improperly constructed and operated or in cases in which fractures connect the injection zones with overlying fresh water aquifers, movement of the highly conductive injected fluids into the overlying fresh water aquifers could create a conductive electrical target which contrasts sharply with the surrounding material. In such cases, electrical methods may indeed be useful in detecting and mapping the contaminated zones.

The success of geophysical surveys is critically dependent on the clear definition of exploration objectives. The objectives of surveys using electrical geophysical methods must be stated in terms of geoelectric sections. A geoelectric section displays the variation in electrical resistivity laterally and vertically across a vertical plane passed through some line on the surface. The detectability of the contamination will vary with different sections and methods. Detectability can often be evaluated through the use of mathematical models.

The use of mathematical models is essential in interpreting electrical geophysical data in terms of a geoelectric section composed of of horizontal strata of different resistivities. Current practice usually relies on 1-dimensional models for this interpretation. While it is often possible to observe lateral resistivity changes in the data from electrical geophysical surveys, the limited lateral resolution of electrical methods makes the determination of the geoelectric section difficult where rapid lateral changes exist. In such cases, relatively sophisticated 2-dimensional and 3-dimensional models are needed. However, the use of these more advanced models is still not routine in electrical prospecting.

The use of such models usually substantially increases interpretation costs for routine surveys; they also require additional data which are often unavailable.

The important criteria for evaluating the applicability of various electrical methods to exploration objectives are as follows:

o practical depth of exploration
o lateral resolution
o vertical resolution
o sensitivity to geologic noise
o survey productivity (cost, ease of operation, personnel qualifications)

Table 5.1 summarizes the discussions of Chapters 3 and 4 concerning the capabilities of D.C., frequency-domain EM, TDEM, CSAMT, and IP. For cases where conductive contamination lies very near the surface (<30 meters depth), continuous, frequency-domain electromagnetic induction is likely to be useful in mapping the areal extent of the brines. D.C. resistivity may be successful at slightly greater depths although cultural interferences (power lines, pipelines, fences) and geologic noise are likely to cause problems. Neither of these methods are likely to produce useful information at depths approaching a typical injection horizon (thousands of meters).

However, because the earliest measurements for time-domain electromagnetic (TDEM) systems are on the order of 50 to 100 microseconds, near-surface layers can not often be determined with this method (Fitterman and Steward, 1986). Cultural interferences (powerlines, pipelines, fences) in the vicinity of the loop arrays may also cause problems. However, because of its ability to achieve substantial depths of exploration with relatively small loop arrays, time-domain electromagnetic induction (TDEM) appears to offer the greatest chance of success at depths approaching injection horizons. The case studies reviewed above tend to support this assertion. However, even TDEM will need a relatively large conductivity contrast (factor of two or greater) between the target and surrounding background to do successful mapping. The target must have lateral dimensions and a thickness which are a substantial fraction of the depth of exploration to be detectable; mapping requires targets which have dimensions greater than the depth of exploration.

Table 5.1. Summary Table f Surface-Based Electrical Surveys

Method	Maximum Effective Depth of Investigation	Sensitivity to Geologic Noise	Vertical Resolution	Lateral Resolution	Survey Productivity	Comment
D.C.	1000 meters (with large arrays)	High	Limited by Geologic Noise	Poor	Low	Requires large arrays for deep exploration
Frequency-Domain EM	30 meters (for Geonics EM34) [400 Hz]	High	Fair	Good	High	Requires good conductivity contrast between soil and target
TDEM	3000 meters	Low	Good	Good	Fair	Cannot be applied to uppermost layer
CSAMT	100 meters	High	Poor	High (If anomaly is manifested near surface)	Good	Often difficult to use for determining resistivity layering
IP	1000 meters (with large arrays)	High	Limited by Geologic Noise		Low	Brines unlikely to cause detectable IP effects; requires large arrays

REFERENCES

1.1 U.S. Environmental Protection Agency, 1984; National Primary Drinking Water Standards, Title 40, Code of Federal Regulations.

1.2 McKee and Wolfe, Water Quality Criteria, 2nd Edition, California State Water Quality Control Board Publication No. 3-A (1963).

1.3 Fairchild, D.D., "Review of Data Bases On Injection Wells," Environmental and Ground Water Institute, University of Oklahoma, Norman, OK; June 1984.

1.4 U.S. Environmental Protection Agency, Office of Drinking Water, Report to Congress on Injection of Hazardous Waste, Washington, D.C., May 1985.

1.5 Scalf, M.R., Keely, J.W., and Lafevers, C.J., Ground Water Pollution in the South Central States," EPA-R2-73-268, Washington, D.C., 1973.

1.6 Miller, D.W., Waste Disposal Effects on Ground Water, Berkeley, CA, 1980

1.7 Collins, A.G., "Saline Groundwater Produced with Oil and Gas," EPA-66012-74-010, Washington, D.C., 1974.

1.8 U.S. Environmental Protection Agency, "The Report to Congress: Waste Disposal Practices and Their Effects On Ground Water," EPA 570/9-77-001, Washington, D.C., 1977.

2.1 Greenhouse, J.P., "Surface and Borehole Geophysics in Contaminant Hydrogeology," Notes from Hydrogeology Field School, CFB Borden, 1982.

2.2 McNeill, J.D., "Electrical Conductivity of Soils and Rocks," Technical Note TN-5, Geonics Limited, Mississauga, Ontario, Canada, October 1980.

2.3 Telford, W.M.; Geldart, L.P.; Sheriff, R.E., Keys, D.A., Applied Geophysics, Chapter 5, Cambridge University Press, 1976.

2.4 Keys, W.S., and L.M. MacCary, "Applications of Borehole Geophysics to Water Resources Investigations," in Techniques of Water Investigations, U.S. Geological Survey, Ch. E1, Book 2, 1972.

2.4 Guyod, H., "Interpretation of Electric and Gamma Ray Logs in Water Wells," Log Analyst, v.6, 1966, p 29-44,

2.5 Sawyer, Clair N., and McCarty, P.L., Chemistry for Sanitary Enjineers, McGraw-Hill Series in Sanitary Science and Water Resources Engineering, McGraw Hill, 1967.

3.1 Kaufman, A.A. and G.V. Keller, Frequency and Transient Soundings, Elsevier, New York, 1983.

3.2 Kaufman A.A., "Tutorial Distribution of Alternating Electrical Charges in a Conducting Media," Geophysical Prospecting, v. 133, p. 17:, 1985.

3.3 Alpin, L.M., "Source of the Field in the Theory of Electroprospecting by Direct Current," Applied Geophysics, v. 3, 1947.

3.4 Van Nostrand, R.G., and K.L. Cook, "Interpretation of Resistivity Data," Geological Survey Professional Paper 499, 1966.

3.5 Newman, G.A., Gerald W. Hohman, and W.L. Anderson, "Transient Electromagnetic Response of A Three-Dimensional Body in a Layered Earth," Geophysics, v.51, p. 1608, 1986.

3.6 Strangway, D.W., Swift, C.M., and Holmes, R.C., "The Application of Audio-Frequency Magnetotellurics (AMT) to Mineral Exploration," Geophysics, v.38, p. 1159, 1973.

3.7 Hoekstra, P., "Electromagnetic Methods for Mapping Shallow Permafrost," Geophysics, v.43, p. 782, 1978.

3.8 Olhoeft, G.R., "Electrical Properties of Rocks," in The Physics and Chemistry of Rocks and Minerals, p. 261, 1975, John Wiley & Sons, N.Y.

3.9 Ogilvy, A.A. and E.N. Kuzmino, "Hydrogeological and Engineering Geologic Possibilities for Exploring the Method of induced potentials," Geophysics, v.37, p. 839, 1972.

4.1 "Study of Subsurface Contamination with Geophysical Monitoring Methods at Henderson, Nevada," E.G. Walther, D. LaBrecque, and D.D. Weber, Lockheed Engineering and Management Services Company, Inc., and R.B. Evans and J.J. van Ee, EMSL-LV, USEPA, Proceedings of the National Conferences on Management of Uncontrolled HGazardous Waste Sites, 1983, Washington, D.C.

4.2 Olhoeft, Gary R., and D.R. Capron, "The Use of Geophysics in Hazardous Waste Investigations," U.S. Geological Survey, Denver, CO, 1986

4.3 Wightman, W.E., A.A. Kaufman, and P. Hoekstra, "Mapping Gas-Water Contacts in Shallow Producing Formations with Transient EM," presented at 53rd Annual Meeting, Society of Exploration Geophysics, Las Vegas, Nevada (1983)

4.4 Ra inovich, B.I., and V.S. Surkov, "Results of the Use of the 2 SB Method in the Siberian Platform," in Theory and Use of Electromagnetic Fields in Exploration Geophysics, Akad. Nouk, USSR, Novosibirsk, p. 3, 1973.

4.5   Fitterman, D.V., P.V. Raab, and F.C. Frischknecht, "Detection of Brine Contamination from Injection Wells Using Transient Electromagnetic Soundings," EPA, pre-issue copy, January 1986.

4.6   Sy..d, T., K.L. Zonge, S. Figgins, and A.R. Anzzolin, "Application of the Controlled Source Audio Magnetotellurics (CSAMT) Survey to Delineate Zones of Ground-Water Contamination: A Case History," presented at the Second National Conference and Exposition on Surface and Borehole Geophysical Methods in Ground-Water Investigations, National Water Well Association, Fort Worth, TX, February 12-14, 1985.

4.7   Reed, P.C., K. Cartwright, and D. Osby. "Electrical Earth Resistivity Surveys Near Brine Holding Ponds in Illinois," Illinois State Geological Survey, 1981.

4.8   Fitterman, D.V., and M.T. Steward, "Transient Electromagnetic Sounding for Groundwater," Geophysics, V. 51, p. 995-1005, 1986.

APPENDIX I: 1984 EPA INJECTION WELL INVENTORY

EPA REGION	STATE	CLASS I	CLASS II	CLASS III	CLASS IV	CLASS V	STATE TOTAL	REGIONAL TOTALS
I	CT	0	0	0	0	173	173	
	MA	0	0	0	0	35	35	
	ME	0	0	0	0	18	18	
	NH	0	0	0	0	33	33	
	RI	0	0	0	0	42	42	
	VT	0	0	0	0	1	1	
		0	0	0	0	302		302
II	NJ	0	0	0	0	1327	1327	
	NY	23	3859	249	0	2324	6455	
		23	3859	249	0	3651		7782
III	DE	0	0	0	0	3	3	
	MD	0	0	0	3	965	968	
	PA	5	4073	0	11	15942	20031	
	VA	0	1	24	3	1748	1776	
	WV	7	370	17	0	169	563	
		12	444	41	17	18827		23341
IV	AL	9	207	10	0	249	475	
	FL	105	136	0	3	4360	4604	
	GA	0	0	0	0	4	4	
	KY	2	4357	0	0	307	4666	
	MS	8	1223	0	0	118	1349	
	NC	3	0	0	2	45	45	
	SC	0	0	0	3	33	36	

EPA REGION	STATE	CLASS I	CLASS II	CLASS III	CLASS IV	CLASS V	STATE TOTAL	REGIONAL TOTALS
	TN	0	13	0	12	33	58	
		127	5936	10	20	5149		11242
V	IL	9	18493	0	0	372	18875	
	IN	15	3798	0	0	28	3841	
	MI	86	1193	110	0	2768	4157	
	MN	0	0	0	0	19	19	
	OH	18	3911	2	0	2814	6745	
	WI	0	0	0	0	0	0	
		129	27395	112	0	6001		33637
VI	AR	8	1172	0	0	55	1235	
	LA	80	4399	227	0	0	4706	
	OK	15	14091	0	0	0	14106	
	NM	1	4344	114	1	104	4564	
	TX	160	47189	30739	0	436	78524	
		264	71195	31080	1	595		103135
VII	IA	0	0	0	0	705	705	
	KS	59	30081	394	0	931	31465	
	MO	0	300	0	0	254	554	
	NE	0	942	0	0	88	1030	
		59	31323	394	0	1978		33754
VIII	CO	1	998	59	2	6	1066	
	MT	0	1447	0	0	1	1448	
	ND	1	570	4	0	0	575	
	SD	0	8	0	0	0	8	
	UT	0	504	30	0	7	541	
	WY	3	4416	898	0	10	5327	
		5	7943	991	2	24		8965
IX	AZ	0	6	484	5	27	522	
	CA	39	13844	6	22	2	13913	
	HI	0	518	0	0	1	519	
	NV	0	6	0	0	13	19	
		39	14374	490	27	43		14973

APPENDIX 1 (cont'd)

EPA REGION	STATE	CLASS I	CLASS II	CLASS III	CLASS IV	CLASS V	STATE TOTAL	REGIONAL TOTALS
X	AK	0	160	0	1	3	164	
	ID	0		0	0	2042	2042	
	OR	0	1	0	0	712	713	
	WA	1	0	0	10	6357	6368	
		1	161	0	11	9114		9287
		659	166630	33367	78	45684		246418

STATE	AVERAGE DEPTH TO TOP OF INJECTION ZONE (feet)	AVERAGE THICKNESS OF INJECTION INTERVAL (feet)	LITHOLOGY	FORMATION NAMES
ALABAMA	4095	72	SS, CLAY, MARL	NAHEOLA NANAFALIA
ALASKA	2032	115	SH, SILT, SS	TERTIARY, SAGAVANIRKTOK
ARKANSAS	2867	108	SS, SH, CLAY	GRAVES, TOKIO BLOS, SOM.
MEAKINS				
CALIFORNIA	6139	751	SS, SILT	RIO BRAVO
FLORIDA	2067	513	LS	CEDAR KEYS, LAWSON, LOWER FLORIDIAN
ILLINOIS	2512	574	DOL, SS, LS	POTOSI, EMINENCE, MT. SIMON, SALEM
INDIANA	2332	1420	SS	MT. SIMON, BETHEL, CYPRESS, TAR
SPRING				
				EAU CLAIRE
KANSAS	3257	559	DOL, LS, CHERT	ARBUCKLE LIR
KENTUCKY	3115	2590	DOL	KNOX
LOUISIANA	3267	281	SS, CLAY, SILT	HOSSTON, FLEMING, SPARTA
MICHIGAN	3447	379	SS, LS, DOL	MT. SIMON, EAU CLAIRE GALESVILLE, FRANCON IA, DUDEE
TRAVERSE				
MISSISSIPPI	4413	1212	SS	HOSSTON
OHIO 2	3479	177	SS, DOL	MT. SIMON, MAYNARD-VILLE, ROME
OKLAHOMA	1361	964	DOL, LS, SS, CHERT	ARBUCKLE
PENNSYLVANIA	1611	70	LS	BOSS ISLAND
TEXAS	5371	702	SS, CLAY, SHALE	CATAHOULA, OAKVILLE FRIO, SAN ANDRES, BLOSSOM, JACKSON, ANHUAC, LOWER
GRANI				
				WASH, GLORIETTA
NATIONAL AVERAGE (by well)	4063	556		

LEGEND: SS - SANDSTONE   SH - SHALE   DOL - DOLOMITE   LS- LIMESTONE   SILT - SILTSTONE

APPENDIX 3

CONFINING ZONE CHARACTERISTICS
OF
CLASS I INJECTION WELLS

STATE	AVERAGE CONFINING ZONE THICKNESS (ft)	LITHOLOGY	FORMATION NAMES
ALABAMA	150	CLAY	
ALASKA	15000	SS	PERMAFRONT
ARKANSAS	521	SH, MARLS, CHALK	SARATOGA, ANNONA, BROWNSTOWN, OZAN
CALIFORNIA	700	SS, SH, SILT	FREEMAN-JEWETT, VALLEY SPRING-IONE
FLORIDA	311	CLAY, DOL, ANHY	CEDAR KEYS, BUCATUNNA
ILLINOIS	319	SH, LS, DOL, SILT	PRAIRIE DU CHIEN, EAU CLAIR, MAQUOKETA, NEW LABANY, ST. GENEVIEVE
INDIANA	256	SS, SH, SILT	EAU CLAIRE, TAT SPRINGS
KANSAS	3089	LS, SH, SS	WELLINGTON TO SIMPSON
KENTUCKY	700	DOL, LS	TRENTON, BLACK R, CHAZY
LOUISIANA	442	SH, CLAY, SS, SILT	SLIGO, BURKEVILLE, FLEMING
MICHIGAN	538	SH, DOL, LS	ANTRIM, PRAIRIE DU CHIEN, ELLSWORTH, BELL, BAYPORT-MICHIGAN
OHIO	1254	DOL, SH, LS	EAU CLAIRE, ROCHESTER, ROME, TOMSTOWN
OKLAHOMA	83	SH, LS	WOODFORD, CHATTANOOGA
PENNSYLVANIA	395	SH, LS, CHERT	
TEXAS	1442	SH, CLAY, SS	ANAHAU, JASPER, BEAUMONT, OAKVILLE, LAGARTO, LISSIE, MONTGOMERY, BETTY, GRAYBURG, YATES, FRIO, FLEMING, BURKEVILLE, ANAHUAC, GLENROSE

NATIONAL AVERAGE 928
(by well)

LEGEND
SS - SANDSTONE
SH - SHALE
DOL - DOLOMITE
LS - LIMESTONE
SILT - SILTSTONE